ÇUKUROVA UNIVERSITY
INSTITUTE OF NATURAL AND APPLIED SCIENCES

PhD THESIS

Leila NAJAFI

NUMERICAL AND EXPERMENTAL INVESTIGATION OF FLOW DOWNSTREAM OF PERFORATED CYLINDER AT LOW REYNOLDS NUMBER

DEPARTMENT OF MECHANICAL ENGINEERING

ADANA-2022

ABSTRACT

Phd THESIS

NUMERICAL AND EXPERMENTAL INVESTIGATION OF FLOW DOWNSTREAM OF PERFORTED CYLINDER AT LOW REYNOLDS NUMBERS

Leila NAJAFI
ÇUKUROVA UNIVERSITY
INSTITUTE OF NATURAL AND APPLIED SCIENCES
DEPARTMENT OF MECHANICAL ENGINEERING

Advisor : Prof. Dr. Hüseyin AKILLI
Year : 2022 Pages: 115
Jury : Prof. Dr. Hüseyin AKILLI
: Prof. Dr. Beşir ŞAHİN
: Prof. Dr. Sami AKÖZ
: Assoc. Prof. Dr. Bengi ŞANLI
: Assoc. Prof. Dr. Tahir DURHASAN

The aim of present study is to investigate the effects of deployment of perforated cylinder on vortex street suppression and flow structure on downstream of a circular cylinder in deep water and at low Reynolds numbers by using numerical simulations along with the technique of high-image-density Particle Image Velocimetry (PIV), in this purpose, during the sudies, porosity of perforated cylinder and diameters of cylinders were kept constant. This study carried out with the related to six diffrent of Reynolds numbers between750 to 2000 for PIV study and ten various value of Reynolds number is considered from range of 150 to 2000 for CFD analysis.For validation purposes, numerical investigations were run for solid cylinder cases to achieve agreement between the simulations and the experimental results as a case study. Furthermore, numerical simulations were performed to see the effect of placing the perforated cylinder around the solid cylinder, concentrically. In this regards, Velocity and vorticity contours, turbulent kinetic energy, and streamline topologies were investigated in the wake region in order to reveal the differences in flow structuers of circular cylinder among various distance rates at different Reynolds numbers. As a conclusion, According to the results, suppression of Karman vortex street is receivable with utilize of perforated cylinder around single cylinder. At all Re numbers according to the both numerical and expermental results, after perforated cylinder was concentrically placed with respect to the circular cylinder was obvioused a reduction approximately 20% to 45% in Drag coefficient.

Key Words: Circular cylinder**,** Perforated cylinder, PIV, Vortex shedding, Velocity, Turbulent kinetic energy, Drag

ÖZ

DOKTORA TEZİ

DELİKLİ SİLİNDİRİN AKIŞININ SAYISAL VE DENEYSEL İNCELENMESİ DUSUK REYNOLDS SAYLILARINDA

Leila NAJAFI

ÇUKUROVA ÜNİVERSİTESİ
FEN BİLİMLERİ ENSTİTÜSÜ
MAKİNA MÜHENDİSLİĞİ ANABİLİM DALI

Danışman : Prof. Dr.Hüseyin AKILLI
Yıl: 2022, Sayfa:115
Jüri : Prof. Dr.Hüseyin AKILLI
: Prof. Dr. Beşir ŞAHİN
: Prof. Dr. Sami AKÖZ
: Doç. Dr. Bengi ŞANLI
: Doç. Dr. Tahir DURHASAN

Bu çalışmanın amacı, derin suda dairesel bir silindirin mansabında vorteks sokak bastırma ve akış yapısı üzerine delikli silindir yerleştirilmesinin etkilerini sayısal simülasyonlar ve yüksek görüntü yoğunluklu tekniği kullanarak düşük Reynolds sayılarında araştırmaktır. Bu çalışmalar sırasında delikli silindirin porozitesi ve silindirlerin çapları sabit tutulmuştur.PIV çalışması için 750 ile 2000 arasında değişen altı farklı Reynolds sayısı ile CFD analizi için 150 ile 2000 arasında değişen on farklı Reynolds sayısı değeri ile ilgili olarak bu çalışma yapilmiştir. Validasyon amacıyla sayısal incelemeler yapılmıştır. Simülasyonlar ve deneysel sonuçlar arasında bir kiyaslama çalışması olarak anlaşma sağlanmiştir. Ayrıca, delikli silindirin katı silindirin etrafına eşmerkezli olarak yerleştirilmesinin etkisini görmek için sayısal simülasyonlar yapılmıştır. Bu bağlamda, farklı Reynolds sayılarında çeşitli mesafelerde, dairesel silindirin akış yapılarındaki farklılıkları ortaya çıkarmak için akiş bölgesinde hız ve girdap konturları, türbülanslı kinetik enerji ve akım çizgisi topolojileri incelenmiştir. Sonuç olarak, sonuçlara göre, tek silindir etrafında delikli silindir kullanımı ile Karman girdap sokağının bastırılması mümkündür. Hem sayısal hem de deneysel sonuçlara göre tüm Re sayılarında, delikli silindir dairesel silindire göre eşmerkezli olarak yerleştirildikten sonra ,Drag katsayısında yaklaşık %20 ila %45'lik bir azalma görülmüştür.

Anahtar Kelimeler: Dairesel silindir, Delikli silindir, PIV, Vorteks, Hız, Türbülanslı kinetik enerji, Drag

EXTENDED ABSTRACT

Considering that the circular cylinder is widely used in the engineering of underwater and marine structures, bridges and towers, physical and biomechanical engineering, etc., the behaviour and changes of the fluid flow around them require to carry out high accuracy investigation due to helps to increase the lifespan of structures by eliminating harmful effects of fluid flow around bodies during designs is the important subject. When the fluid flow passes over a cylindrical or circular object, fluid flow separation phenomenon occurs at shear layers of around bluff bodies. This phenomenon of flow separation is the main cause of vortex generation at the downstream of the cylinder, causing vortex shedding, which leads to vortex-induced vibration (VIV). In addition, the interaction of the vortex pair due to these vortices that are formed in the region near the wake can have harmful and destructive effects on the bluff winds, that is why controlling the adverse effects caused by the fluid flow around the structures is extremely important. Based on the studies of scientists in the last hundred years about the structure of flow around bluff objects, many control techniques have been presented, which are generally classified into two basic categories as passive and active control techniques. In each of the two categorized flow control methods, they have good features and relative formations, but despite this, passive control techniques are more preferred in engineering because of their economic and easy application, and because they do not require external energy input. According to passive control techniques we use perforated cylinder with fixed porosity rate =0.5 due to study for controlling wake region at the downstream by experimental method PIV and Numerical method.

ANSYS software was used to simulate the effect of placement of the perforated cylinder around the solid cylinder. An average number of the total number of nodes, tetrahedra, pyramids, prism, and elements were 951479, 4809070, 0, 51040, 4860110 for the case of adding the perforated cylinder, to solve

the Navier-Stokes momentum and continuity equations and the mesh-independence criteria achieved with error less than or equal to 10e-04 double precision. The fluid (water) was considered Newtonian. The flow was transient with 0.01 seconds time steps. Parameters were assessed based on the time-averaged fashion. In this study, all experiments have been performed in a large-scale water channel at the Fluid Mechanics Laboratory at cokurova University. In order to establish the correctness and accuracy of the measurement method for the flow structure around the cylinder, firstly the solid circular cylinder was examined at Reynolds 750 1000 1250 1500 1750 2000. also, it was analysed at Reynolds 150 and1500 numerically. Particle Image Velocimetry (PIV) method, which is a non-intrusive flow measurement method, was carry out to have quantitative results about the flow characteristics. at the PIV method, the floating particles movement of flow measured which can be clearly seen with the help of a pulsed laser source at a specific and limited time. In these experiments analysed the behaviour of the fluid flow behind a solid cylinder with a diameter of 10 mm also Perforated cylinder with diameter of 20 mm, was located as a outer cylinder with inner solid cylinder concentrically. In order to investigate the flow controlling by decreasing Drag forces with using perforated cylinder, various Reynolds number was calculated based on solid cylinder diameter with free stream velocity that changes during of experiments (Re=750v1000v1250v1500v1750 and 2000) and numerical studies (Re=150,250,350,500,1000,1250,1500,2000). Porosity rate value was fixed during all studies β =0.5. Totally this value has introduced as a most effective porosity rate at the previous studies due to provide a successful flow control performance at the wake region of behind cylinder, so it used on perforated cylinder all Reynolds numbers. according to investigate with PIV experiments and Numerical, some results were gained such as the time averaged streamlines $\langle\psi\rangle$, time average of velocity contours time averaged vorticity contours $\langle\omega\rangle$ and TKE contours. Based on the results shown, it can be concluded that the perforated cylinder has a tremendous effect on the flow structure. With the increase of the Reynolds number,

there is a visible decrease in the values of the drag coefficient and TKE and the size of the vortex area. Also, it can obvious clearly the effective controlling of the perforated cylinder on the vortex shedding of past region of the single cylinder .so, the location of the saddle point generated on the horizontal axis of the centre line of the cylinder has been reduced by 80% and pulled back, so it has been significantly reduced in the vortex shedding. It was shown that the deployment of perforated cylinder will eliminates the region of negative <u/U> contours behind the cylinder in both longitudinally (streamwise) and in traverse (spanwise) directions for all tested Reynolds numbers. In addition, the separation point angle value compared of the single cylinder has also improved, and although we expected to have 82 °, but it occurs at 90 ° to 120°, so this angle made to generate the back flow and the weak wake region in gap region. According to change of the separation angle after located the perforated cylinder and approaching the stokes flow state behind the cylinder reduces the drag coefficient and makes to eliminate the turbulence of the flow behind the cylinder or vortex shedding. This is a sign of shedding swept and disappeared by the jet-alike mechanism which helps preventing the well-known Karman Street. And the value of flow vorticity <ω> has decreased by 78% compared to the single cylinder. Thus, for this case, β= 0.5 and d/D =0.5 can be presumed as the most effective at all Reynlds Numbers in this study. In additional, these PIV results match up with Numerical results and this configuration can be regarded as successful to control the flow. the drag coefficient, $<C_d>$ of the cylinder is obtained with 20% and 22% lower than the bare cylinder case at Re=1000 and 2000, respectively.

In conclusion, the flow structure downstream of cylinder is significantly affect the drag coefficient, $<C_d>$ of the cylinder is obtained with 20% and 22% lower than the bare cylinder case at Re=1000 and 2000, respectively. the drag results and the PIV measurements are in close agreement with each other in the scope of this investigation. This reveal that the C_d can be effectively reduced by applying perforated shrouds cylinder.

GENİŞLETİLMİŞ ÖZET

Dairesel silindirin sualtı ve deniz yapılarının, köprü ve kulelerin mühendisliğinde, fiziki ve biyomekanik mühendisliğinde vb. yardımcı olması nedeniyle alanlarda yaygın olarak kullanıldığı göz önüne alındığında, etraflarındaki sıvı akışının davranışı ve değişiklikleri, yüksek doğrulukta incelemeler yapılmasını gerektirir. Tasarımlar sırasında cisimlerin etrafındaki sıvı akışının zararlı etkilerini ortadan kaldırarak ,yapıların ömrünü artırmak önemli bir konudur. Akışkan akışı silindirik veya dairesel bir nesnenin üzerinden geçtiğinde, blöf cisimlerinin etrafındaki kayma katmanlarında akışkan akışı ayrılma olayı meydana gelir. Bu akış ayrılması olgusu, silindirin aşağı akışında girdap oluşumunun ana nedenidir ve girdap dökülmesine neden olur ve bu da girdap kaynaklı titreşime (VIV) yol açar. Ayrıca iz yakın bölgesinde oluşan bu girdaplar nedeniyle girdap çiftinin etkileşimi blöf rüzgarları üzerinde zararlı ve yıkıcı etkilere sahip olabilir, bu nedenle yapıların etrafındaki sıvı akışının neden olduğu olumsuz etkilerin kontrol edilmesi son derece önemlidir. Son yüz yılda bilim adamlarının blöf nesnelerin etrafındaki akışın yapısı hakkında yaptığı çalışmalara dayanarak, genellikle pasif ve aktif kontrol teknikleri olarak iki temel kategoride sınıflandırılan birçok kontrol tekniği sunulmuştur. Kategorize edilen iki akış kontrol yönteminin her birinde, iyi özelliklere ve göreceli oluşumlara sahiptirler, ancak buna rağmen, pasif kontrol teknikleri, ekonomik ve kolay uygulanabilmeleri ve harici enerji girdisi gerektirmemeleri nedeniyle mühendislikte daha fazla tercih edilmektedir. Pasif kontrol tekniklerine göre, akış aşağısında iz bölgesini deneysel yöntem PIV ve Sayısal yöntemle kontrol etmek için yapılan çalışma nedeniyle sabit gözeneklilik oranı = 0,5 olan delikli silindir kullanıyoruz.

Delikli silindirin katı silindirin etrafına yerleştirilmesinin etkisini simüle etmek için ANSYS yazılımı kullanıldı. Navier-Stokes momentum ve süreklilik denklemlerini ve ağı çözmek için delikli silindirin eklenmesi durumunda toplam düğüm, tetrahedra, piramit, prizma ve eleman sayısının ortalama sayısı 951479,

4809070, 0, 51040, 4860110 idi. - 10e-04 çift kesinliğe eşit veya daha az hatayla elde edilen bağımsızlık kriterleri. Akışkan (su) Newtonian olarak kabul edildi. Akış, 0.01 saniyelik zaman adımlarıyla geçiciydi. Parametreler, zaman ortalamalı moda göre değerlendirildi. Bu çalışmada, tüm deneyler Cokurova Üniversitesi Akışkanlar Mekaniği Laboratuvarı'nda büyük ölçekli bir su kanalında gerçekleştirilmiştir. Silindir etrafındaki akış yapısı için ölçüm yönteminin doğruluğunu ve doğruluğunu tespit etmek için öncelikle dolu dairesel silindir Reynolds 750 1000 1250 1500 1750 2000'de incelenmiştir. ayrıca Reynolds 150 ve 1500'de sayısal olarak analiz edilmiştir. ayrıca Reynolds 150 ve 1500'de sayısal olarak analiz edilmiştir. Kesintisiz bir akış ölçüm yöntemi olan Parçacık Görüntülü Hız (PIV) yöntemi, akış özellikleri hakkında nicel sonuçlar elde etmek için gerçekleştirilmiştir. Kesintisiz bir akış ölçüm yöntemi olan Parçacık Görüntülü Hız (PIV) yöntemi, akış özellikleri hakkında nicel sonuçlar elde etmek için gerçekleştirilmiştir. PIV yönteminde, belirli ve sınırlı bir zamanda darbeli bir lazer kaynağı yardımıyla açıkça görülebilen, akışın yüzen parçacıkların hareketi ölçülür. Bu deneylerde, 10 mm çapında katı bir silindirin arkasındaki sıvı akışının davranışını da analiz eden 20 mm çapında delikli silindir, iç katı silindir ile eş merkezli olarak yerleştirilmiş bir dış silindir olarak yerleştirildi. Düşük Reynolds sayılarında delikli silindir kullanarak Sürükleme kuvvetlerini azaltarak akış kontrolünü araştırmak amacıyla, deneyler (Re=750v1000v1250v1500v1750 ve 2000) ve sayısal çalışmalar (Re=750v1000v1250v1500v1750 ve 2000) sırasında katı silindir çapına dayalı olarak çeşitli Reynolds sayıları hesaplanmıştır. =150,250,350,500,1000,1250,1500,2000). gözeneklilik oranı değeri tüm çalışmalar sırasında sabitlendi β =0.5. Tamamen bu değer, silindir arkasının iz bölgesinde başarılı bir akış kontrol performansı sağladığı için önceki çalışmalarda en etkili gözeneklilik oranı olarak tanıtılmış, bu nedenle delikli silindirde tüm Reynolds numaralarını kullanmıştır. PIV deneyleri ve Sayısal ile yapılan araştırmaya göre, zaman ortalamalı akım çizgileri $<\psi>$, hız konturlarının zaman ortalaması, zaman ortalamalı girdap konturları $<\omega>$ ve TKE konturları gibi bazı sonuçlar elde edildi. Gösterilen sonuçlara dayanarak, delikli silindirin akış yapısı üzerinde muazzam bir etkiye sahip olduğu sonucuna varılabilir. Reynolds sayısının artmasıyla sürüklenme

katsayısı ve TKE değerlerinde ve girdap alanının boyutunda gözle görülür bir azalma vardır. Ayrıca, katı silindirin arka bölgesinin girdap dökülmesinde delikli silindir ile etkin akış kontrolünü açıkça görebilinir. Bu nedenle, silindirin eğri noktasinin mesafesinde 80 % azaltılmıştır ve geri çekilmistir i, bu nedenle girdap dökülmesinde önemli ölçüde azaltılmıştır. Delikli silindirin yerleştirilmesinin, test edilen tüm Reynolds sayıları için hem uzunlamasına (akış yönünde) hem de çapraz (açıklık yönünde) yönlerde silindirin arkasındaki negatif <u/U> kontur bölgesini ortadan yok olmasi gösterilmiştir. Ayrıca, Iki silindi arasindaki bölge de tek silindire göre ayırma noktası açısı değeri de iyileşmiştir ve 82° olmasını beklememize rağmen 90° ile 120° arasında gerçekleşme nedeniyle bu açı geri akış ve düşük iz oluşmasını sağlamistir . Delikli silindir yerleştirildikten sonra ayırma açısının değişmesine ve silindirin arkasındaki stokes akış durumuna yaklaşılması, sürtünme katsayısını azaltır ve silindir arkasındaki akışın türbülansını veya girdap dökülmesini ortadan kaldırmayı sağlar. Bu, ünlü Karman Sokağı'nı engellemeye yardımcı olan jet benzeri mekanizma tarafından süpürülen ve kaybolan bir dökülme belirtisidir. Ve akış vortisitesi <ω> değeri, tek silindire kıyasla %78 oranında azalmıştır. Dolayısıyla, bu durumda, β= 0,5 ve d/D = 0,5'in bu çalışmadaki tüm Reynlds Sayılarında en etkili olduğu varsayılabilir. Ek olarak, bu PIV sonuçları, Sayısal sonuçlarla eşleşir ve bu konfigürasyon, akışı kontrol etmede başarılı olarak kabul edilebilir. Silindirin sürtünme katsayısı $<C_d>$, Re=1000 ve 2000'de çıplak silindir kasasından sırasıyla %20 ve %22 daha düşük olarak elde edilir.

Sonuç olarak, silindirin akış aşağısındaki akış yapısının sürtünme katsayısını önemli ölçüde etkilediği, silindirin $<C_d>$'si, Re=1000 ve 2000'de çıplak silindir kasasına göre sırasıyla %20 ve %22 daha düşük olarak elde edilmiştir. Bu araştırma kapsamında sürüklenme sonuçları ve PIV ölçümleri birbiriyle yakın bir uyum içindedir. Bu, delikli örtü silindiri uygulanarak C_d ve buyuk olcude grdaplari ve karman caddesinin etkili bir şekilde azaltılabileceğini ortaya koymaktadır.

ACKNOWLEDGEMENT

I would like to express my deepest appreciation to my supervisor Prof. Dr. Hüseyin AKILLI Prof who continuously supported and his constructive suggestions during the planning and development of this research work Also, I would like to express my gratitude to Prof. Dr. Beşir Şahin for his support and encouragement.

I would like to thank Associate professor. Dr. Tahir DURHASAN and Research Assistant Sergen TÜMSE for their invaluable assistance during my experiments. I would also like to extend my thanks to Laboratory technician Sefa MERAL for their help in offering me the resources in running the program during my journey.

I would like to express my special thanks to my dear husband Ahmet GURBUZ who was with me during my PhD studies and giving me strength and moral with his presence.

And I would like to thank my cute little angels, my twin daughters; Duru and Derya that been very patient that they were my major motivation source in this difficult way.

For their great patience and support during my PhD study, my sincere thanks go to my dearest family. I express my deepest gratitude, especially to my dear mother and dear father, and to my sisters and brother who have continuously encouraged me along the way of my PhD studies.

CONTENTS **PAGE**

LIST OF TABLES **PAGE**

LIST OF FIGURES **PAGE**

LIST OF ABBREVIATONS

D	: Perforated Cylinder diameter
d	: Diameter of inner cylinder (Solid single cylinder)
H	: Depth of the water in the channel
ν	: Kinematic viscosity
β	: porosity value
h_L	: Laser sheet height
h_W	:Water level
Re	: Reynolds number
U	: Free stream velocity
$< u'u' >$	: Streamwise Reynolds normal stress
$< v'v' >$	: Transverse Reynolds normal stress
$< u'v' >$	: Reynolds shear stress
$< u >$	: Streamwise velocity
TKE	: Turbulent Kinetic Energy
Δt	: Time interval
S	: Saddle point
S_t	: Strouhal number
f	: Frequency
L_c	: Length of the cylinder
<ψ>	: Time averaged vorticity contours
<ω>	: Time averaged vorticity contours

1. INTRODUCTION

The fluid flow at the past of the circular cylinders have been extensively investigated because of its practical main in engineering and scientifical studies relevance in fluid mechanics like the marina engineering, platform pillars, pipelines and high-rise buildings on the engineering and physics fields, there is several systems and machines in mechanical, civil and naval engineering where circular bodies are used. examples of some machines and systems are like heat exchangers, chimneys, and sea offshore platforms. In scientific items, the fluid flow past of circular cylinders exhibit different importance physical cases, such as separation point, vortex shedding and turbulence in the wake, at relatively with low flow velocity circular shape flow is determined with a wide region of separated flow where is named as wake region that it includes different states of flow inconsistency. The famous flow instability is which cause to the regular generation and shedding of spanwise vortices, which are often well known as Karman vortices.

While the cylinders are categorized in proximity, the flow field and the forces affected with the cylinders are entirely various from those seen while they are isolated at the fluid flow. The impact of the attendance of other shapes in the fluid flow is named flow interference, and it is too important in aerodynamics and hydrodynamics systems an machines. Such as, in all the bodies and systems mentioned at this section it is usual to have circular cylindrical structures categories with each other.

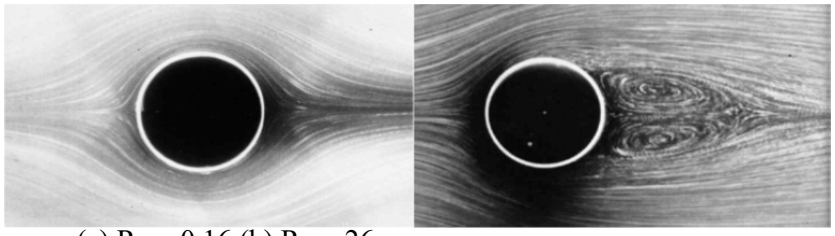

(a) Re = 0.16 (b) Re = 26

Figure 1.1. Visualization of low Reynolds number flows around a circular cylinder.(a) creeping flow, (b) steady symmetric separated flow. Flow is from left to right.Adapted from Van Dyke (1982).

The three-dimensional intricacy that these flows systems Couse them a considerable case of study by means of experimental and numerical investigations, the flow around of the circular cylinder or bluff bodies shapes that have achieved most of the attention during lasted last 50 years (see for instance the work by Zdravkovich, 1997). Due to this issue the vortex shedding controlling is a important case of numerical and experimental investigation.

1.1. APPLICATION

For most bodies and shapes which are at the versus of flow, there is a probability of generation fluctuations and vibrations whose are induced by the fluid flow. Phenomena associated are known as a flow induced vibration with fluid flow. These Phenomena related happen in many engineering fields, such as an example, it can be mentioned to design of structures and building such as bridges, electrical transmission lines, airplane wings, offshore plat forms, risers on oil pipes extraction, heat exchangers, pipelines, marine cables, and submarine components.

These uncontrolled vibrations can be a Couse of destruction to structures. One of the important reasons of generating vibrations in these bodies, due to occur flow separation and occurring vortex structures on the wake. The vortex shedding Couse to structures vibration with their fluctuating of aerodynamics forces on them. The group of vibrations induced by fluid flow wake region is known Vortex Induced Vibration (VIV), which the intrinsic parameter of this phenomena due to happen vortex shedding in downstream of bluff bodies.

Due to cylindrical bodies were used in most of building widely, investigation of fluid flow past bluff bodies and analyzed the forces on these shapes has a interesting subjects today. Therefore, in recent years and with Investment in improvement of measurement equipment related of fluid flow behavior in the other hand, also development of software's as ways for calculated and simulated of fluid, different studies has been carry outed on this filed. One of the most important fields, is Oil and Gas Extraction Risers from Sea depth. These Risers have

cylindrical structures, And the vibrations problems are the most challenge. Various methods to reduce and eliminate this vibration have been proposed by studying the flow around the circular bodies.

Figure 1.2. (a)Oil platform - (b) Oil and Gas extraction Risers

1.2. Flow around a Circular Cylinder

Investigation and understanding of the complex fluid flow past of bluff bodies have become indispensable due to its significance in engineering applications like marine structures, cables, platform pillars, floating wind turbines, towers, and tall structures. The flow structure around cylinder has been investigated for more than a century, starting with the fundamental work of Strouhal on the relationship between the frequency of vortex shedding, free-stream velocity, and cylinder diameter. Porter (2020) was done an experimental investigation using smoke visualization. Taneda (1956) conducted experiments in a towing tank and investigated wakes behind the cylinder and plates photographically for the Reynolds number between 0.1 to 2000. Zdravkovich (1998) studied the flow past a circular cylinder as a baseline case of more complex flows. In the In the widely studies with Zdravkovich (1997), three amperemeters of

the flow past a circular cylinder (and past a bluff shaps totaly) are cited: the boundary layer, the sepereation point, shear layers and the wake region (shown at figure 1.4). In the lace of roughness of body's surface and occlusion ffects, these interacting components under to the a transition systems to turbulent flow that in depended to only parameter of the fluid flow that called the Reynolds number, Re, that is indicated as review made by Zdravkovich(1997).

$$\mathrm{Re} = \frac{UD}{\nu}$$

by U is the velocity of fluid flow, D the cylinder diameter and v the kinematic viscosity of the fluid. Some process of this transition steps as Reynolds increases are mentioned in this part.

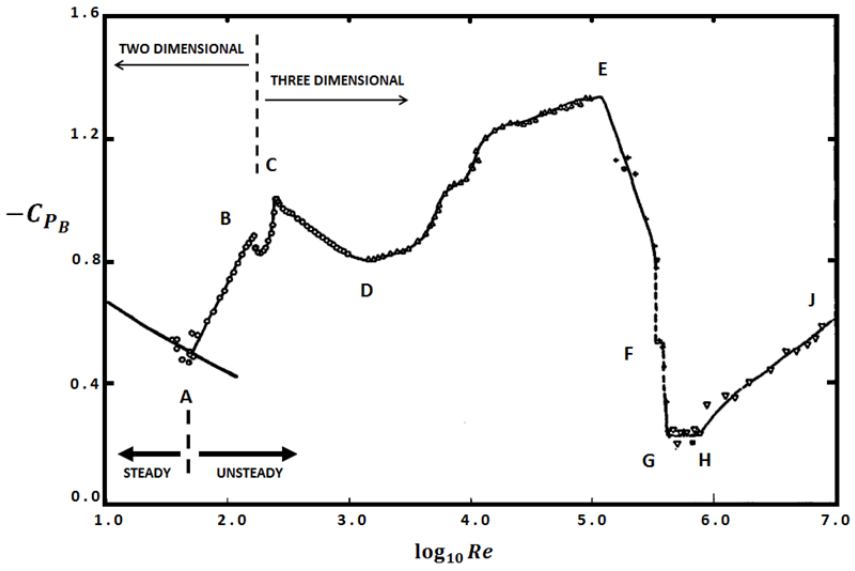

Figure 1.3. Classification of flow regimes according to the plot of base suction coefficients (CPB) over a large range of Reynolds numbers (Williamson, 1996)

The drag force is formed by surface friction and flow pressure. From Stokes flows (Re <<1) to fully turbulent flows (Re≈ 107) there are various flow regimes that can be categorized like bellow image (Figure1.4);

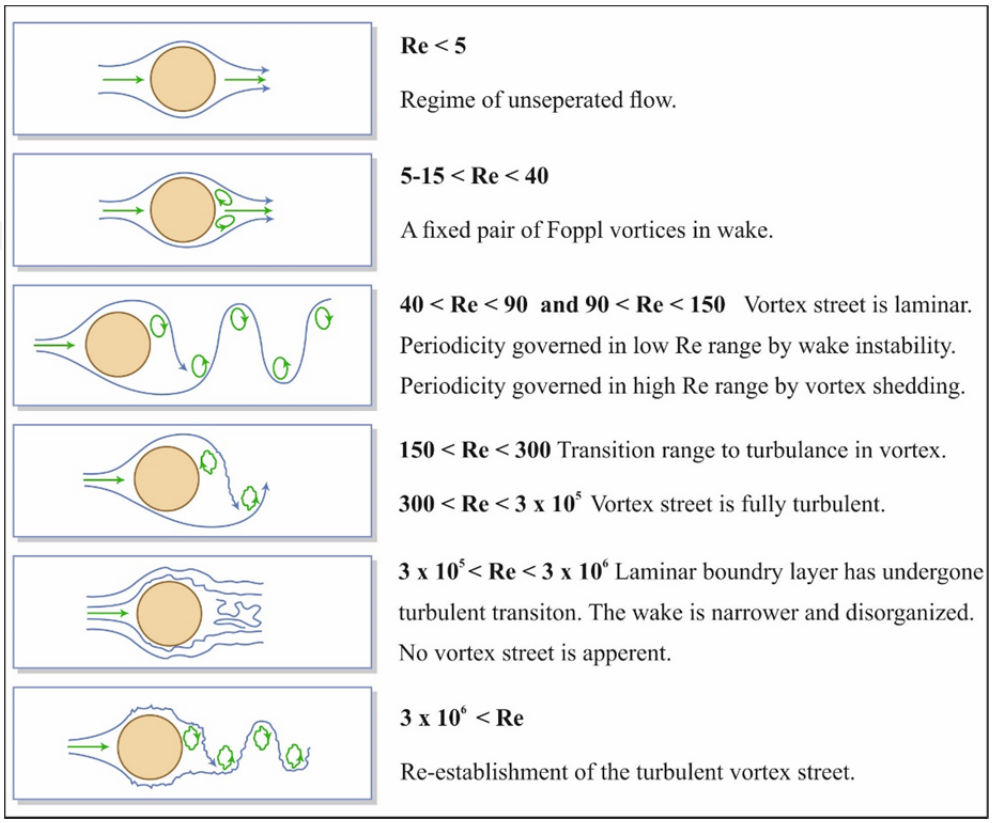

Figure 1.4. Flow regimes of circular cylinder depending on the Reynolds number (Lienhard, 1966 and Figure by MIT OCW.).

For Re < 5, the flow is steady and two-dimensional by just one separation point at the rear stagnation point. For the regime of 5 < Re <40, the fluid flow is steady yet also flow separates from the trailing edge of the cylinder. After that, stationary vortex pair (Figure 1.4) happen in the wake region that rotentional length grows as the Reynolds number increases.

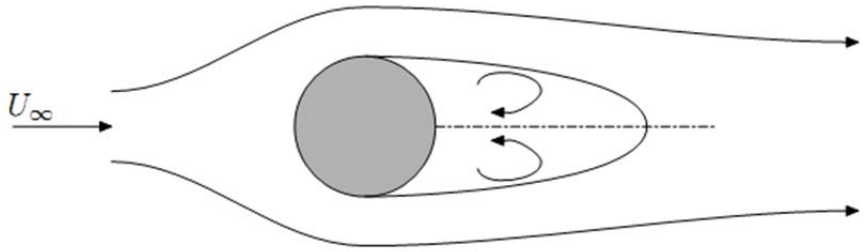

Figure 1.5 Schematic of Steady wake

At the important number (Re≈ 49), all the imposed location are starting held steady, inconsistency increases and vortex shedding generating on the past of the circular cylinder, addithinaly , it can be seen the well known von Karman vortex street. (Figure 1.3)

The mechanism of vortex shedding proposed by Gerrard (1964) was shown in Figure 1.6. The main cause of the generating vortex-street wake is interaction between the two separating shear layers up and down. A vortex, called as upper vortex, goes on to increase by feeding with circulation from its touched shear layer until it draws the opposing shear layer against the wake region. These drawn shear layer (greating bottom vortex) transports fluid with oppositely marked vorticity along by it and exterminates and cutting source of circulation to the upper vortex shedding that results in the shedding of the upper vortex. In the next turn, this lower vortex grows sufficiently, it would draw the upper shear layer along the wake region and a result of extirpation bottom vortex would be shed and transfers to downstream.

This cycle repeats and alternates vortex shedding from two side occurring a vortex street downstream of the body. Gerrrard's vortex-formation model observes that entrainment has a main impact to form a vortex street which is mentioned before. In Figure 1.6, Gerrard shows entrainment flows in vortex generation. At this model, entrained fluid "a" is pulled into the growing vortex while fluid "b" transfers into the developing shear layer. And some fluid "c" is go into the wake region that make to grow vortex shedding.

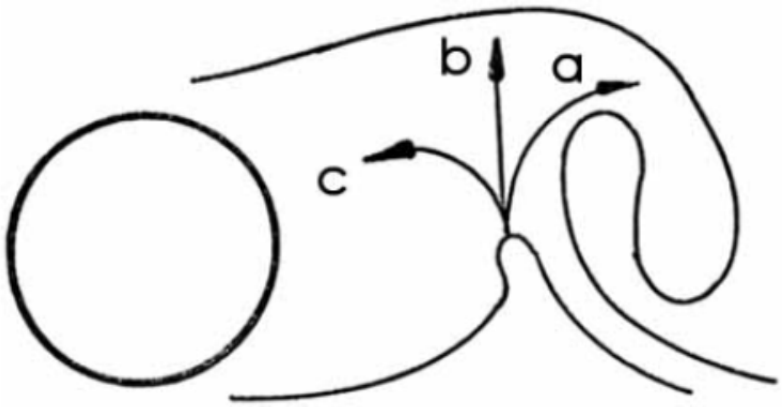

Figure 16. The vortex shedding mechanism by Gerrard (1964)

Between 40 < Reynolds number < 190 (Figure 1.4) the recirculation area growes instabilities whose strength and amplification grow with Re resulting in alternating high and low pressure area on the lee side of the body. As the instability of wake becomes amplified, the impacts of Reynolds stresses in the near wake region improve, the generation length shortens, the base suction increases consistently.

For 190 < Re < 260 (regime B-C: 3D wake transition regime), the wake first develops a secondary instability and intrinsic three dimensionality which seems in a regular spanwise structure in Williamson's (1988) flow visualization. In the kind of higher Reynolds values, i.e., Re > 200, the flow becomes three dimensional and turbulent.

For regime C-D (increasing disorder in the fine-scale three dimensionalities: 260 < Re < 1000), at Re = 260, the peak Reynolds stresses and a particular ordered 3-d streamwise vortex shedding behavior in the near wake ragion are effective on the base section. As Re is rised towards point D, three dimensionality began to be disordered. Therefor, decreasing in the two-dimensional Reynolds stresses, a consistent decreasing in base part and an increasing length of the generation region are observed.

In the shear layer transition regime (D-E: 103 < Re < 2x105), the base section and the 2-D Reynolds stresses increase, whereas the strouhal number and the formation length of the mean recirculation region decrease. And there is an increase in base suction and drag as the turbulent transition point in the separating shear layers moves upstream and Re increases. In addition, for this regime, it is thought that three dimentional structures on the scale of the shear layer vortices develop as well as three dimensionality on the scale of the Karman vortices.

Critical transition (E-G) regime is called “critical transition” in that base part and drag diminish significantly, because of a separation-reattachment bubble. This bubble revitalizes the boundary layer, and it transfers the final separation point further downstream on the cylinder to about 140°. This transition continues until point F. At this point, a separation- reattachment bubble typs on only one side of the body, causing a large avreage lift force (C_L= 1).

In the supercritical regime (G-H), the flow is symmetric ,too. With two separation-reattachment bubbles. A few of fluctuations are discovered in the wake at big Strouhal numbers of about 0.4. The Reynolds stresses of the boundary layer following the separation bubble are extremely greater and this makes the boundary layer to survive a larger adverse pressure gradient than at the around of cylinder critical regime, where transition finally exists before of separation occuring.

For regime H-J (Boundary-layer transition regime or post-critical regime), the boundary layer is fully turbulent, and the separation occurs further forward on the cylinder at about 100°, yielding higher drag and base section and a wider downstream wake than in the previous regime.

1.2.1. Flow Separation

The appearance of the fluid viscosity retardeds the fluid particles very close to the solid surface and takes shape like a thin fluid layer called a boundary layer. The flow velocity is zero at the surface because of the no-slip boundary condition.

According to the flow divulges to a powerful viscous force of flow strength, flow momentum is substantially goes to be lower around the boundary layer. due to of this reason the boundary layer flow is effective parameter to the external pressure difference that is the form of a pressure force effecting fluid particles around cylinder

In the state of flow that the pressure decreasing in line with the flow the pressure gradient is said to be favorable. In this state, the pressure force can help the fluid transfer and the fluid flow doesn't reduce velocity. But, when the pressure is increasing in the line of the flow, against the pressure difference condition as so it is called exist. Furthermore, the presence of a strong viscous force, the fluid particles must act against of the increasing pressure forces. As a conclusion the flow particles able to stop or reversed, due to the near particles to transfer far from of the surface. This occurrence is known the boundary layer separation phenomena. finally, when the velocity at the wall be zero or lower than zero and an peak point exists in the velocity profile so a positive pressure region or adverse pressure difference create in the flow directional flow separation point is revealed according to Figure 1.7 separation of flow has been seen

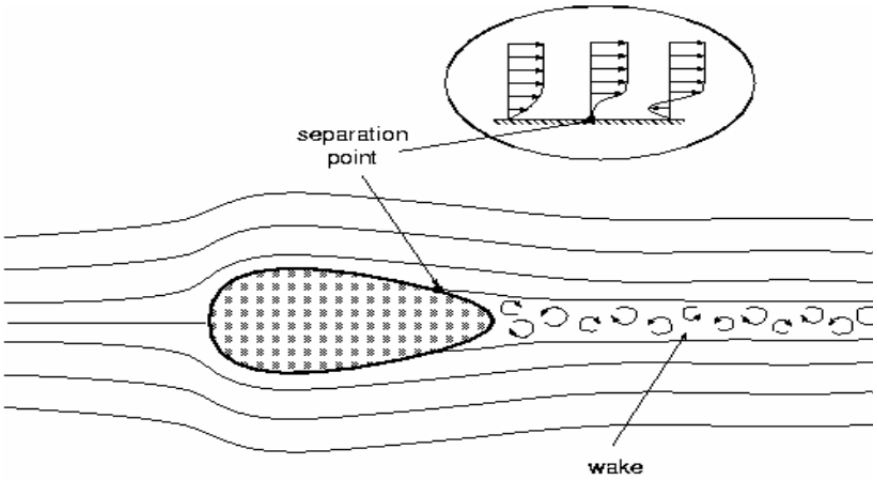

Figure 1.7. Flow Separation

1.3. Flow Control past a Circular Cylinders

Flow control may be applied to delay/advance transition, to suppress/enhance turbulence, or to prevent/promote separation depends on desired objectives. The resulting of flow over a cylinder may be the vortex induced vibration, the acoustic noise, the lock-in phenomenon and increasing lift and drag fluctuations, due to reasons in the previous section. to avoid or minimize these results, the flow control techniques have been studied since discovery of the boundary layer by Prandtl (1945). The flow control techniques base on the principle of modification of the geometry or the wake flow to change the behaviors of the boundary layer or free-shear layers. The flow control techniques can be divided into two categories name as active and passive flow control. The active flow controls need to external energy whereas the passive flow controls. Therefore, the passive flow control techniques are more applicable than the active flow control techniques. A comprehensive study on the classification of the flow control techniques was performed by Gad-el-Hak (2000) .

1.3.1. Passive Flow Control

The passive flow controlling process are extended applied since they have like benefits that can make easier their implementation, lower cost and more resistant. Zdravkovich (1981) categorized the passive flow controlling methods in to three group in according to vortex shedding as surface roughness, shrouds, and near-wake stabilizers. He also was performed another group in according to with flow direction as omnidirectional and unidirectional. The omnidirectional mean is effective irrespective of the flow direction when the unidirectional means to effective only direction of flow.

1.3.1.1 Surface Protrusion

Separation lines and or separated shear surfaces are as the surface protrusions that can be impact to flow fluid. The helical protrusions have been wildly carrying out in the application of offshore plat form of see engineering and industrial chimneys instruction as shown figure 1.5. The helical bumps are omnidirectional. Although the helical protrusions are considerably effective on the prevention of the vortex shedding induced vibration, they can make to increasing of the drag force. when helical bumps with rectangular cross -section are known as helical strakes, helical protrusions by cylindrical cross -section (wire) are known as helical wires. also, the surface prominences have been applied for the flow controlling such sawing wire, scaffold, and bump. explanatory sketches are shown in figure 1.8

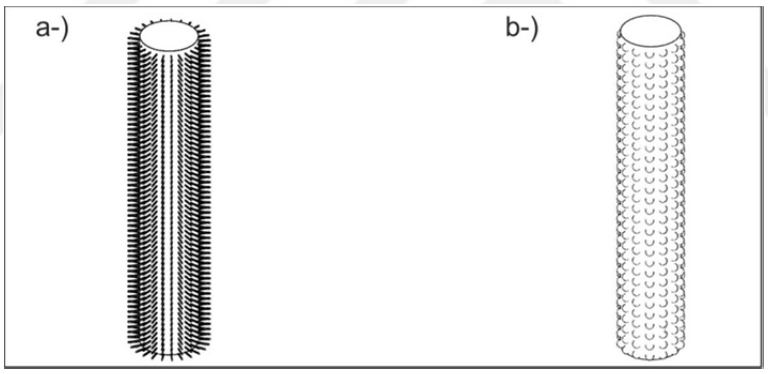

Figure 1.8. Schematic representation of surface protrusions; a) fin, b) bump

1.3.1.2 Shrouds

The shrouds area has an impact the bubbles area and then can be decreases the darg forces. The fairings carried out at the improvment opreation usually like cover in offshore, vessel and undersea. this kind of shrouds are the best method to lock up vortex induced vibration and, they dramatically make lower the drag forces. The shrourds can be all directinal or one way in regarding of needed. An

example of its application is obvioused in Figure 1.9. presentation of perforated area is another way to reduce the vortex shedding ragion around cylinder.

The perforated plate or cylinder desighend likea circular or rectangular. Usually, due to Figure 1.9 we obvious the perforated cylinder and the vertical slut monted on a bloff body. It fixed with very thin metal on cylinder which was kept the main cylinder with legs. The so significant benifit of the perforated area is that it able to deacreasing drag.

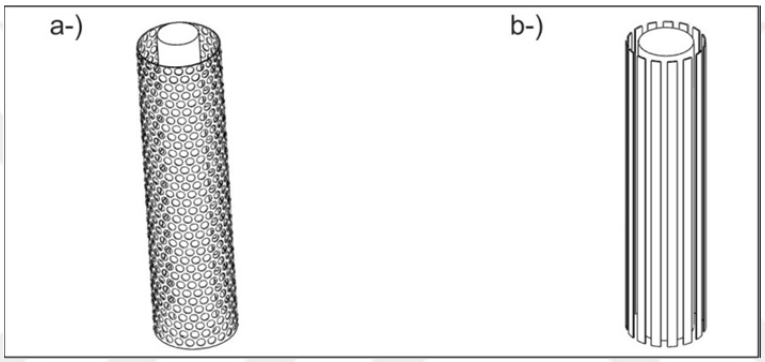

Figure 1.9. Schematic representation of shrouds; a) perforated cylinder, b) axial sluts

1.4. Present Study

The recently numerical investigations about flow behavior around of circular shapes were done on steady flows employing the flow function-vortex generation and finite gradiant dissocation method These numerical investigations include the studies of Thom (1933) Kawaguti (1953) and Apelt (2021) at Re =40 and 44 which show an approximate linear growthing of the vortex shedding with the changies of Reynolds number.

S. Behara and S. Mittala (2010) numerically investigated yawed shedding at the laminar flow around a numericaly two-dimensional circular cylinder by a stabilized finite element method. Sen et al. (2009) studied an extensive research of flow past a circular cylinder at low Reynolds numbers by a stabilized finite element

method, deployment of two methods of boundary layers conditions, namely, the no slip condition and towing tank position. Wei et al. (2016) carried out the struchers of aerodynamic loads applied on two cylinders at a low Reynolds number =100 with using finite volume discretization method. Valencia (2019) discloses the fluctuating impact results of direct numerical simulation of fluid flow around a circular cylinder under the efficacy of an imapact of KC = 7, 9 and Reynold numbers of Re= 40, 100, 150, 200, 250, 300, 500 and 1000. In the study of B. Molin (1993) asymptotic theoretical methods was crried out to show vortex shedding induced drag force by minimaized of the geometric factores, like the cylinder gap, the open ragion ratio, and the kinde of of the openings, and showed that vortex induced vibration (VIV) could be deacrese with fitting perforated skin, but in this model the drag of cylinder growth to high.

Furthermore, vortex shedding around past of circulars cylinders is a main couse of VIV twhich if notgood controled make to great damage onthe shaps.

To decreas or delet the harmful impacts of vortex shedding there are two ways can be done: active and passive thechnics. while the active method require energy source, passive flow control thechnics took high attention for controlling the vortex flow around cylindrical shaps in dealy investigation, like perforated cylinders E. Pinar, (2015), helical wires or strakes A. Ekmekci, (2002)-T. Durhasan (2018), and helical strake (2017) H. Akilli et al. splitter plate (2005),(2013)small rod S.-J. Lee, S.-I. Lee (2004),(2011) (2011) roughness elements A. Kahraman (2002) and O-ring H. Lim and S.-J. Lee, (2004) hollow cylinders (2017) rotating vortex control cylinders (2017). To reduce or delet VIV behinde of circular cylinder and elimneat the drag force effect at subcritical Reynolds numbers by diffrence factors, the foil couples were applied in the study of Galvao et al. (2008) Najafi et al (2016) studied on timeaveraged nearwake of a cylinder with yaw angles from 0° to 45° by 5° steps at a Reynolds number Re=5000 based on the cylinder diameter. As yaw angle increased, the counter-

rotating vortices in the near-wake of the cylinder detached, moved to downstream and disappeared, due to increase in the streamwise velocity.

Therefore, the value of the normalized timeaveraged wakes vorticity, decreased more ever the drag coefficient. as a result, the highly turbulent flow domain past of the yawed cylinder was whashed and went toward of downstream. Durhasan (2018) generaly studied the flow behavior of perforated circular cylinders with doing the technique of high image density Particle pictures Velocimetry (PIV) at the fixe and highe Reynolds number Re = 10,000 with the cylinder diameter (D = 100 mm. In this investigation the impact of diffrence porosity ratio, β on the flow struchers of cylinder's vorticity analized by the porosity ratio from 0.25 to β 0.80 and it was showed that the increasing the porosity ratio, β, is elonged with decreasing of turbulent fluctuations at the vortex shedding region on the cylinder.

There are some investigations in regards to the crry out of splitter plate like an impressive passive flow control method further more with using the perforated cylinders.hereof, Akilli et al. (2005) studied the impactof attached splitter plate on the flow of circular cylinder with variouse lengths at the shallow water. In this experimental investigation, the length of the splitter plates were normalized by the diameter of the circular cylinder, and it was tried to discover the most impactful ratio of splitter plate length L to circular cylinder diameter, d. They showed that while the ratio of the length of the splitter plate on the circular cylinder diameter was higher than L/d = 1.2, shedding of large vortices were deleted without pay attantion of the thickness of the plate. in the other handr similar sresearch was crried out by Gozmen. (2013) with changing the ratio of splitter plate length, L on the circular cylinder diameter, d to show the change of flow behaviourson the downstream of the circular cylinder, in additional the ratio of the plate height to the water height was variused to minimized the facores of the control method. Molin (2011) obvioused a hydrodynamic model of perforated or slotted body and obvioused which the perforating shaps of marine or offshore bodies can be an

efficient means for decreasing inertia force and disarrange forces, and for growth up of the damping of aggractive responses. His suggest was tocarry experimental investigation to clear the drag coefficient and water inlet of procity shape arrangements compleatly.

Akilli et al. (2005) investigetd the flow struchers behinde of vertical circular cylinder located in shallow water and with contolling the vortical flow behavior by applayment of splitter plate inserted at diffrent positions. They determined that the splitter plates have a dramaticaly impact on disappearing of the vortex shedding for the gap ratio from 0 to 0.75 d.

Pinar et al. (2015) has determaind which the passive flow control method the helping of perforated cylinders have a dramaticaly effect on the unsteady flow behavior on the downstream of the circular cylinder. by increasing the diametr's of holes on tge perforated cylinder, the vortices generated on the top and bottom shear layers are longed near the stream direction with reducing their magnitudes compared to the single cylinder sample. in additional, they obviosed that the distance of porosity ratio from 0.4 to 0.8 is very impactful for the effective suppress of Karman Vortex Street there for that the drag coefficient on the circular cylinder diluted.

Durhasan et al. (2016) searched the impact of perforated circular cylinders on the flow characteristics around a cylinder of d=50 mm diameter in downstream direction with different porosity ratios and arc angles with usage of the Particle Image Velocimetry (PIV) technique. They revealed that the most impactful suppression of vortex street located at porosity ratio of $\beta = 0.5$ becouse of the decreased effect of shear layers and make weak momentum transfer to wake region.

To the results measured with PIV experments, it was showed that focouse of general kinetic energy (TKE) along the shear layer reduced, and wake generation of the cylinder longed by the tendance of perforated surface. additionaly, the vortex shedding frequency reduced down to 50% with usage of a

perforated surface by a = 180 arc angle compared to the single cylinder sample. They atlast obviosed how with using of a perforated surface can suppress the vortex shedding behind downstream onthe circular cylinder and be another way through widerange passive control methods in both practical and theoretical situations. Durhasan et al. (2019) investgated that the wake flow region around the circular cylinder can be impactful controlled with helping various porosity formations becouse of the limitation of flow rate.

Load measurements were also carried out in the wind tunnel to do the impact of shroud on the drag coefficient on bihind of circular cylinder. It was discoverd that the drag coefficient on the cylinders dicreased considearbly in sample of shrouds compared to that include from the bare cylinder sample. Yaqing Jin (2020) studythe complex fluid–structure interaction of perforated bodies with diffrance degrees of porosity.

According to scientific literature a great vale of work about flow behavior of perforated circular cylinders past of a solid cylinder has been carry out with higher Reynolds numbers (e.g. H. Akilli (2015) 2018), (2017))in order to these investigtaion, with increasing of porosity, βeta , the flow wake are substantially decreased in the wake region due to the PIV measurment E.PINAR (2017) with utilize the perforated circular cylinder, the magnitude of turbulent images has been weaked to a significant, extent in comparison with single cylinder's results T. Durhasan (2018) it was observed that concentration of TKE along the shear layer decreased and wake generation of the cylinder longes by the presence of perforated surface. The most impacted suppression of vortex street was seen for β = 0.5 and 0.6 sampels depended to on weakened shearlayers.

In this study, it was aimed to investigate the flow structures downstream of a solid cylinder after perforated cylinder placement in deep water based on a fixed porosity (β =0.5) for the Reynolds numbers between 750 and 2000 with the help of a combination of numerical simulations and the Particle Image Velocimetry (PIV) technique.

2. PRELIMINARY WORK

2.1. Flow around a Cylinder

Cylinder same behavior can be discovered both alone and in categories in the designs for heat exchangers, cooling systems for nuclear power plants, offshore construction, buildings, chimneys, power lines, struts, grids, screens, and cables, in both air and water flow. In many of these industerial applications, Karman vortex shedding is accountable for difficulty by flow induced vibration and noise. A full realization of the fluid dynamics of the flow behinde a circular cylinder includes some mainly isusses as the boundary layer, separation point, the free shear layer, the wake ragion, and the dynamics of vortex sheding.

2.2. Flow Control Techniques

Flow control investigations have been carrying out from Prandtl (1904) found the boundary layer. They utilized steady state ways and mechanisms of flow control. Some of main scientists like Bearman (1984, 2011), Sarpkaya (2004) and Williamson and Govardhan (2004) have more over emphasization importance of vortex shedding eliminated on downstream of a 2D bluff shape like circular cylinder. More detailed researches were carried out by Lachman (1961) and Gad-el Hak (2000) . last recently, same studies were done by Choi et al. (2008) , Kumar et al. (2008) and Rashidi et. al. (2016) . Choi et al. (2008) make shorter the active and passive control methods in his research. He, also, determinde the impact of Reynolds number to control drag and control 's randoman. A same investigate was done by Oruc (2017) on the passive and active flow control methodes for bluff shaps.

2.2.1. Passive flow control

A completly study on the passive flow control method was shown by Zdravkovich (1981). He categoried the passive flow control ways in to three

classes according to factual systems of vortex shedding as skin protrusions, shrouds and near wake stabilizers. A study of drag decreasing method and cover modification ways were carried out by Bandyopadhya impacts of cover modifications on turbulent boundary layers. Another simillar study by Kumar et al. (2008) obviused only passive control ways. The rstudy showed that patented passive control systems are utilized for practical applications like marine deepwater environments.

2.2.1.1 Surface Protrusion

Ahmed and Bays Muchmore (1992) studied flow behind of the wavy cylinder as expermentally. They mettioned that in spite of symmetrical geometry, asymmetrical flow behaviour is greated. Their results also determined that the partial drag coefficients at the geometric nodes are more than at the geometric saddle point.

Nebres and Batill (1993) were carried out experimental review in wind tunnel to study the impact of the single perturbation on the flow structuers of circular cylinder. They showed that Strouhal number is affected remarkably by disturbance angular location, disturbance size and Reynolds number.

Lee and Kim (1997) carried out the experimental investigate to disclose the flow structure on the downstream of a circular cylinder with helically wrapped three small wiresby diffrent steps of pitch. They determined that the surface protrusions notably impacted the wake generation of the cylinder. The vortex generation region elongated and the vortex shedding frequency and spanwise elongated compared to the single cylinder.

Owen et al. (2001) experimentally investigated that the impact of simple geometry repairof a circular cylinder on the drag and vortex shedding induced vibration reducing. They gain to vortex shedding elimination and drag reducing up to 47 percent for the blof body by a wavy axis. They also mentioned that the

cylinder by bumps make decreased drag and vortex shedding up to 25 percent compared to the circular cylinder model.

Bearman and Brankovic (2004) studied the vortex shedding induced vibration of a circular cylinder and with utilize the skin protrusion tools: strakes and bumps at the Reynolds number from of 103 to 104. They beholded that the usual vortex shedding in the wakes of fixed cylinders with strakes or bumps become visible a little. however, the amplitudes of vibration were discoverd, they are lower than field cylinder.

Lim and Lee (2004) show that using of Orings decrease the role of the drag coefficienton the cylinder. They were done out experiments for diffrent compositions of pitch distance at Reynolds numbers in the limit from Re = 78×102 to120×103. It is cleared that the maximum drag decreasing value of about 9% compared with the single cylinder was obtained at Re = 12×104, the cylinder coverd by O rings of d = 0.0167D in a pitch spaceing of 0.165D. however the vortex shedding frequencies of the Oring cylinders are near to that of the smooth cylinder up to a Reynolds number of 32×103, the vortex shedding alternation rise and looke the vortex shedding almost eliminate at high Reynolds numbers.

Lam et al. (2004) performed and experimental studies to measure the velocity counturs of the wake downstream of a wavely cylinder in the range of Re=3×103 to 9×103 with utulize a Laser Doppler Velocimetry (LDV) method. They concluded that the long vortex generation length of wavy cylinder should makes the drag reducing and eliminate of vortex that led to vibration.

Nakamura and Igarashi (2008) invesigated decreasing of the drag and lift forces on the circular cylinderby fitting cylindrical rings along the span of a cylinder at an distance of diffrent diameters at Reynolds numbers in the range of Re = 3×103 and 38×103. They noted that the drag force of the cylinder with fitting cylindrical ring was less than for the 2d cylinder, although the projected area of the cylinder with attaching cylindrical ring was higher than the 2d cylinder. They obviused that maximum reducing of drag force was received by 15% for the rate of

D/d = 1.3, W/d = 1.0, and P/d = 6 at Re=30×103, where D is the ring diameter, W is the spanwise width of the ring, and P is the spanwise step of the ring.

Zou and Lin (2009) performed the numerical studing of cross flow behinde a wavy cylinder at Re = 3×103 with present the load cell measurement for the confirmation. In the research, they present the load cell evulation for the validation experment, and they compared the avrage flow field and the around wake ragion behavior of the wavy sinusoidal cylinder by the circular cylinder at the similar Reynolds number. They discoverd that the avrage drag coefficient for the wavy cylinder is decreased becouse of the generation of a longer wake vortex ragion created by the wavy cylinder. The fluctuating lift coefficient of the sinusoidal wavy cylinder is remarlbly decreased, too. In this investigatin, they also obviused that such free shear layers only roll up into ripe vortices at far from of downstream location and notably change thearound of wake behaviour and the pressure distributions counturs behinde of the wavy cylinder.

Kiu et al. (2011) managed the experimental investigation to reveal the impacts of uniform skin roughness on vortex induced vibration of circular cylinders representation of offshore spar platforms at the range of subcritical Reynolds numbers. They determined that the roughness of cylinder is rised the Strouhal number, however drag coefficient decreased when compare with the smooth circular cylinder.

Gao et al. (2015) analysed the impacts of surface roughness on the vortex shedding with vibration (VIV) respond of a flexible cylinder. Their measurments detected that the surface roughness notably impacts on the VIV response and displacment respond reducing and the vortex shedding frequency rise up with increasing surface roughness. Thay were discoverd that lock in region of rough cylinder is thin than a smooth cylinder.

Recently, Zhou et al. (2015) were investigated byto compare flow structure of those cylinders about flow behinde of the smooth, grooved, and dimpled cylinders. Their measurments results obviused that the stability of vertex shedding

of the chanalleand the dimpled cylinders went to weaker and drag of those cylinders is less than the smooth cylinder. Wang et al. (2015) used a water drop model fairing for controlling the wake ragion and suppressing Karman vortex street generation on downstream of a circular cylinder with using CFD method. The fairing elements evidently decreased the drag and lift forces as well as influenced the frequency of vortex shedding compared to the single cylinder.

Ozkan et al. (2017) investigated the impact of fitted permeable plates on the eliminate of the vortex shedding from a circular cylinder. They showed that with using of a permeable plate notably repress the vortex shedding downstream of the circular cylinder for the porosity rate value of β=0.4 and 0.5 with the plate angle in the range of $35o \leq \theta \leq 90o$

2.2.1.2. Shrouds

First timethe experimental research with using of shroud cylinder as passive flow control methods was carried out by Price (1956) . He examined diffrent porous shrouds to study their impacts on suppression of the vortex- excited vibrations. He indicated that the vortex excited vibrations are suppressed by shrouded cylinders becouse of the delay in generation the normal Karman Street.

Zdravkovic and Soutworth (1973) sudied that the impact of shroud eccentricity on elimination of flow induced vibrations. Their results revealed that an eccentricity in any way and of any magnitude always decreased the amplitude of vibration subcritical wake region in comparison with that of a concentrically shrouded cylinder.

Every et al. (1982) performed the practical aspects of vortex excited structural vibrations around the marine surroundingby particular stress on methods of their suppression. also in the some part of this study, they focused on the impact of shrouds on the flow control, noted a general literature and faumase that shrouds with the optimum dimension gave a 50% decreasing in oscillations of a plain investigation on suppressing flow induced vibrations (Every and King, 1979)

Molin (1993) determined computational outcomes of how vortex induced vibrations being reduced with using shroud through sevral range of cylinder and shroud couples.

Boorsma et al. (2010) showed that perforated fairings could decreas noise of landing rib depends on the position of perforation and the porosity of fairing.

Zhao and Cheng (2010) indicated numerical studies due to investigate the impacts of porous media on the reducing of lift coefficient of circular cylinder. They review that the value of decreasing widely depends on the Reynolds number, the permeability.

Ozkan et al. (2012) carriedout permeable cylinders with various porosities to control the flow behavior of wake region of sevral circular cylinders owing to various diameter ratios. It was reported that shear layers on each side of the blunt body being lengthened along streamwise path as a proof of attenuation of organized vortex shedding street in their studies.

Ruck et al. (2012) studied the impact of porous coating on the drag Coefficient of cylinder. They indicated that the covering only on leeward side can decrease the drag forces. This can be conceived as a mixture of a smooth surface on the windward (smallest friction) and permeable wall layer on the leeward side.

Gozmen et al. (2014) carried out experimental research to flow control downstream of a circular cylinder with using permeable cylinder in deep water. Their PIV measurments results show that the permeable cylinder notably eliminates the vortex shedding downstream the cylinder with increasing porosity.

Flow past a semi-circular cylinder was studied numerically by Mimeau et al. (2014). They showed that introducing porous layers only at the upper and lower of the solid body permits to better manipulate the vortex and to receive relevant control performances.

Oruc et al. (2016) studied the impact of a drop shaped mesh on the suppress Karman vortex street generation in the near wake of the cylinder. It was observed that large scale vortical flow behaviour was not developed and the

maximum amounts of both turbulent kinetic energy and Reynolds shear stress distributions were strongly attenuated.

Durhasan et al. (2016) carried out the impact of the perforated semi circular fairing on the vortex street deleting by employing PIV technique in the shallow water,experimentally. They indicated that the elimination of vortex shedding street in the downstream is recieved for porosity of β= 0.6 and arc angle α=180o.

2.2.1.3 Near-wake Stabilizers

Roshko (1954) was espacially one of the first to show periodic vortex fgeneration suppression with using a circular cylinder attached with a splitter plate for a Reynolds number of 1.45×104. He also reported that,with positioning this splitter plate atsevral fixed distances in the full progressed cylinder wake, the Strouhal number St diminishes as the distance between the cylinder and the plate growth up to a limit situation (G □2.7D). He also performed that a splitter plate of chord 5D, fitted to the cylinder, results in suppression of vortex shedding. A plate of tendon 1d does not prevent of generation of vortices but changes the shedding frequency very light.

Roshko (1955) obviused flow behaviour at Re=1.45×104 when splitter plates were monted behind a cylinder. When the plate was fitted on the cylinder base and the long of the splitter plate, it was larger than 5D, the vortex shedding disappeared, and thus drag was significantly reduced. also, he also indicated flow struchers as the plate of l=d moved to downstream. When the splitter plate was taked palce on downstream less than 4d, the Strouhal number, St reduced, and themain pressure increased as the splitter plate moved on downstream. However, when the splitter plate was taken place farther downstream, the flow field did not show more variuse model the natural vortex shedding.

2.2.2. Experimentally Investigated for Flow Past of Bluff bodies

Flow around of bluff shaped in widely encountered in industrial applications, like cable suspension bridges, overhead cables, tow cables, chimney stacks, towers, offshore structures, etc.

How to complatley realize the complicated flow phenomena behind of cylindrical cable and which way to decrease their shapes drag and lift force are main subjects for engineering design. In basic study, flow around past circular cylinders have been extensively studied both methods of numerically and experimentally. Many important physical phenomena were indicated. For flow past a circular cylinder, Roshko (1954) determined flow regimes predicated on measurement of velocity counturs, spectra, and frequency for variouse Reynolds numbers. Gerrard (1966) presented the generation region of the vortices as seen Figure 1.6. He brings up the physical issues for two simultaneous paramiters of the shedding process. Further experimental investigations had been carried out by Shirakashi et al. (1984), Lourenco et al. (1992) and Hayashi and Kawamura (1995).

In the studies of B. Molin asymptotic theoretical research was performed to clear vortex induced drag with minimized of the geometric factores, such as the cylinder gap ragion, the open area ratio, and the shape of the openings, and showed that vortex induced vibration (VIV) could be decrease by attached perforated shrouds, but in this subject the drag of cylinder increased.

There are some studies related to the use of splitter plate as an effective passive flow control technique in addition to the use of perforated cylinders. In this regard, Akilli et al. (2017) investigated the effect of attached splitter plate to the circular cylinder with different lengths in shallow water. In this experimental study, the length of the splitter

Hsiao and Shyu (1991) studied experimental research to measure velocity and pressure distribution of circular cylinder under internal acoustic stimulation. Their results depicted that the internal acoustic excitation makes a growth in lift

and a notably decreasing in drag. (Active flow) Akilli et al.(2005) studied the flow structures around a vertical cylinder placed in shallow water and controlled the vortical flow behaviour by employing a splitter plate inserted at diffrent locations. They achived these results that the splitter plate has a substantial impact on suppression of the vortex shedding for the gap ratio from 0 and 0.75 d. Pinar et al. (2015) has noted that the passive flow control methods with the use of porosity cylinders has a remarkably effect on the unsteady flow behaviour on downstream of the cylinder. By increasing porosity rate, the vortices generated on the top and bottom shear layers are elongated along the flow path by losing their magnitudes compared to the single cylinder case.

further more they obviused that the distance of porosity ratio $0.4< \beta <0.8$ is very impactful for theeffective suppression of Karman Vortex Street therefor that the drag coefficient on the cylinder decreased. Durhasan et al. (2016) investigated the effect of perforated cylinders on the flow characteristics behind a cylinder of D=50 mm diameter in downstream path with various porosity ratios and arc angles with using the Particle Image Velocimetry (PIV) method. They revealed that the most impactful suppression of vortex street locates at porosity ratio of $\beta = 0.5$ becouse of the weakened shear layers and decrease momentum movment into wake region. Due to the results evaluated from expermental measurements, it was obvioused that concentration of total kinetic energy (TKE) along the shear layer reduced and wake generation of the cylinder elongated by the attendance of perforated surface. Additionaly, the vortex shedding frequency decreased down to 50% with utilize of a perforated surface with a = 180 arc angle compared to the single cylinder model. They also showed how using of a perforated surface can disappear the vortex shedding downstream of a circular cylinder and be an alternative way through wide range passive control methods in both practical and theoretical aspects.

Durhasan et al. (2019) stated that the wake flow region behind the cylinder can be effectively controlled by using different porosity configurations due to the

restriction of flow rate. Force measurements were also performed in the wind tunnel to reveal the effect of shroud on the drag coefficient of cylinder. It was found that the drag coefficient of the cylinders reduced significantly in case of shrouds compared to that obtained from the bare cylinder case. Yaqing Jin (2020) analysed the complex fluid–structure interaction of perforated bodies with various degrees of porosity.

To the best of authors knowledge, a great vale of work about flow behavior of perforated circular cylinders past of a solid cylinder has been carry out with higher Reynolds numbers (e.g. H. Akilli (2015) 2018), (2017))in order to these investigtaion, with increasing of porosity, βeta , the flow wake are substantially decreased in the wake region due to the PIV measurment E.PINAR (2017) with utilize the perforated circular cylinder, the magnitude of turbulent images has been weaked to a significant, extent in comparison with single cylinder's results T. Durhasan (2018) it was observed that concentration of TKE along the shear layer decreased and wake generation of the cylinder longes by the presence of perforated surface. The most impacted suppression of vortex street was seen for $\beta = 0.5$ and 0.6 sampels depended to on weakened shearlayers. Son et al. (2011) tested feedback control in order to suppress the vortex shedding of the circular cylinder. They discoverd that applying P, PI and PD controls to cylinder remarably decreased the avrage drag and lift vibrations.

Feng and Wang (2010) investigated on control of a flow behavior around a circular cylinder by blowing and suction. It located at the avrageof rear stagnation point and experiments were indicated in a water channel at Re=950. They reported that although the synthetic jet notabley affects the global flow field, it is still dominated by the large -scale coherent behavior.

In this study, it was aimed to investigate the flow structures downstream of a solid cylinder after located perforated cylinder in deep water based on a fixed porosity (β =0.5) for the Reynolds numbers between 150 to 2000 in numerical

study and 750 to 2000 in experimental, with the help of a combination of numerical simulations and the Particle Image Velocimetry (PIV) technique.

2.3. Numerical Investigated

2.3.1. Numerical Simulations for Flow Past of Bluff bodies

The early numerical simulations about flow behavior around bluff bodies were investigated on steady flows employing the stream function of the vorticity formolation and finite variouse discretization method. These numerical studies include the research of Thom (1993), Kawaguti (1953) and Apelt (1958) at Re =40 and 44 which performed an approch linear growth of the standing vortex couple by the Reynolds number

S. Behara and S. Mittala (2010) numerically studied skewed, vortex shedding in the laminar regime for the flow past a nominally two dimensional circular cylinder by a stabilized finite element method. Sen et al. (2009)studied an wide analysis of flow past a circular cylinder at low Reynolds numbers by a stabilized finite element way, employing two kinds of boundary layers conditions, namely, the no slip condition and towing tank condition. Wei et al. (2016) indicated the parameters of aerodynamic forces exerted on a twisted cylinder at a low Reynolds number of 100 using finite volume discretization method. Valencia 2(019) studied the oscillating impact results of direct numerical simulation of fluid flow around a cylinder under the effect of KC = 7, 9 and Reynold numbers of Re= 40, 100, 150, 200, 250, 300, 500 and 1000.

Kuo et al. (2007) numerically investigated the passive wake control downstream of a circular cylinder in uniform flow for Re ranging from 80 to 300. They utilize two small control cylinders, by diameter ratio d/D = 1/8, located at x/D = 0.5 and y/D = ±6 and Reynolds numbers is variouse from 80 to 300. Their mechanism, which can notably decrease the fluctuating lift force FL and the form drag force FD on the baise cylinder, is explored without completely suppressing the vortex shedding street for Re = 80to300. They obvioused that, by this control,

the vortex street downstream of the single cylinder is still maintained but the vibration of lift force FL and the form drag force FD on the main cylinder have a reduction monotonously with increasing the Reynolds number.

Kuo and Chen (2009) obvioused the wake flow behavior downstream of a circular cylinder manipulated with two small control cylinders and clarified the primary mechanism that leads to a deacreasing of the lift and the pressure drag on the single cylinder. They found that the fluctuating lift on the singlecylinder shows a 70 to 80% reduction without completely suppressing the vortex street.

A numerical work by Mittal and Raghuvanshi (2001) was carried out to study the influence of putting of a control cylinder in the near wake of the main cylinder for flows at low Reynolds numbers in the limite of $60 \leq Re \leq 100$. Results were compared by those from flow past a main cylinder at alike Reynolds numbers. It has been performed that the suitable location of the control cylinder resulted with a nearly complete suppression of the vortex shedding downstream of the single cylinder.

A numerical studies on the flow control downstream of perforated cylinder with using exerting an external magnetic field was carried out by Bovand et al. (2015). They indicated that the vortex shedding is elimineated notably with the external magnetic ragion for small Darcy number.

Zhang et al. (2010) investigate the numerical study to control the flow downstream of a cylinder employing alternative path implicid algorithm and Fast Fourier Transform. They undrestand that the total drag coefficient is reducing and oscillations of drag, and lift are suppressed notably.

Muddada and Patnaik (2010) numerically investigated the flow over a circular cylinder with the helpping of a control algorithm by utulize multiple feedback sensors and actuators at the subcritical Reynolds number. They demonstrated the impact of rotary kind actuators on the flow behaviours downstream of the circular cylinder.

3. MATERIAL AND METHOD

3.1. Experimental Setup

3.1.1. Water channel

Experiments were carried out in a large-scale water channel located in the Fluid Mechanics Laboratory at Çukurova University. The model of water channel is shown in Figure 3.1. The channel has the following dimensions: a length of 8,000 mm, width of 1,000 mm, and a depth of 750 mm.

The height of the water was kept constant at 650 mm during the experiments. The water channel test section is constructed of transparent Plexiglas with the thickness of 15 mm that interconnect with upstream and downstream fiberglass reservoirs. A honeycomb screen arrangement is placed at the entrance of contraction to regulate the flow and drop the turbulence intensity below 2%. The contraction area ratio of the water channel is 2:1. Before the experiments, freestream velocity that can be adjusted by centrifugal pump was calibrated by PIV software. The speed of the impeller can be controlled by an ABB variable frequency drive controller unit. Thus, desired freestream velocity can be obtained in the test section. The experiments were operated at the freestream velocity that corresponds to a Reynolds number of 750,1000,1250,1500 and 2000.

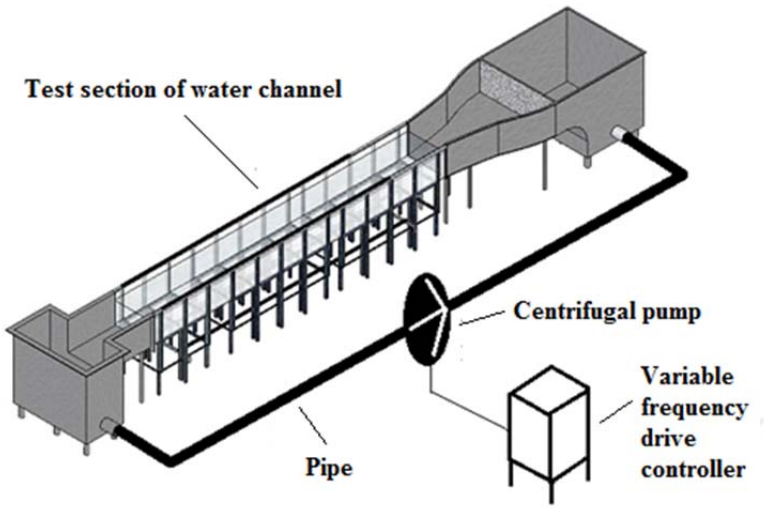

Figure 3.1. The scheme of water channel and main components

3.1.2. Particle image Velocimetry (PIV)

Particle image velocimetry technique is one of the most reliable methods for flow velocity measurement in modern fluid mechanics. It is based on the well known equation:

$$\text{Velocity} = \frac{\text{Distance}}{\text{Time Interval}} = \frac{\Delta x}{\Delta t} \tag{3.1}$$

PIV measures whole velocity fields by taking two images shortly after each other and calculating the distance individual particles travelled (Δx) within this time (Δt). From the known time difference and the measured displacement, the velocity is calculated (URL-1). PIV technique basically consists of two stages: image acquisition and image evaluation (Figure 3.2).

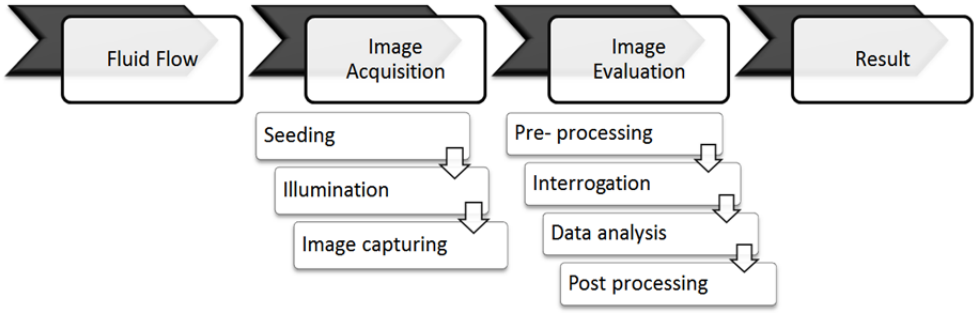

Figure 3.2. General PIV process

The first part of image acquisition is seeding the flow field by suitable seeding particles. Different types of seeding particle are used depending on the nature of the flow for PIV experiments. Seeding particles are added to the flow for tracing the velocity field by means of recording the particle images with a camera. Therefore, particles must remain suspended throughout an experiment. Silver coated hollow glass spheres (S-HGS) are borosilicate glass particles with a spherical shape, a smooth surface and 10 μm in diameter, preferred for the present liquid flow applications (Fig. 3.3). The thin silver coating further increases the reflectivity.

Figure 3.3. Seeding particle (URL-2)

The type of seeding particle is chosen to follow the flow and in order to detect their movement an area of the flow field is illuminated by a light-sheet. The light-sheet, which is generated by a laser and a system of optical components, is not continuous, but pulsed to produce a stroboscopic effect, freezing the movement of the seeding particles. In the experiments, the New Wave Research Solo 120 XT model double-pulsed Nd:YAG laser system was used (Fig 3.4). The laser sheet is adjusted to 8 mm in thickness. The time between the light pulses i.e. repetition rate is 15 Hz.

Figure 3.4. Laser head and power supply of the Nd:YAG laser system

In order to reveal the position of the illuminated seeding particles, a CCD-camera (Charge Coupled Device) is positioned at right angles to the light-sheet, and particle positions will see as light specks on a dark background on each camera frame. In experiments, the movement of particles was recorded by a FlowSense 2M CCD camera with a resolution of 1600 × 1200 pixels (Fig. 3.5). The camera was equipped with a Nikon AF Micro 60 f / 2.8D lens (Fig. 3.5). With the help of a synchronizer (Fig 3.6), the camera and the pulsing light-sheet are synchronized so that particle positions at the instant of light pulse number 1 are registered on frame 1 of the camera, and particle positions from pulse number 2 are on frame 2. The

camera lens images the target area onto the sensor array of a digital camera. The camera is able to capture each light pulse in separate image frames. Once a sequence of two light pulses is recorded, the images are divided into small subsections called interrogation areas (IA). The interrogation areas from each image frame, I_1 and I_2, are adaptive-correlated with each other, pixel by pixel. The correlation produces a signal peak, identifying the common particle displacement, Δx, and thus also the velocity (URL-3). DynamicStudio v3.20 software was used throughout the entire velocity measurements: from setting up the system, calibration, through the acquisition to the final data processing and presentation. Adaptive correlation method was used to process the images prior to 2D-velocity reconstruction with final interrogation area of 32 × 32 and overlap of IA with a value of 50%. A total of 7326 (99 × 74) velocity vectors were obtained for a instantaneous velocity field. Double frame mode was used for PIV operations and a total of 500 frames with 15 frame per second (fps) were obtained.

Figure 3.5. The camera and lens

Figure 3.6. The synchronizer

The number of particles in the flow is important to obtain a good signal peak in the adaptive-correlation. As a rule of thumb, 10 to 25 particles should be seen in each interrogation area. An accurate measure of the displacement, and thus also the velocity, is achieved with sub-pixel interpolation. A velocity vector map over the whole target area is obtained by repeating the adaptive-correlation for each interrogation area over the two image frames captured by the camera (Fig. 3.7).

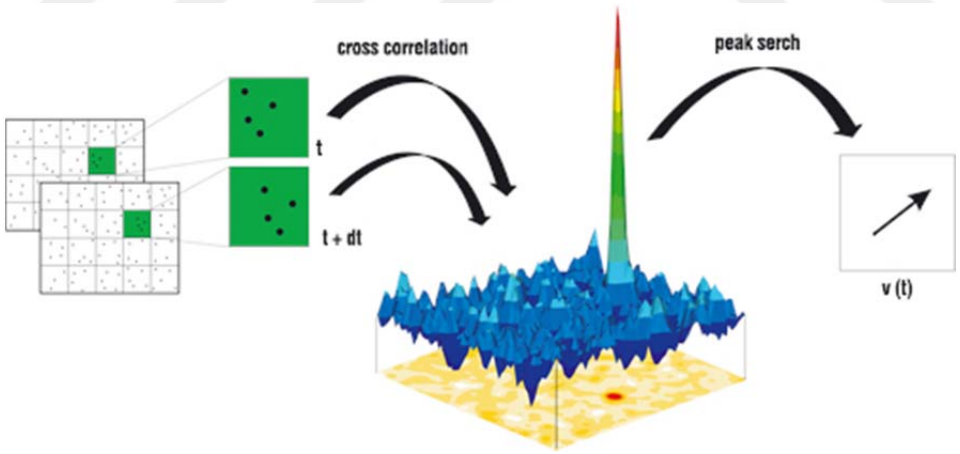

Figure 3.7. Velocity vector detection process (URL-4)

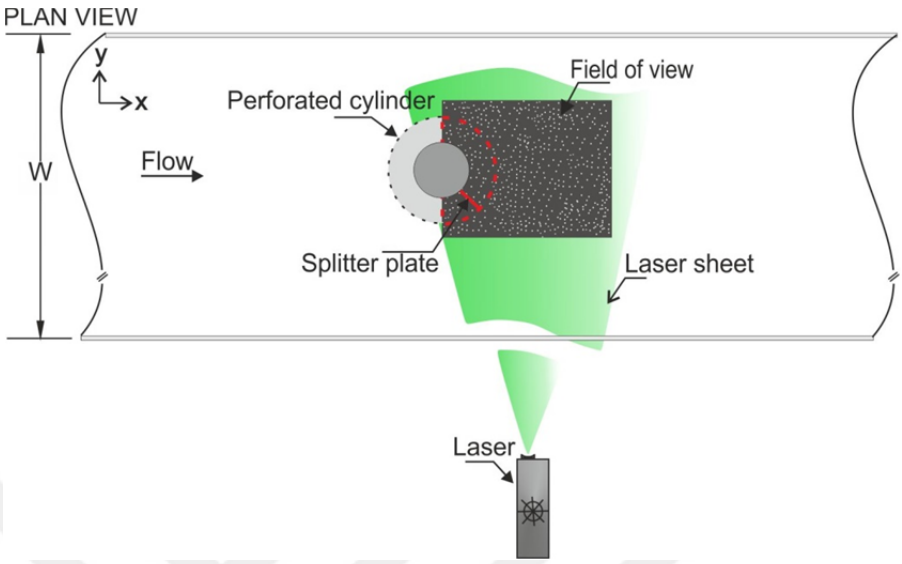

Figure 3.8. Schematic representation of PIV experimental setup.

Figure 3.11 shows schematic representation of plan view setup. The time interval between pulses was 1.75 ms for all experiments and the thickness of the laser sheet illuminating the measurement plane was approximately 2 mm. The time interval and the laser sheet thickness were selected such that the maximum number of particles in the interrogation window was obtained (With the help of a synchronizer, the time between the images to be taken and the laser pulses is synchronized, and the velocity vectors of the flow field were measured by comparing the particle movement between two consecutive images). The number of particles in an interrogation area was in between 20 and 25. The uncertainty in velocity relative to depth averaged velocity is about 2% in the present experiments. The water was seeded with approximately 10 μm diameter aluminum coated sphere particles. The instantaneous images were captured, recorded, and stored in order to obtain averaged-velocity vectors and other statistical properties of the flow field. Spurious velocity vectors (less than 3%) were removed using the local median-filter technique and replaced by using bilinear least squares fit technique between surrounding vectors. The velocity vector field was also smoothed to avoid dramatic

changes in the velocity field using the Gaussian smoothing technique. The vorticity value at each grid point was calculated from the circulation around the eight neighboring points.

3.1.3 Experimental Model

In this study, it was aimed to investigation of flow structure and control of flow in the near wake of cylinder by perforated cylinder. A circular cylinder (inner cylinder) which are made of Steel material was surrounded by the perforated cylinder which is constructed from perforated steel sheet which has 1 mm thickness and diameter value of hole d=2 mm. To prevent the interaction of vortices generated by inner cylinder. Schematic representations of experimental model are showed in Figure 3.9.

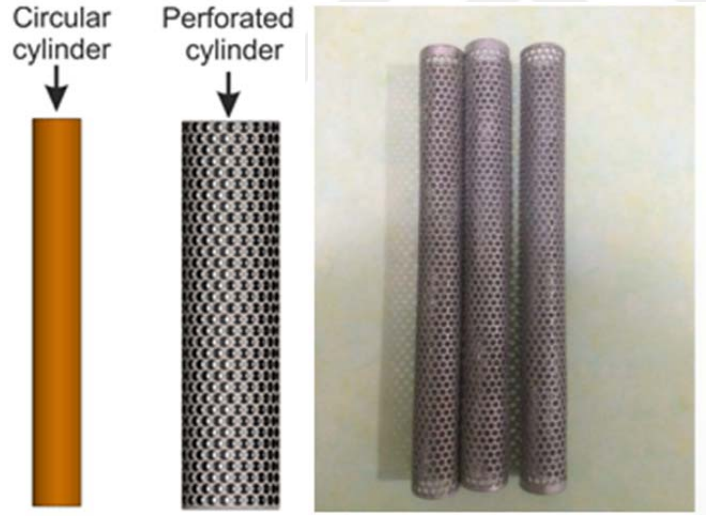

Figure 3.9. Schematic representations of experimental model.

3.1.4 Test models

Circular cylinder (inner cylinder) which are made of steel material was surrounded by the perforated cylinder which is constructed from perforated steel

sheet which has 1 mm thickness and diameter value of hole d=2 mm. Schematic representations of experimental model is showed in Figure Fig 3.10. Both centerlines of the test cylinders are coincided with the mid-plane of the test section that parallel to the side walls. The solid blockage ratio and the aspect ratio of the cylinders were, 5% and 12, respectively.

Measurements were performed in two individual planes as shown below (Fig. 3.11). The field of interest is 216 mm in length and 162 mm in wide. The plan view measurement plane was 300 mm higher than and parallel to the bottom wall.

Figure 3.10. The view of immersed test models

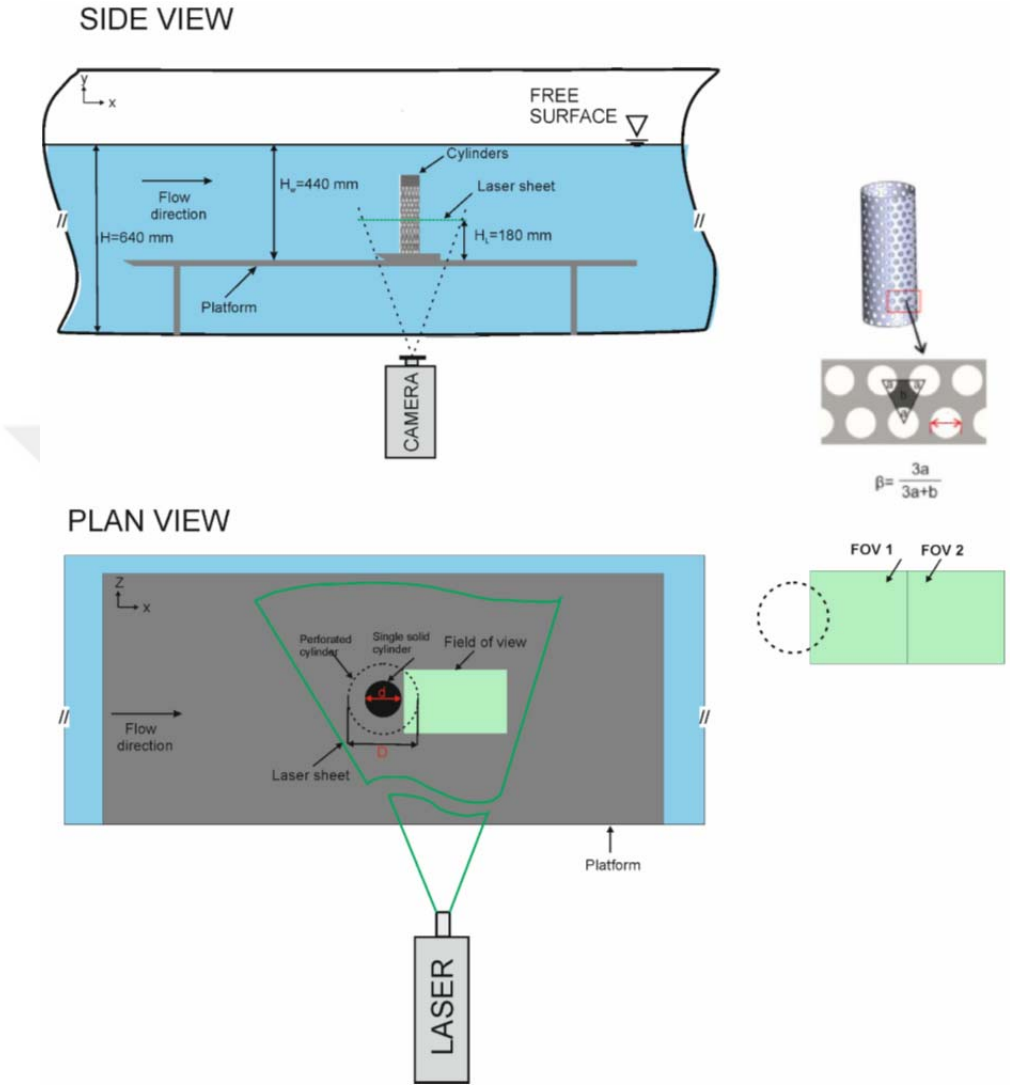

Figure 3.11. The view of immersed test models

3.1.5. Parameters

Firstly, in order to constitute reference experiments were performed for solid single cylinder (d=10 mm). Secondly, the effect of perforated cylinders on the flow control was investigated for six different Reynolds Numbers with fixed porosity (β= 0.5). β is defined as the ratio of the open gap area on the body to whole body surface area (Figure 4.1) . Diameter ratio is ratios of the diameter of

the inner cylinder, d to the diameter of the perforated cylinder D, That in the all expermental and Numerical investigation is d/D=0.5 in this study.

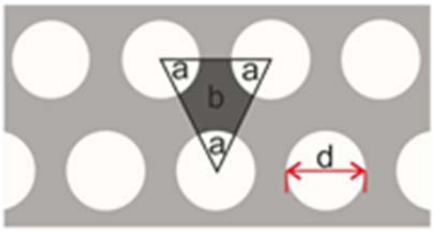

$$\beta = \frac{3a}{3a+b}$$

Figure 3. 12. Definition of porosity, β

3.1.6.Analysis performed has been listed as shown in the following table.

Table 3.1. Reynolds Numbers tested in the thesis

Experimental	x	x	x	x	750	1000	1250	1500	1750	2000
Numerical	150	250	350	500	x	1000	1250	1500	x	2000

3.2. Experimental Method

Throughout this study, three experimental systems were used in order to analyze the two-dimensional flow structure for a defined flow field. One of the systems used is the flow visualization and the other is the Particle Image Velocimetry (PIV) technique. Dye flow visualization experiments were performed to have a direct observation of the flow structure qualitatively in the investigated flow field whereas the PIV experiments was used to measure the velocity vector field which is one of the best non- intrusive techniques within the velocity measurement systems, quantitively. Finally, force measurement was performed to investigate effect of the current method on the drag coefficient of cylinder.

3.3. Numerical Simulation in CFX

3.3.1. Introduction

Computational fluid dynamics (CFD) is a branch of fluid mechanics that uses numerical methods and algorithms to solve and analyze problems that involve fluid flows. Computers are used to perform the calculations required to simulate the interaction of liquids and gases with surfaces defined by boundary conditions. With high-speed supercomputers, better solutions can be achieved. Ongoing research yields software that improves the accuracy and speed of complex simulation scenarios such as transonic or turbulent flows. Initial experimental validation of such software is performed using a wind tunnel with the final validation coming in full-scale testing, e.g. flight tests.

The fundamental basis of almost all CFD problems is the Navier–Stokes equations, which define any single-phase (gas or liquid, but not both) fluid flow. These equations can be simplified by removing terms describing viscous actions to yield the Euler equations. Further simplification, by removing terms describing vorticity yields the full potential equations. Finally, for small perturbations in subsonic and supersonic flows (not transonic or hypersonic) these equations can be linearized to yield the linearized potential equations.

Historically, methods were first developed to solve the Linearized potential equations. Two-dimensional (2D) methods, using conformal transformations of the flow about a cylinder to the flow about an airfoil were developed in the 1930s.

In the twentieth century, with computers' advent and their use in complex calculations science, CFD was born, and they were progressed with the development of computational power. Today, CFD is used as an accurate method for investigating and analysis of the various phenomena related with fluid flow, in industry.

3.3.2. Numerical evaluation

Flow past a cylinder has attracted the interest of many researchers in bluff body aero/hydrodynamics because, in practical applications, chimneys, lamp posts,

bridge supports, offshore structures, etc., have circular cross-section. In the present study, the fluid generally exhibits turbulent behavior due to the Reynolds number (Re = 150,250,350,500,1000,1250,1500 and 2000). Hence, flow was assumed fully turbulent. For the analysis of turbulent flows, the following items were considered:

1- Turbulent flows are completely unsteady. For their simulation, transient analysis should be selected.
2- Turbulent flows are three-dimensional completely. Therefore, the cylinder must be modeled in three-dimensions.
3- To enable the effects of turbulence to be predicted, a large amount of CFD research has concentrated on methods which make use of turbulence models. Advantages or disadvantages, computational cost and accuracy of results should be considered for choosing the appropriate model. In the present study, the k - ω based Shear-Stress-Transport (SST) model which is recommended for accurate boundary layer simulations was adopted.

3.3.3. Turbulence model

Turbulence consists of fluctuations in the flow field in time and space. It is a complex process, mainly because it is three dimensional, unsteady and consists of many scales. It can have a significant effect on the characteristics of the flow. Turbulence occurs when the inertia forces in the fluid become significant compared to viscous forces and is characterized by a high Reynolds Number.

In principle, the Navier-Stokes equations describe both laminar and turbulent flows without the need for additional information. However, turbulent flows at realistic Reynolds numbers span a large range of turbulent length and time scales and would generally involve length scales much smaller than the smallest finite volume mesh, which can be practically used in a numerical analysis. The Direct Numerical Simulation (DNS) of these flows would require computing power which is many orders of magnitude higher than available in the foreseeable future.

To enable the effects of turbulence to be predicted, a large amount of CFD research has concentrated on methods which make use of turbulence models. Turbulence models have been specifically developed to account for the effects of turbulence without recourse to a prohibitively fine mesh and direct numerical simulation. Most turbulence models are statistical turbulence model, as described below. The two exceptions to this in ANSYS CFX are the Large Eddy Simulation model and the Detached Eddy Simulation model.

3.3.3.1.The *k* - ω based SST model

One of the main problems in turbulence modeling is the accurate prediction of flow separation from a smooth surface. Standard two-equation turbulence models often fail to predict the onset and the amount of flow separation under adverse pressure gradient conditions. This is an important phenomenon in many technical applications, particularly for airplane aerodynamics since the stall characteristics of a plane are controlled by the flow separation from the wing. For this reason, the aerodynamic community has developed a number of advanced turbulence models for this application. In general, turbulence models based on the ε-equation predict the onset of separation too late and under-predict the amount of separation later on. This is problematic, as this behavior gives an overly optimistic performance characteristic for an airfoil. The prediction is therefore not on the conservative side from an engineering standpoint. The models developed to solve this problem have shown a significantly more accurate prediction of separation in a number of test cases and in industrial applications. Separation prediction is important in many technical applications both for internal and external flows. Currently, the most prominent two-equation models in this area are the *k* - ω based models of Menter. The *k* - ω based Shear-Stress-Transport (SST) model was designed to give highly accurate predictions of the onset and the amount of flow separation under adverse pressure gradients by the inclusion of transport effects

into the formulation of the eddy-viscosity. This results in a major improvement in terms of flow separation predictions.

One of the advantages of the *k* - ω formulation is the near wall treatment for low-Reynolds number computations. The model does not involve the complex nonlinear damping functions required for the *k* - ε model and is therefore more accurate and more robust. A high-Reynolds *k* - ε model would typically require a near wall resolution of $y^+ > 0.2$, while a low-Reynolds number *k* - ω model would require at least $y^+ < 2$. In industrial flows, even $y^+ > 2$ cannot be guaranteed in most applications and for this reason; a new near wall treatment was developed for the *k* - ω models. It allows for smooth shift from a low-Reynolds number form to a wall function formulation. The *k* - ω models assumes that the turbulence viscosity is linked to the turbulence kinetic energy and turbulent frequency via the relation:

$$\mu_t = \rho \frac{k}{\omega} \tag{3.2}$$

3.3.3.2. Modeling flow near the wall

Near a no-slip wall, there are strong gradients in the dependent variables. In addition, viscous effects on the transport processes are large. The representation of these processes within a numerical simulation raises the following problems:

- How to account for viscous effects at the wall?
- How to resolve the rapid variation of flow variables which occurs within the boundary layer region?

Experiments and mathematical analysis were shown that the near-wall region can be subdivided into two layers. In the innermost layer, the so-called viscous sublayer, the flow is almost laminar-like, and the (molecular) viscosity plays a dominant role in momentum and heat transfer. Further away from the wall,

in the logarithmic layer, turbulence dominates the mixing process. Finally, there is a region between the viscous sublayer and the logarithmic layer called the buffer layer, where the effects of molecular viscosity and turbulence are of equal importance. The figure below illustrates these subdivisions of the near-wall region.

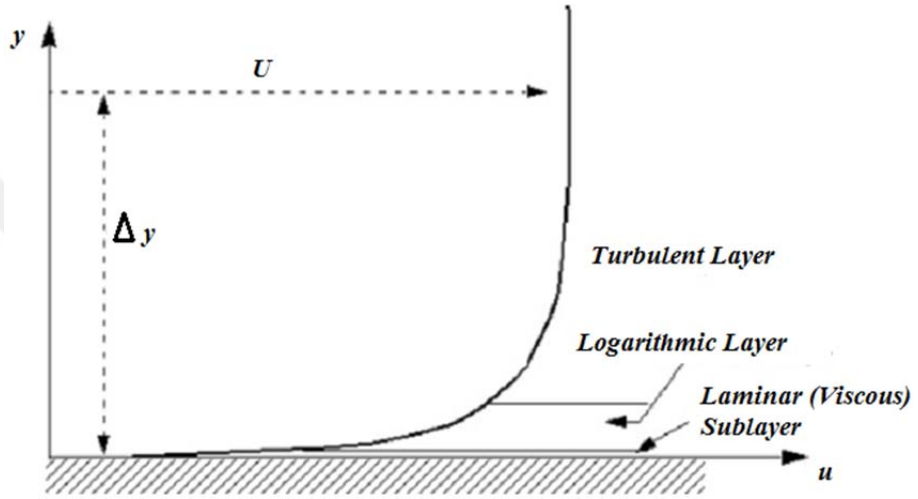

Figure 3.13. Subdivisions of the near-wall region

If the logarithmic profile reasonably approximates the velocity distribution near the wall, it provides a means to numerically compute the fluid shear stress as a function of the velocity at a given distance from the wall.

This is known as a “wall function” and the logarithmic nature gives rise to the well known “log law of the wall”. Two approaches are commonly used to model the flow in the near-wall region:

1- The wall function method uses empirical formulas that impose suitable conditions near to the wall without resolving the boundary layer, thus saving computational resources. All turbulence models in CFX are suitable for a wall function method.

The major advantages of the wall function approach are that the high gradient shear layers near walls can be modeled with relatively coarse meshes,

yielding substantial savings in CPU time and storage. It also avoids the need to account for viscous effects in the turbulence model.

2- The Low-Reynolds-Number method resolves the details of the boundary layer profile by using very small mesh length scales in the direction normal to the wall (very thin inflation layers). Turbulence models based on the ω – equation, such as the SST or SMC – ω models are suitable for a low-Re method. Note that the low-Re method does not refer to the device Reynolds number, but to the turbulent Reynolds number, which is low in the viscous sublayer. This method can therefore be used even in simulations with very high device Reynolds numbers, as long as the viscous sublayer has been resolved.

The computations are extended through the viscosity-affected sublayer close to the wall. The low-Re approach requires a very fine mesh in the near-wall zone and correspondingly large number of nodes. Computer-storage and runtime requirements are higher than those of the wall-function approach and care must be taken to ensure good numerical resolution in the near-wall region to capture the rapid variation in variables. To reduce the resolution requirements, an automatic wall treatment was developed by CFX, which allows a gradual switch between wall functions and low-Reynolds number grids, without a loss in accuracy.

Wall functions are the most popular way to account for wall effects. In CFX, Scalable Wall Functions are used for all turbulence models based on the ε – equation. For k - ω based models (including the SST model), an automatic near-wall treatment method is applied.

3.3.3. Simulation of fluid flow problems

For modeling the flow around a cylinder in this project, Ansys CFX was used. In this section, summary concerning the modeling process, the initial condition and boundary conditions were presented. The following steps will be conducted.

1- Investigate the hydrodynamic forces on the cylinders.
2- Investigate the wake structure of cylinder by changing the yaw angle and center-to-center spacing ratio.
3- Investigate the instantaneous and time-averaged changes in flow characteristics.

Therefore, two types of analysis are considered i.e. quantitative analysis (hydrodynamic forces) and qualitative (the wake flow structure) single cylinder and two cylinders cocentrical. Both categories of the simulations were performed at a various Reynolds numbers according table 3.1 . Cylinders has a constant diameter of 0.01 m and with a height of 0.6 m. The computational domain was 12D in height, 8D in width and 24D in length. The test cylinder is located 4D away from the side walls and 8D downstream of the inlet. Computational domain around single cylinder is shown in the following (Figure 3.14.)

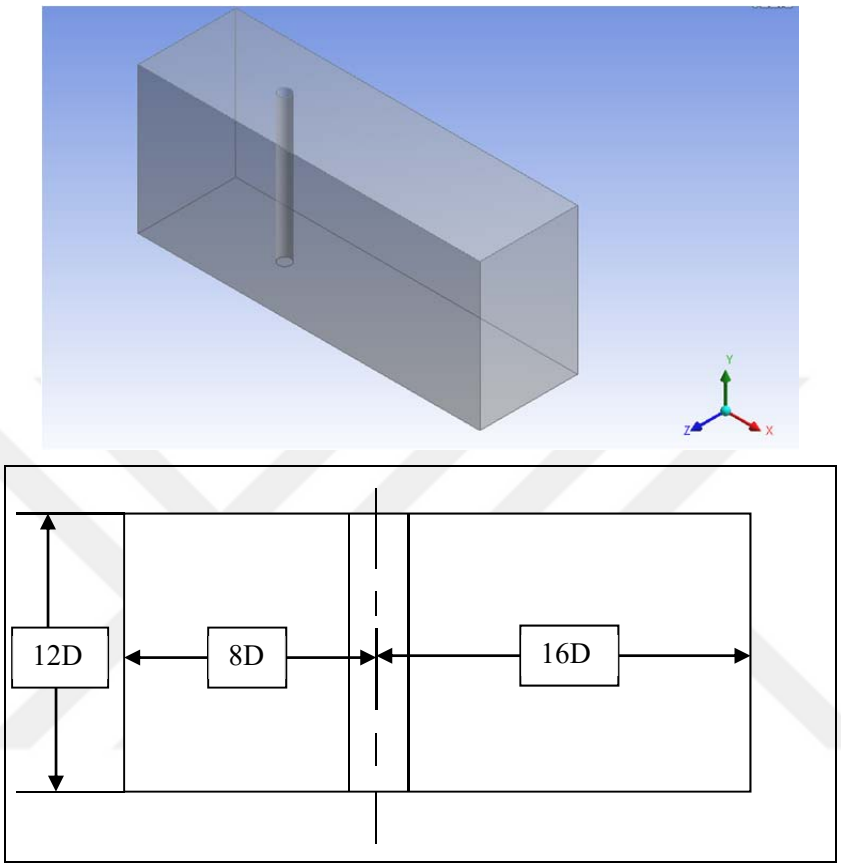

Figure 3.14. Schematic of computational domain

3.3.4. Grid generation

For each analysis carried out by CFD, quality of computational grid created on the model has a dramatic effect on the convergence, accuracy, and precision of results. Especially in the present simulations, accurate prediction of the separation point's position has a significant impact in the amount of force on the cylinder. In CFD analysis were used the different methods for gridding of the flow domain.

3.3.4.1. Hybrid meshes (grids)

A hybrid mesh is a mesh that contains structured portions and unstructured portions. Note that this definition requires knowledge of how the mesh is stored (and used). There is disagreement as to the correct application of the terms "hybrid" and "mixed." The term "mixed" is usually applied to meshes that contain elements associated with structured meshes and elements associated with unstructured meshes (presumably stored in an unstructured fashion).

In the present project, hybrid meshes was used. The intense structured mesh with tetrahedral elements was applied to the surface of the cylinders. Production of this type of elements was provided by “Inflation” option in ANSYS CFX-mesh to gain more accuracy. And the other part of the flow domain comprised of unstructured meshes. Whatever elements were becoming smaller at the range of resolution, gridding can be adapted better on the geometry and solving will be more accurate. On the other hand, shrinking elements means to increase the number of them and smaller time step in the solution process that led a rise in the volume and computational operations, and also it makes to significant rounding error. So in terms of geometric elements may not be large enough that it does not conform to the geometry and not too small that the numerical operations are required too heavy. Hence, for optimization of girding it was essential to have full cognizance of the geometry and the physics of the problem, till to able to identify the regions of the flow with strong gradients changes and where needs for more numerical accurate and finally, the grid of around these regions was just done finer.

In the following figure, a view of created grid around the cylinder was shown. As one can see from the figure, the intense grid distribution around the cylinder started to decrease as moved away from the cylinder.

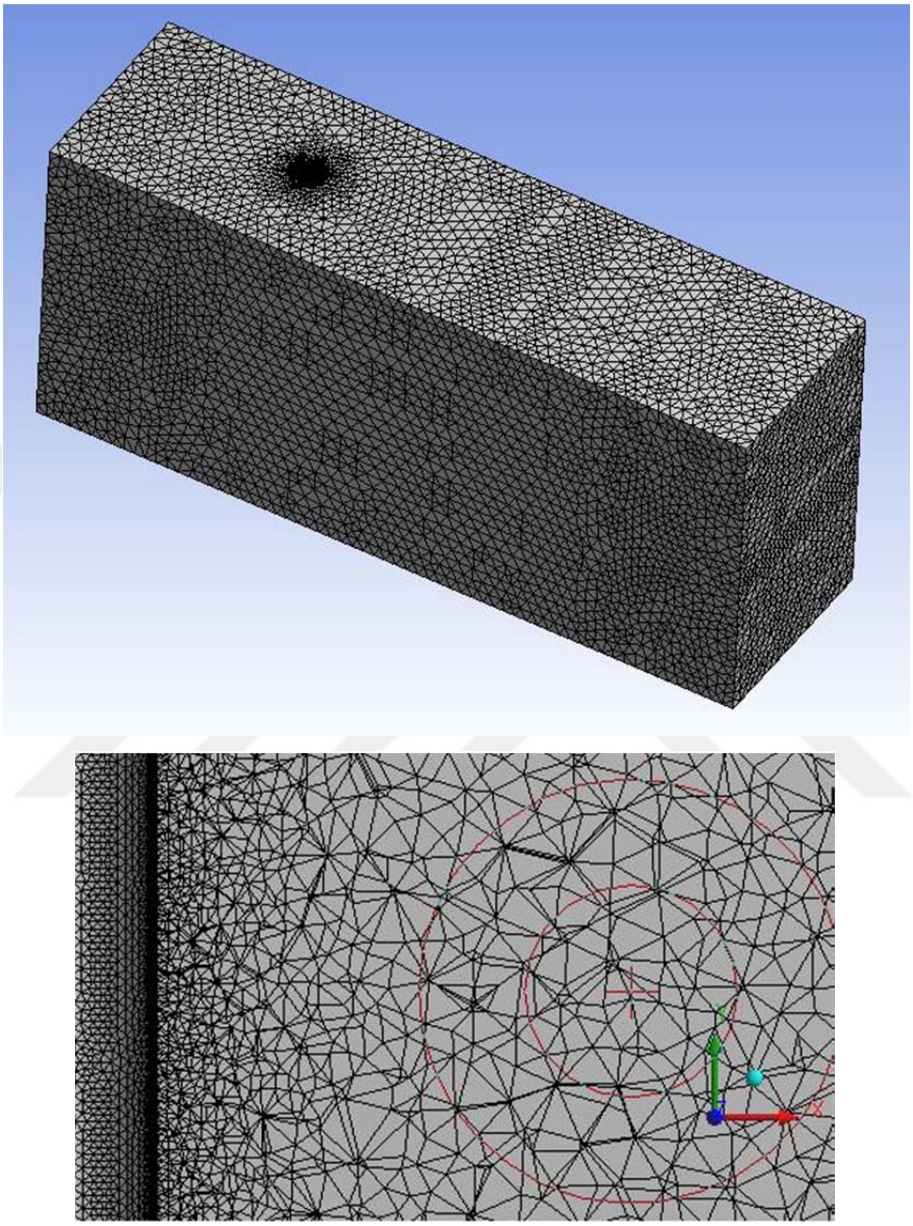

Figure 3.15. The whole flow domain with grid and zoom-in view of the grids around single cylinder

3.3.5. Boundary conditions

According to geometry of flow domain, seven boundaries were detected, and appropriate boundary conditions were assigned to them. Employed boundary conditions can be classified into four categories:

- Inlet boundary conditions for upstream boundary: Fluid is entered from such boundary to solution domain. A various velocity was assigned.
- Outlet boundary condition for downstream boundary: Fluid is exited through the boundary from the solution domain. For this boundary due to be adequate distance and appropriate downstream boundary from cylinder, static pressure was used as a boundary condition. A constant static pressure of 0 Pa was assigned.
- No slip wall boundary condition: The velocity of the fluid at the wall boundary is set to zero. This boundary condition was assigned to the side surfaces and the surface of the cylinder.
- Free slip wall boundary condition: In this case, the velocity component parallel to the wall has a finite value (which is computed), but the velocity normal to the wall, and the wall shear stress, are both set to zero. This boundary condition was applied to the top and bottom walls. When this boundary condition was assigned to a surface, no boundary layer will be formed on the mentioned surface.

3.3.6. Transient solution and determining the time step

Generally, flow analysis is divided to two categories: Steady state and Transient. In the Steady state, analysis is eliminated the time effect, and varying amounts are independent of time. But in the in transient analysis, the changes of parameters are considered with the time and in the equations. In the study, transient analysis is required to simulate the turbulent flow accurately.

Determination of appropriate time step is very crucial in terms of getting accurate data about the concerning flow parameters. Strouhal number is approximately equal to 0.2 in the range of $300 \leq Re \leq 10^5$(Figure 3.14). Thus, the vortex shedding frequency (f_S) can be calculated from the formula below.

$$St = \frac{f_S D}{U} \tag{3.3}$$

By using the above formula, the vortex shedding frequency was determined as 0.4 Hz. The vortex shedding period (T) that is equal to 1/ f_S can be calculated too. It was determined as 2.5 s. The vortex shedding period was divided to 166, so that, time step side was determined as 0.015 s.

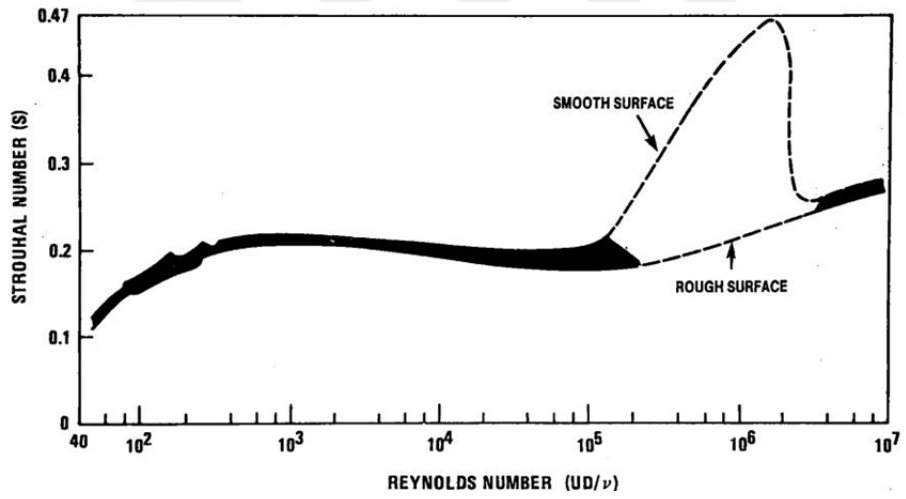

Figure 3.16. Strouhal number changes with Reynolds number for a fixed cylinder

3.3.7. Linear equation solution

ANSYS CFX uses a Multigrid (MG) accelerated Incomplete Lower Upper (ILU) factorization technique for solving the discrete system of linearized equations. It is an iterative solver whereby the exact solution of the equations is approached during several iterations.

3.3.8. Physical Properties of the Fluid

Simulations were carried out in isothermal conditions. The working fluid is water. The properties of the water were shown in table below.

Table 3.2. The physical properties of the working fluid

Property	Unit	Symbol	Value
Density	kg/m^3	ρ_w	997
Dynamic viscosity	kg/ms	μ_w	0.89×10^{-3}
Water temperature	$^{\circ}C$	T	25

3.3.9. Dimensionless parameters

Laboratory and experimental works are often time-consuming and costly. Dimensional analysis is important tool for evaluate the influencing parameters on studied phenomenon. By using non-dimensional parameters which are earned from dimensional analysis, data can be connected by using of minimum possible number of graphs. By using the dimensionless numbers can be indicated the less graphs with higher quality. In the following, other dimensionless numbers were introduced which the effect of their changes were examined (Table 3.2).

Table 3.3. Dimensionless parameters and coefficients

Parameter	Symbol	Equation
Reynolds number	Re	$\frac{\rho\, U\, D}{\mu}$
Strouhal number	St	$\frac{f_S\, D}{U}$
Drag coefficient	C_d	$\frac{F_D}{0.5\, \rho\, U^2 (D \times h)}$
Lift coefficient	C_l	$\frac{F_L}{0.5\, \rho\, U^2 (D \times h)}$

3.3.10. Grid independence tests

A high-quality grid is critical to an accurate CFD solution; a poorly resolved or low-quality grid may even lead to an incorrect solution. It is important, therefore, for users of CFD to test if their solution is grid independent. The standard method to test for grid independence is to increase the resolution (by a factor of 2 in all directions if feasible) and repeat the simulation. If the results do not change appreciably, the original grid is probably adequate. For single cylinder case, the medium sized grid found adequate. On the other hand, the number of elements increased and reached to 19211228 in for two cylinders..

Table 3.4. The results of grid independence test for single cylinder

	Number of element	Number of node	Time-averaged drag coefficient
Coarse grid	17088123	3196803	1.515
Medium sized grid	8,294,400	936,478	1.53
Fine grid	10,163,209	1,442,254	1.54
Very fine grid	19,211,228	3,502,041	1.55

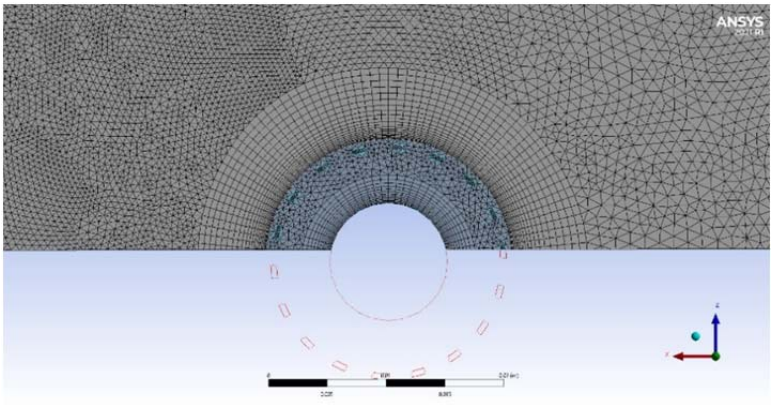

Figure 3.17. 20 layers with the distance of the first element from the surface of the cylinder 0.07 mm

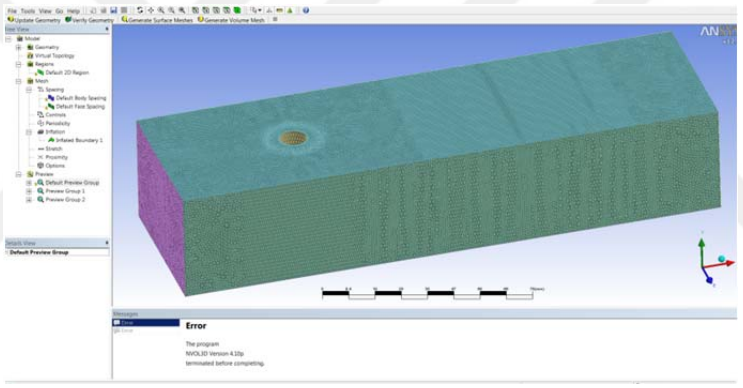

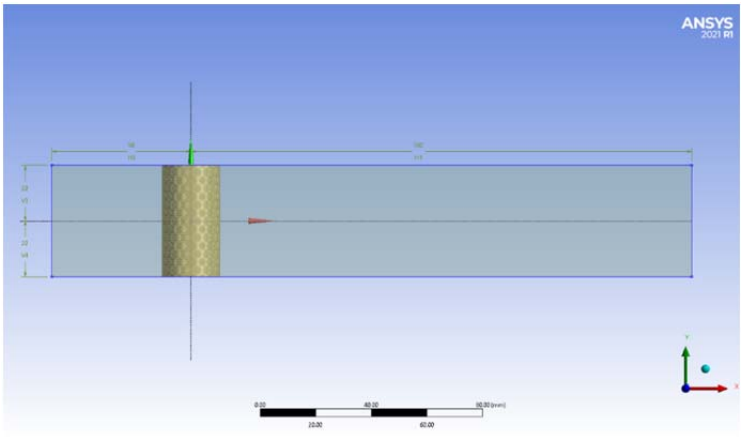

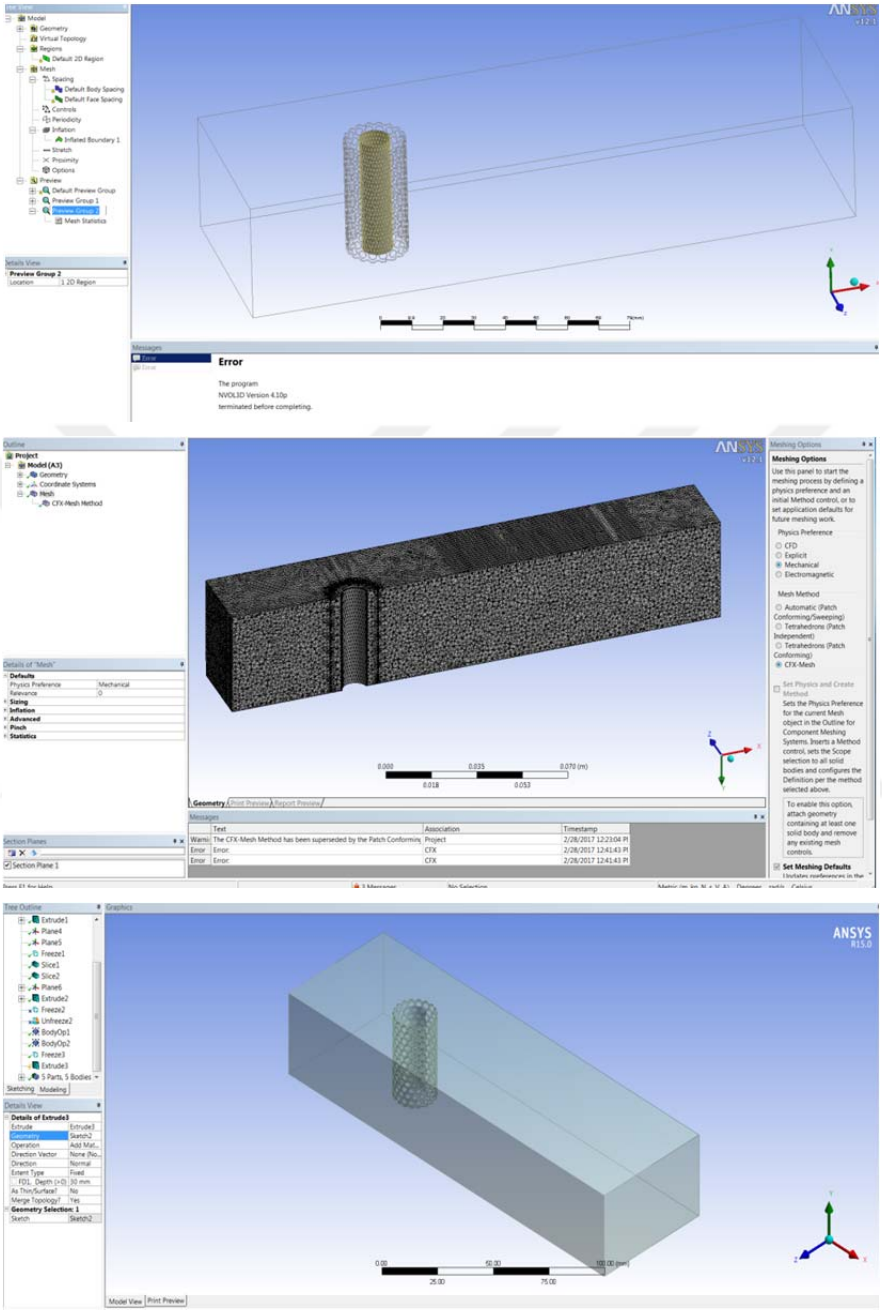

Figure 3.18 More pictures of numerical setup

4. RESULTS AND DISCUSSIONS

This part of the study consists of two subsections. The first chapter is done with numerical numerical and experimental data of the flow struchers around of a single circular cylinder case. The second subsection is about the single and perforated circular cylinders located co-centerical.

4.1. Single Circular Cylinder

When analyzing the flow structure of control elements (perforated circular cylinder around circular inner cylinder), a control case is needed to comprehend the effectiveness of these control elements. For this reason, flow around the circular cylinder (single solid cylinder with the diameter of 10 mm) was investigated without perforated cylinder to take it as a base point and to make comparison with the other experimental results.

To form a reference point and comprehend the basic flow behavior around a circular cylinder, According to Figure 4.1 a ,4.1.b and 4.1.c presents superposed with Time averaged streamlines <ψ> Numerical and expermental and Time averaged vorticity contours <ω> respectively , Numerical result of instantaneous velocity distribution and instantaneous votex sheding formation around a circular cylinder at Re = 150 at time t = 500 was observed at the Figure 4.2 . By the aid of PIV technique, 1000 instantaneous images were taken, and these two images were acquired.

Acorrding figure 4.1 <c> for time averaged vorticity contour the leastes and incremental values were considered as ±1 and 1, <ω> respectively. Negative and positive vorticity contours formed in a symmetrical structure with respect to the horizontal center line of the single cylinder on the shear layers of the sides of the central line of the single cylinder, as symmetrical. The significant area of reverse flow is obvious at the downstream region of single cylinder due to the momentum transferred from the free stream flow region to wake flow region.

The time averaged streamline topologies, <ψ> were illustrated where the fluid flow velocity value becomes zero which is called as saddle point determined by S in the figure. The position where the saddle point is formed, determines the length is defined as the distance from the base of the single cylinder to the saddle points on the centerline (Aydin et al., 2010).

The separation point and rotational motion flow in the near wake region is clearly observed for flow of past of single cylinder region with the help of visualizing tools . According numerical results (figure 4.1<a>) it is apperceived clearly from the instantaneous velocity region further of the single cylinder which alternating vortex shedding and the well known Karman Vortex Street are happend on the wake ragionpast of single cylinder.

As it can be seen from the figure <4.1.a>, the time average streamlines constitute focal points F1 and F2 in the wake region around of single cylinder.They appear in a symmetrical order as it is anticipated, and they are getting closer to each other. From figure <4.1.c>, it is also can be seen that symmetrical time average vorticity contours <ω> takes place and it is in accordance with streamline topology result.

This vortex structure applies unsteady loads on the bluff bodies or any object located downstream of these bluff bodies. These unsteady loads cause fatigue and shorten the life of bluff bodies and objects. In the meantime, Meanwhile, these vortex shedding are an environmental concern subjects. Because they can be the reason erosions and forwarding sediments and pollutants from the underneath of the rivers and shallow lakesrecently studies have been investigated to control the unsteady vortex shedding structure by variouse ways. Taking fluid flows generated around a circular cylinder flow as an object of case study, a series of analyses using CFX software and PIV were performed for a diffrent Reynolds number. The results were found to be in good agreement with those of earlier studies Kuo et al. (2007) and Schlichting (1979). As a outcome, we have obtained comprehensive knowledge and findings that can be carry out this CFX setting up

for associating with fundamental approximationof the flow filde around the circular single cylinder in the variouse low Reynolds numbers.

According to numerical result of flow around of circular cylinder at Re = 1500 at figure 4.2 , It can be seen instantaneous vortices are created, upper and lower shear layers generated by the single solid cylinder and give rise to unsteady flow in the downstream region of the cylinders .So these eddies cause sound and vibration around bluff badies, there force it is very important to control the vortex shedding around them. Before dealing with the main topic of our research, to prove the correctness of the research method experimentally and numerically. First, we checked the flowe around single cylinder and after reciving to a good and significant agreement between the numerical and experimental results ware seen in the single cylinder and also the result of the drag number obtained of numerical method was compared with the previous research and an acceptable result was obtained.

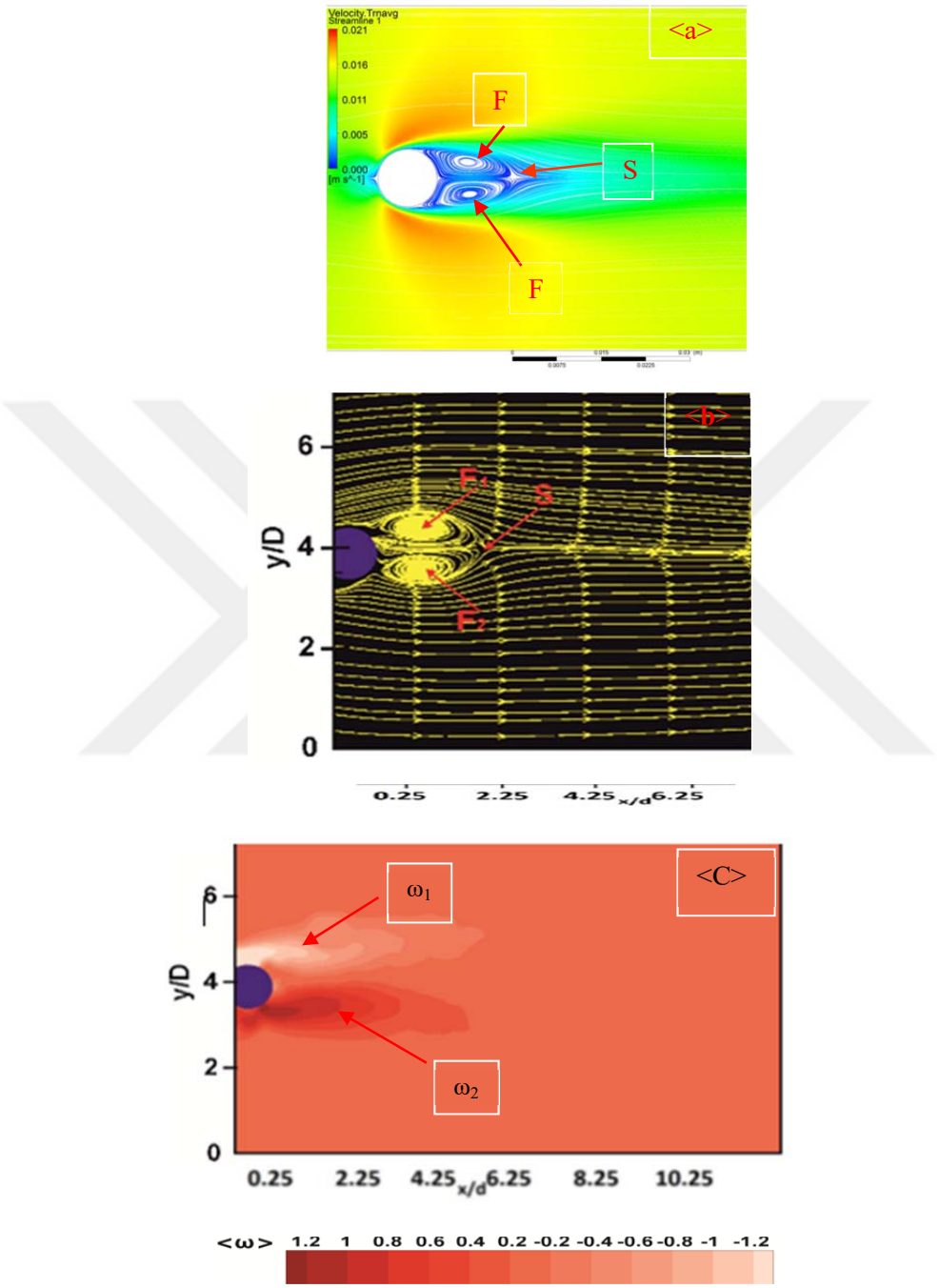

Figure 4.1. Time averaged streamlines <ψ> for Re=1500 < a> Numerical <b>Expermental. <C> Time averaged vorticity contours for Re=1500 <ω> Expermental.

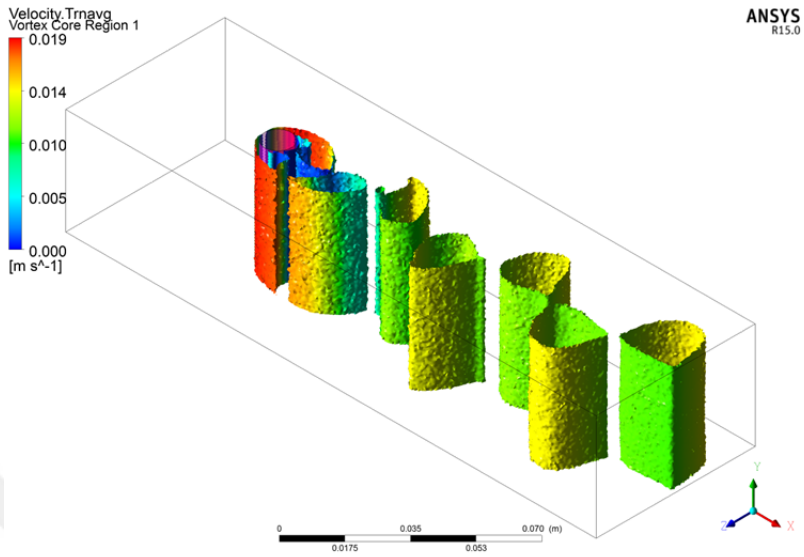

Figure 4.2. Instantaneous dye visualization picture. Flow around a circular cylinder (Re = 150) at time t = 500,(Numerical)

4.2. Validation of the numerical model

When we look to figure 4.3 it can be seen about Re= 10, separation starts occurring on the rear of the body with vortex shedding starting at about Re =90. The region of separation increases with increasing Reynolds number up to about Re =10^3. At this point, the drag is mostly (about 95 percent) due to pressure drag. The drag coefficient continues to decrease with increasing Reynolds number in this range of 10 < Re <10^3. (A decrease in the drag coefficient does not necessarily indicate a decrease in drag. The drag force is proportional to the square of the velocity, and the increase in velocity at higher Reynolds numbers usually more than offsets the decrease in the drag coefficient.) In the moderate range of 10^3 < Re < 10^5, the drag coefficient remains relatively constant. This behavior is characteristic of blunt bodies. The flow in the boundary layer is laminar in this range, but the flow in the separated region past the cylinder or sphere is highly turbulent with a wide turbulent wake. There is a sudden drop in the drag coefficient somewhere in the range of 10^5 < Re <10^6 (usually, at about 2 x10^5). This

signification reduction in C_D is becouse of the turbulant flow in the boundary which transfers the separation point further on the rear of the cylinder, reducing the size of the lenghth ans spanwise of wake and thus the value of the pressure drag. This is in mutuality to streamlined bodies, when creating an increase in the drag coefficient (mostly due to friction drag) when the boundary layer gets turbulent.

To validate the numerical model, flow past a circular cylinder for

Re= 150,250,350,500 ,1000, 1250,1500 and 2000 was compared with data of Figure 4.3. As can be seen in the above table, the drag coefficient calculated has a good aggreement with the experimental value of Anderson. The difference is less than 3.2%. Finally, it shows that the result is reasonable and numerical tool is suitable for the present study.

Table 4.1. Comparing the drag coefficient amounts obtained from the numerical results with the previous investigation results with Schlichting 1979 ,at Re=150

	Present simulation	Schlichting 1979
Time-averaged drag coefficient	1.55	1.6

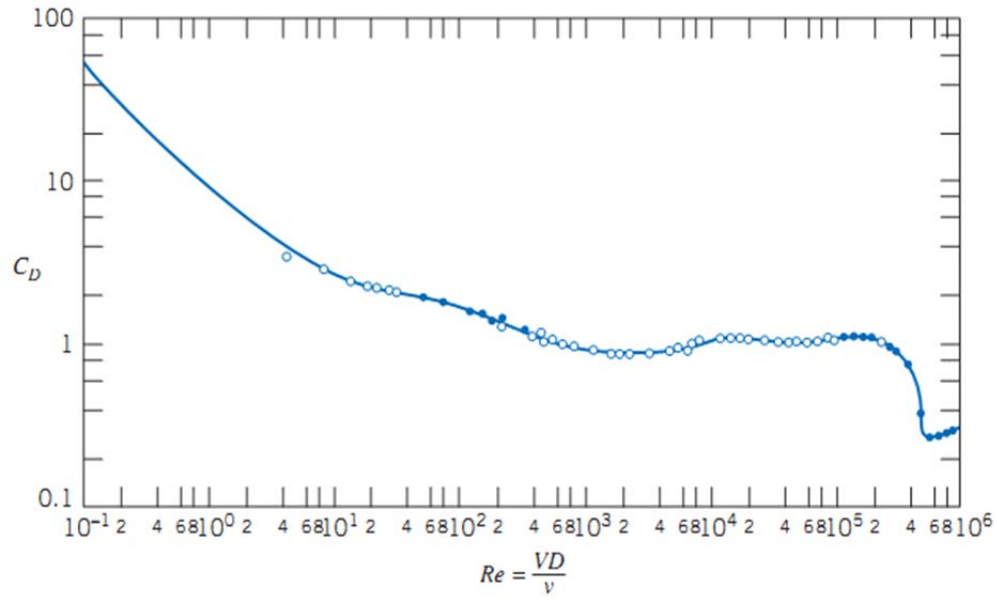

Figure 4.3. Drag coefficient for a smooth circular cylinder as a function of Reynolds Number (Schlichting, 1979)

4.3. Comparing Flow structure downstream of the single cylinder between experimental results with numerical results

By studying the figure 4.4 <a,b>, we find the time-averaged streamline patterns <ψ> at the downstream of the alone solid cylinder at Reynolds number of 1000 based on PIV and numerical simulation, Computational Fluid Dynamics, (CFD). The purpose of these figures was to have a preliminary consideration about the flow, and comprehension of the reynolds number and impact of preforated cylinder for down stream of cylinder effects to the flow structureand compertion between numerical and expermental results.

According to figure 4.4, it shows the time-averaged streamline patterns downstream of the solid cylinder alone at Reynolds number of 1000 based on PIV and numerical simulation, Computational Fluid Dynamics, (CFD). This is a sample of simulations to show the general agreement between the simulations and PIV measurements of flow structure downstream of the solid cylinder, more

importantly on the wake and backflow formation as opposed to the perforated cylinder post-deployment scenario, where it justifies the validity of the CFD results. (al., 2010 ref.). The separated and recirculating flow in the near wake region with the help of visualizing tools is clearly seen for the single cylinder.

As shown in Figure 4.4<a>, there is a saddle point <S> for the CFD simulation at <x/d> = 2.48 (streamwise) and <y/d> =-0.35 spanwise direction. The PIV measurement show the saddle point at <x/d> = 2.19 streamwise and <y/d> =-0.05 spanwise direction. The wake region in CFD simulation elongates more than what PIV shows (51.7% more streamwise) and the saddle point <S> is significantly shifted more downward (spanwise) than what is in the PIV measurements (140%), however, there is a general agreement between both the CFD and the PIV on the formation of the wake and also its pattern behind the solid cylinder, as is opposed to the case when the perforated cylinder will be placed concentrically around the solid cylinder that shows no wake formation except for Re = 2000, discussed also later in this study.

Figure 4.5 shows the three-dimensional time-averaged velocity streamlines past the solid cylinder after placement of the perforated cylinder at Re = 1000. It is observed that wake and flow instabilities delay in streamwise direction until <x/d> = 9.41, i.e., all streamlines are parallel and there is no backflow before this point. After <x/d> = 9.41 Karman Street is clearly seen. The same happens for all other Re numbers, i.e., the Karman Street significantly forms far away from the cylinders. Therefore, to reduce the effects of Karmen Street downstream of the flow around the cylinder, the perforated cylinder solution can be very effective. Also, the width of wake spanwise seen to be narrower, this is due to despite the inertial forces of the fluid flow, overcomes the viscous forces and causes to carry forward of Karmen Street after located perforated cylinder around single cylinder

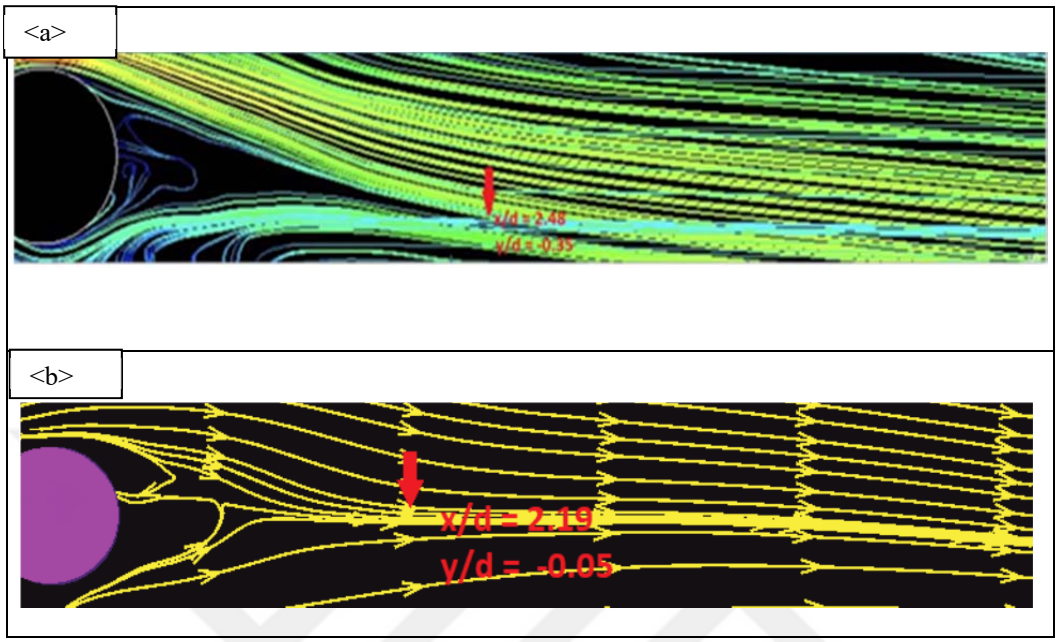

Figure 4.4. Time-averaged streamline topologie <Ψ> for the solid cylinder at Re = 1000, top<a> the CFD simulation, and bottom<b> the PIV measurement. Images are not with identical scales.

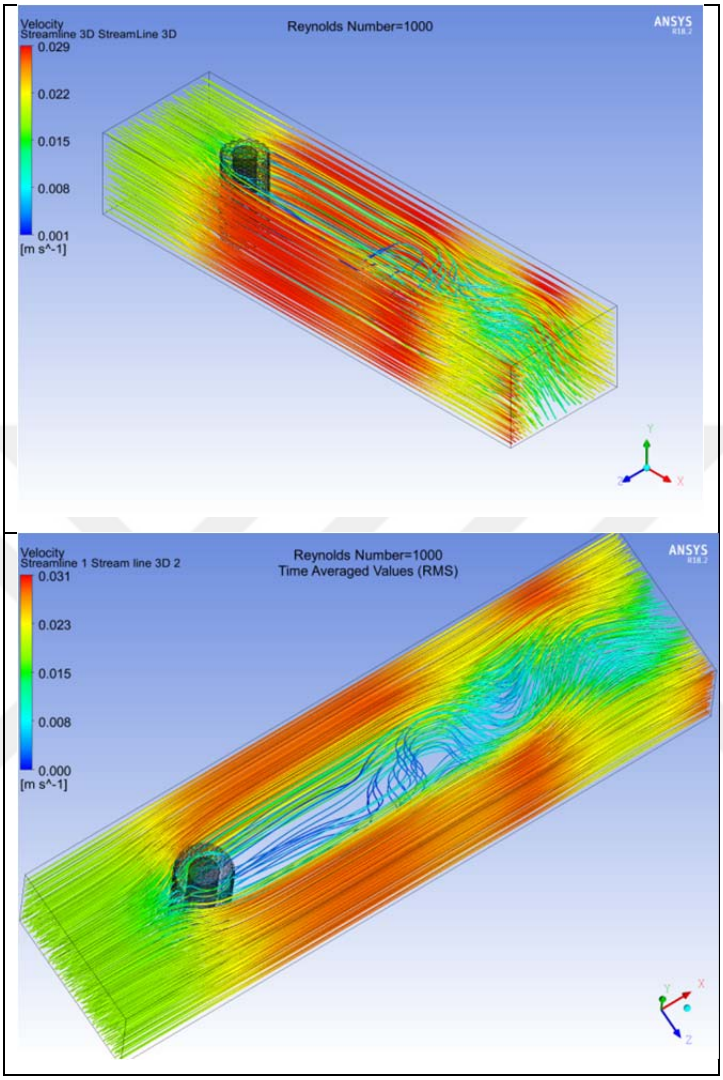

Figure 4.5. Three-dimensional velocity streamlines for Re = 1000 after placement of the perforated cylinder (Numerical)

4.4. Effects of Perforated Circular Cylinder at Different Various Reynolds Numbers

In the current research, Reynolds number determinant and variable parametre is designated initially to investigate the flow structure according to their presence. These are the porosity of outer circular cylinder with respect to flow

direction. Accordingly, in the first step, flow behavior of inner cylinder and outer perforated circular cylinder configuration was examined thoroughly fixed porocity value of $\beta = 0.5$. Also, more far-reaching investigation was carried out in this stage with CFD about the process of interpretation of vortex shedding.

In the figure 4.6 we can obviuse that the first column shows the time averaged streamlines $\langle\psi\rangle$ of the PIV measurements for the solid cylinder along with the CFD simulations after placement of the perforated cylinder to understand the effect of adding the perforated cylinder on the flow structure behind the solid cylinder was been shown at the second column. In this figure ,< F> symbols stand for the circulating flow structures and they indicate the complicated flow structure. In the first columns, upper and bottom shear layers created by the single solid cylinder and make to rise to unsteady flow in the downstream region of the cylinders. This situation can also be seen from time averaged vorticity contours $\langle\omega\rangle$ in figure 4.10. the second column of figure 4.6 ,as initially expecte base on previouse studies upper and bottom shear layers get blocked and became weak by the perforated cylinder wall, generating circulation pairs wake occured far from cylinder side in such a way that they are dispersed in downstream of the cylinder.It is clearly seen from figure 4.6 after located perforted cylinder around single cylinder , the, suppression of Karman Vortex Street is achieved for all Reynolds number.

In the figure 4.6 all the cases with the solid cylinder alone show wake and backflow behind the cylinder in PIV measurements, which will be enlarged both streamwise and spanwise as Reynolds number increases; at Re = 1000 and 1250, there are backflows behind the cylinder. This situation shows that the recirculation zone of the cylinder is restricted by the perforated cylinder. Moreover, the size of the recirculation zone and wakeragion length increasing with the increasing Re numbers. But there is not any occurrence of reverse flow in the near-wake region restricts to momentum transfer in the near-wake region of perforated cylinder.

For Re = 1500 and 2000 the wake region, the two focal points <F_1> and <F_2> a saddle point <S> are clearly observed for both cases. The saddle point for Re = 1000 is locate d at

<y/d> = -0.05 which means the flow is shifted slightly downward; for Re = 1250 the flow is shifted upward as the saddle point is located at <y/d> = +0.06, i.e., 220% upward; this trend continues for Re = 1500 where the saddle point is located at <y/d> = +0.43 and the flow is significantly shifted upward until the Re = 2000 which again the saddle point returns to <y/d> = 0. In order to analyse the flow structure after deployment of the perforated cylinder, we divide the flow into two regions: (1) the gap between the cylinders, and (2) outside of the gap. Except for Re = 2000 and for all other Re numbers, the wake region behind the solid cylinder is washed out by the jet-alike flow.

Formations of foci <F_1 >and <F_2 >are asymmetrical with respect to the centerline of the cylinder and the saddle point <S >disappears for all Reynolds number due to opposition of inertial forces to viscous forces in down stream except Re = 2000 , figure 4.11 .In additinal,wake region exhibits ‘S’ shaped unsteady oscillating flow behavior similar to the Von Karman vortex street and moves further downstream in the main flow direction .However, it is clear that with using the perforated cylinder remarkably effects on the flow wake ragin of the cylinder. For Re =2000 there is a backflow in the gap region located at the lower half behind the solid cylinder. The reason for this phenomenon can be explained as follows that with increasing the Reynolds number of fluid particles while passing through the cylinder holes of perforated cylinder, due to velocity increasing at the constant passing hole surface, therefore, this fluid acceleration causes the formation of akind of stream line in the gap area. However, the wake ragion gnerated in this area is much improved compared to the wake ragion formed behind the single cylinder, because both the spainwise width and wake length is reduced and it is formed only in the bottom region of the center line, and the saddle point is also pulled back. For comparison purposes, the results for the bare cylinder are also included.

The focal point is located at <x/d> = 0.12 versus <x/d> = 0.66 compared to the pre-deployment of the perforated cylinder which shows 450% decrease in the length of the backflow similar to the results obtained for higher Reynolds numbers like the study of Re = 5000 [T. Durhasan,2019] in which the focal points would shift to locations closer to the solid cylinder after deploying the perforated cylinder. There is a separation point at angle 82° for the solid cylinder which agrees with the reports in literature. While there is not a separation after placement of the perforated cylinder except for Re = 2000, the separation point is shifted from 82° to 104° (27% enhancement) for this Re number. For all Re numbers except 2000, the flow will be shifted upward after placement of the perforated cylinder, while for Re = 2000, it is seen that the flow becomes symmetrical with respect to the short axis of the cylinders.

In the figure 4.7, we can obviouse clearly the effective controling of the perforated cylinder on the vortex shedingof past ragion of the single cylinder .so, the location of the saddle point genarated on the horizontal axis of the center line of the cylinder has been reduced by 80% and pulled back, so it has been significantly reduced in the vortex sheding.

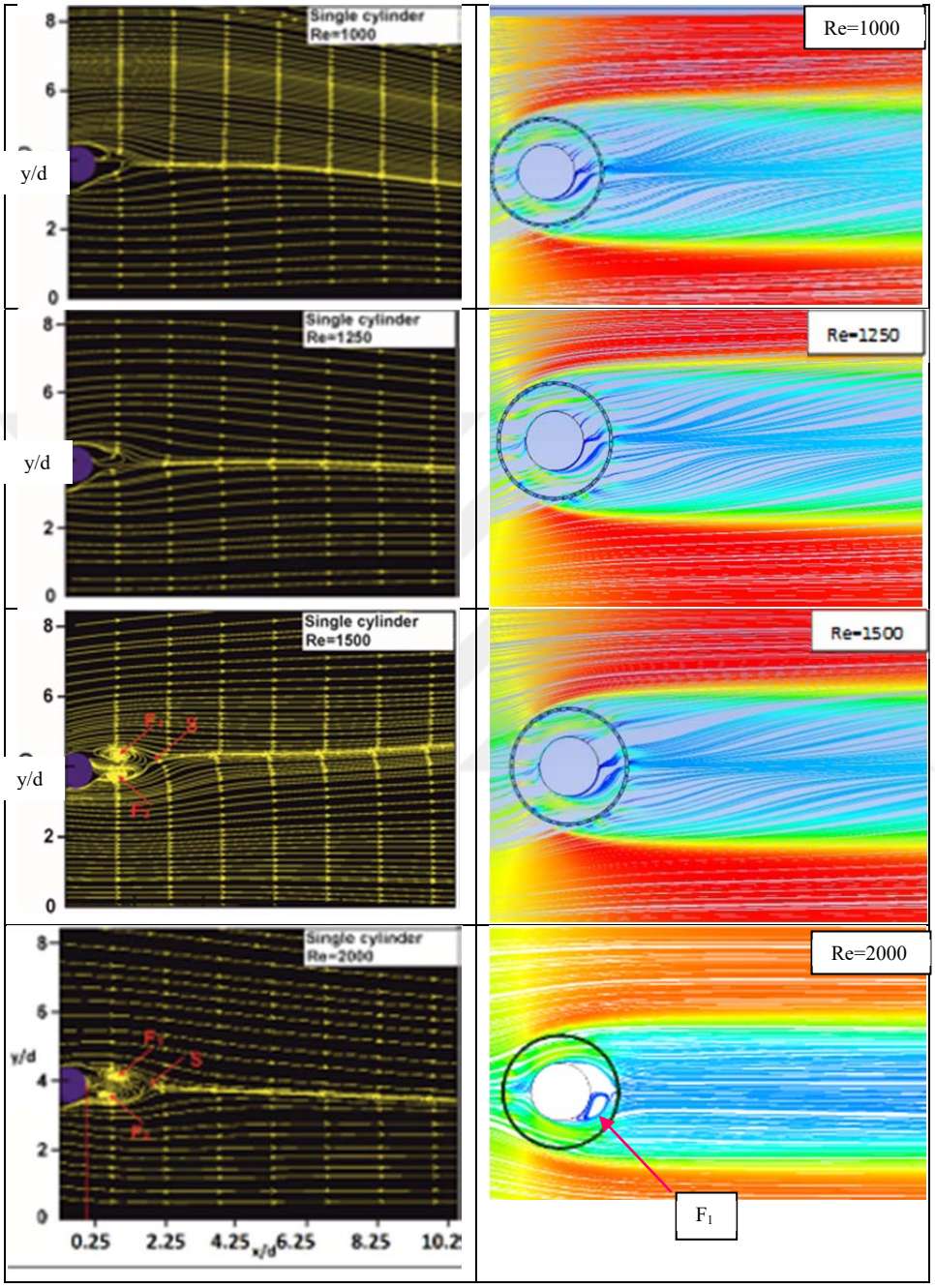

Figure 4.6. The effect of the perforated cylinder employment on the time-averaged streamline patterns <ψ> at Reynolds number between 1000<Re<2000 (left column:Expermental, Right column:Numerical)

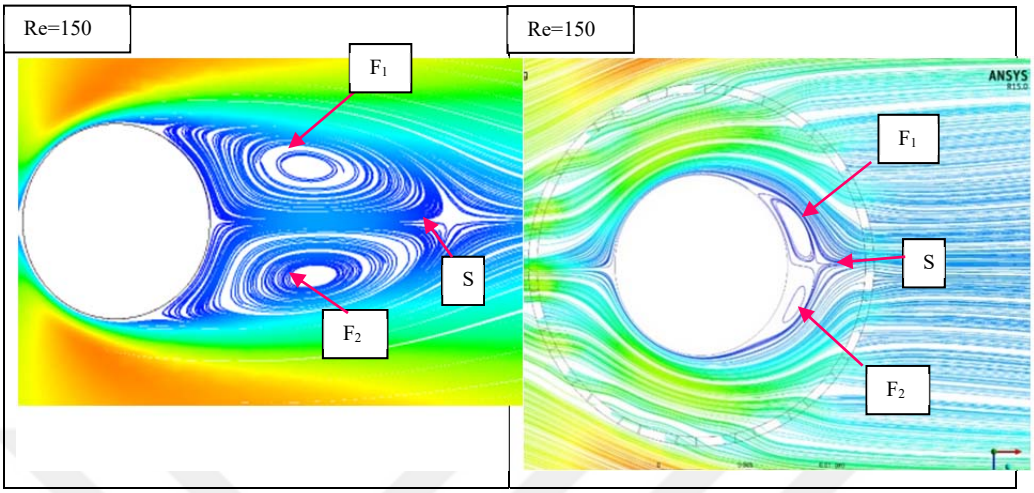

Figure 4.7. The comparison effect of the perforated cylinder employment on the time-averaged streamline patterns <ψ> with single cylinder at the Reynolds number =150

According to Figure 4.8, first column illustrated t the velocity distribution <u/U> around single cylinder that achieved with experimental results and second column that obvoied velocity distribution <u/U> around single cylinder after placment perforated cylinder . It can be obviused the first coulmn that it indicated more extended effect of the perforated cylinder use on the contours of normalized velocity <u/U> in flow direction. In this figure, the streamwise distance, <x> is nondimensionalized with the diameter of the single solid cylinder <d> It is shown that the deployment of perforated cylinder will eliminates the region of negative <u/U> contours behind the cylinder in both longitudinally (streamwise) and in traverse (spanwise) directions for all tested Reynolds numbers except for a small gap region for Re = 2000; instead, placement of the perforated cylinder accelerates the flow because of the holes provided by the surface of the perforated cylinder. So, in this case the flow wake ragine occures between solid inner cylinder and outer cylinder is like flow structure around the single cylinder becouse in this opposition, inertial and viscous forces is disturbed, and here it can be seen that viscous forces have overcome inertiaforce, but not to the extent that occurred in the

case of a single cylinder. Also,This is in accordance with the results obtained from time averaged streamline patterns <ψ> which denotes that the utilization of perforated cylinder makes the focal <F_1,F_2>and saddle points <S> either disappear (for Re other than 2000) or which went quite close to the solid cylinder after placement of the perforated cylinder for Re =2000, according to Figure 4.6.In additional , the separation point angle value compared ofthe single cylinder has also improved, and although we expected to have 82 °, but it occure at 104 ° , so this angle made to generate the back flow and the weak wake region in gap raigion.

This situation should also give rise to decrease in the drag force over the cylinder surface, due to the increase in Reynolds number and the subsequent increase in velocity, it leads to transfer the momentum of the fluid flow and the viscous forces are overcome to iteria forces (figure 4.20). Also, after placing the perforated cylinder, a considerable portion of the wake region is shifted from the back of the cylinder (downstream) to the gap between the cylinders.

The jet-alike phenomena described in the previous studies is clearly seen. This can be more understood by looking at the vorticity distribution assessed as follows figure 4.8.

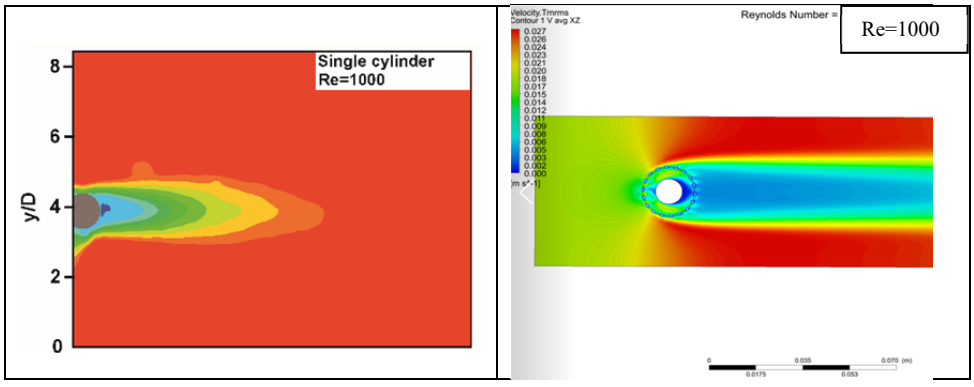

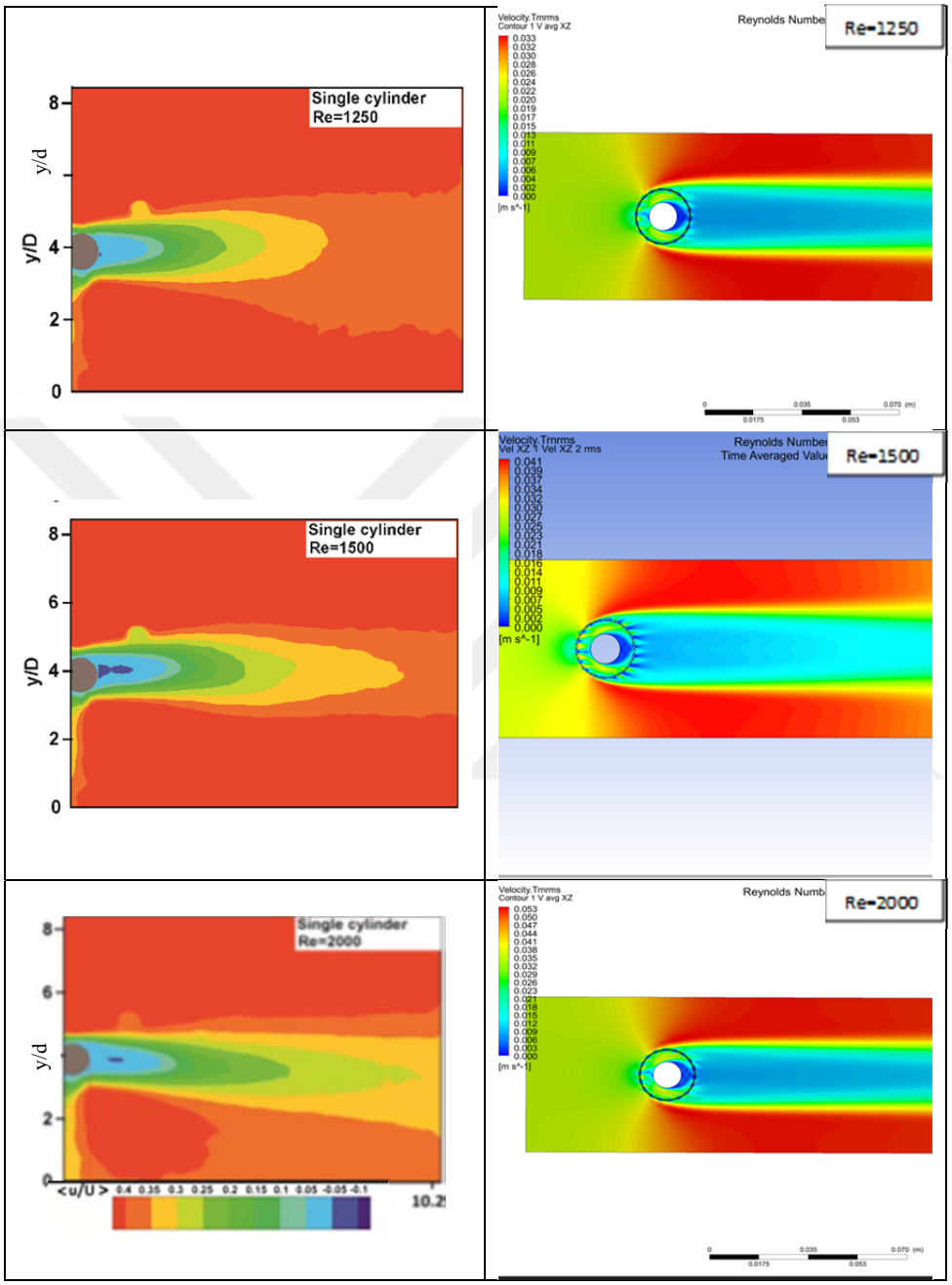

Figure 4.8. The influence of the perforated cylinder utilization on the time-averaged streamwise velocity distribution <u/U> at Reynolds numbers1000<Re<2000(Left Column: Expermental, Right:Numerical)

At the first glance to figure 4.9, it can be seen the vorticity around cylinder after placement of perforated at the horizontal section and secound column obviouse of side face of the time averaged vorticity <ω> concentration that resultes of numerically study. When we look at the time averaged vorticity contours <ω> in figure 4.9 and 4.10 we can inferthe impact of the deployment of perforated cylinder on the time-averaged vorticity contours of various Reynolds numbers with the high and low intensity regions and the reference ribbon. So, these regions of high $<\omega_1>$ and low vorticity $<\omega_2>$ intensities get closer to each other because of shedding of the vortices downstream of the cylinder, and with increasing of Reynolds numbers, the area of vortex shedding increases and the tendency for two positive and negative layers to approach each other is seen. This phenomenon leads to vibration and destruction of bluff bodies over time, Therefore, the suppression of these vibrations is one of the most important structural engineering issues In the figure 4.10. In this regard, after deploying the perforated cylinder, the regions for vorticity assessment does not show any negative regions (clockwise) since all the flow field is accelerating towards the downstream of the cylinder. This shows that adding the perforated cylinder in place concentrically to the solid cylinder would eliminate the vortex shedding considerably, these results that gaind of Numercal study has been indicated at secound column of figür 4.10.

Increasing the separation angle after located the perforated cylinder and approaching the creeping flow state behind the cylinder reduces the drag coefficient and maks to eliminate the turbulence of the flow behind the cylinder or vortex shedding. This is a sign of shedding swept and disappeared by the jet-alike mechanism which helps preventing the well-known Karman Street. Only, for the gap region at Re = 2000, just a small vortices are present.

It was stated in the before investigations that $\beta = 0.5$ is an effective parameter as a prosity rate for suppression of the vortex shedding and for prevention of the Karman Vortex Street, according to the inner and outer perforated cylinder configuration in figure 4.9 and 4.10. And it was also proposed

that vortex pair generated from the inner cylinder needs to be controlled to prevent the interaction of them and to eliminate the unsteady vibration and forced due to the importance of this issue in environmental conditions and engineering designs . So, in the same direction to annihilate the unsteady effects of vortex pair inter actio perforated cylinder was also utilized and investigated for the cylinder porosity of $\beta = 0.5$ application.

According to figure 4.11, the time averaged streamlines of flow $<\psi>$ and 4.9 and 4.10 the time averaged vorticity contours of flow $<\omega>$ were exhibited. At the first glance, seems to suppress the vortex interaction and Karman Vortex Street formation in both annular and wake region after using perforated cylinder, And the value of flow vorticity $<\omega>$ has decreased by 78% compared to the single cylinder. Thus for this case, $\beta = 0.5$ and $d/D = 0.5$ can be presumed as the most effective at the all Reynlds Numbers in this study. In additional, these PIV results match up with Numerical results and this configuration can be regarded as successful to control the flow.

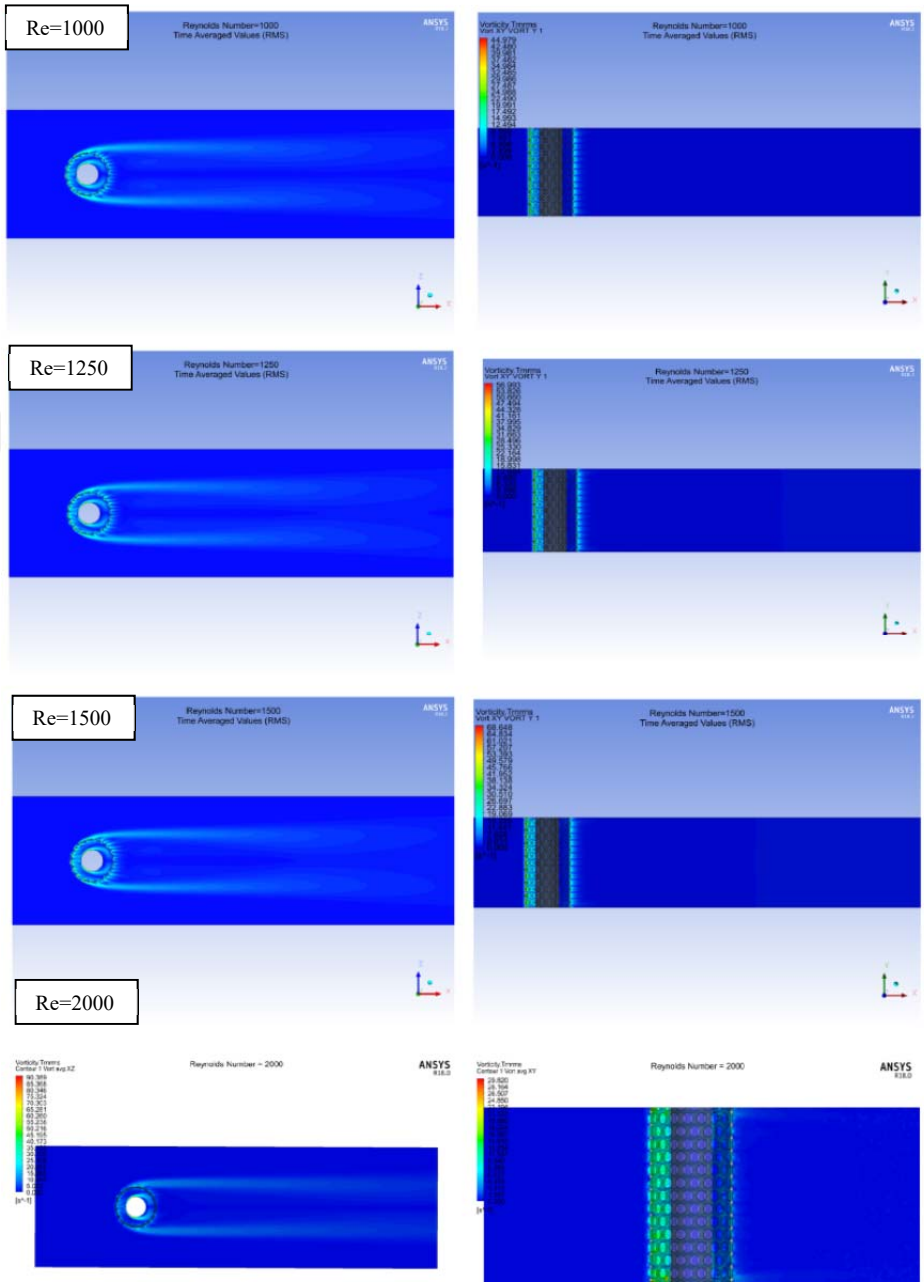

Figure 4.9. The impact of the perforated cylinder placement on the time-averaged vorticity <ω> concentration around the cylinder After located Perforated cylinder at Reynolds numbers from top view and side view of numerical results at 1000<Re<2000 (Numerical Results)

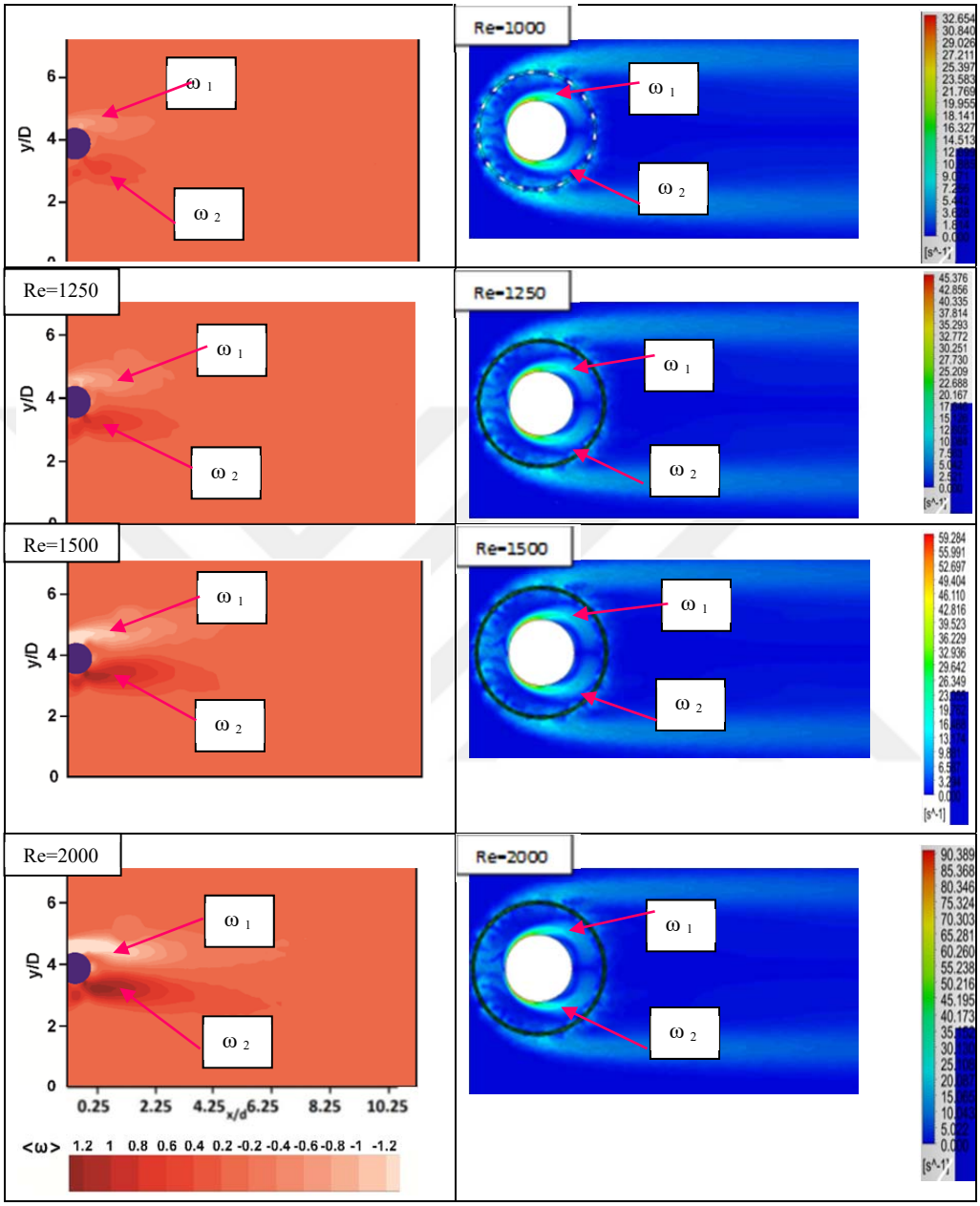

Figure 4.10. The impact of the perforated cylinder placement on the time-averaged vorticity <ω> concentration around the cylinder at Reynolds numbers 1000<Re<2000 (left column:Expermental,Rightresults:Numerical)

In Figure 4.11 the time averaged streamlines <ψ> of numerical results are indicated. In this Figure <F_1 >and <$F_{2>}$ symbols stand for the circulating flow structures and they indicate the complicated flow structure. For Re=150,250,350 and 2000, upper and bottom shear layers generated by the solid cylinder, interact with each other up to the outer perforated cylinder, becouse more fluid flow can not pass through the perforated cylinder according to lower reynolds number (Re=150,250 and 350), So, the natural flow of fluid occurs in this area. The main reason for the formation of the flow wake ragion is the non-predominance of inertial forces over viscous forces, and the angle of the separation point is greater than 82 °, and the separation occurs later. Therefore, the fluid flow has enghugh power to great vortex shedding, and this is clearly seen in the figures.

From Re=500 to Re =1500,upper and bottom shear layers get blocked initially by the perforated cylinder wall , so, generating circulation pairs and then they are dispersed in downstream of the inner cylinders with increasing Reynolds Nomber from Re= 500 to 1500 except Re=2000 , At the all Reynolds numbers, it is seen from figure 4.11 that any circulation points <F> did not take place in downstream of the perforted cylinder, suppression of Karman Vortex Street is achieved for all Reynolds, this acceptable result is due to the presence of a perforated cylinder, which is a significant result.

In figure 4.11, it is seen that jetlike flow dose not take place for this porosity in all Reynolds numbers.

And also in figure 4.6 Karman Vortex Street takes place very far from the perforated cylinder, it goes as far as 4d from solid cylinder, also perforated cylinder can dispersed the flow structure caused by the flow separation (Re=500 to 1500), thus generating of Karman Vortex Street can be seen more far from of perforted cylinder in the down stream of perforated cylinder at all Reynolds number. This situation is valid in all Reynolds Numbers for procity rate of β=0.5 and this porosity is effective for controlling the downstream of the single cylinder.

Here in, perforated cylinder can be regarded as the transient parameter for controlling the downstream region. Yet, high magnitude vortex pairs and unsteady flow take place in the annular region between inner solid cylinder and outer perforted cylinder for Re=150,250 and 350. It can be concluded that, this vortex formation is developed out interaction of reverse flow and jet streams at the outer cylinder.However, according to figure 4.7 , have been obtained around the single cylinder we can justify the comparison results in the way that the spanwise and the length of the flow wake ragion have been significantly reduced, so it has been reduced from 2d to less than 0.5d at the Re=150. After inserting the perforated cylinder, and can be seen only in the gap area, this result is considered a good and impressive performance for this process.

In additinal according Figure 4.11. When we look at the flow configuration, the narrow wake region and absence of Karman Vortex Street draws attention. So these PIV results at the figure 4.6 match up with numerical visualization results and this configuration can be regarded as successful to control the flow. Creating of karman street and vortex formation was been seen very further then cylinder in this regard it is seen at leas 4d more then of cylinder center at the Reynold 500. Consequently, this configuration also seems to be effective control case for contolling wake ragion around cylinder that lead to decreas drag forces. It can be concluded that, this vortex formation is developed out interaction of reverse flow and jet streams at the outer cylinder. So, in the light of obtained CFD results that the flow structure of the cylinder in the near-wake region are is significantly affected by the perforated cylinder for all Reynolds.The perforated cylinders are dominat on the flow structure for this porosity value of β=0.5.

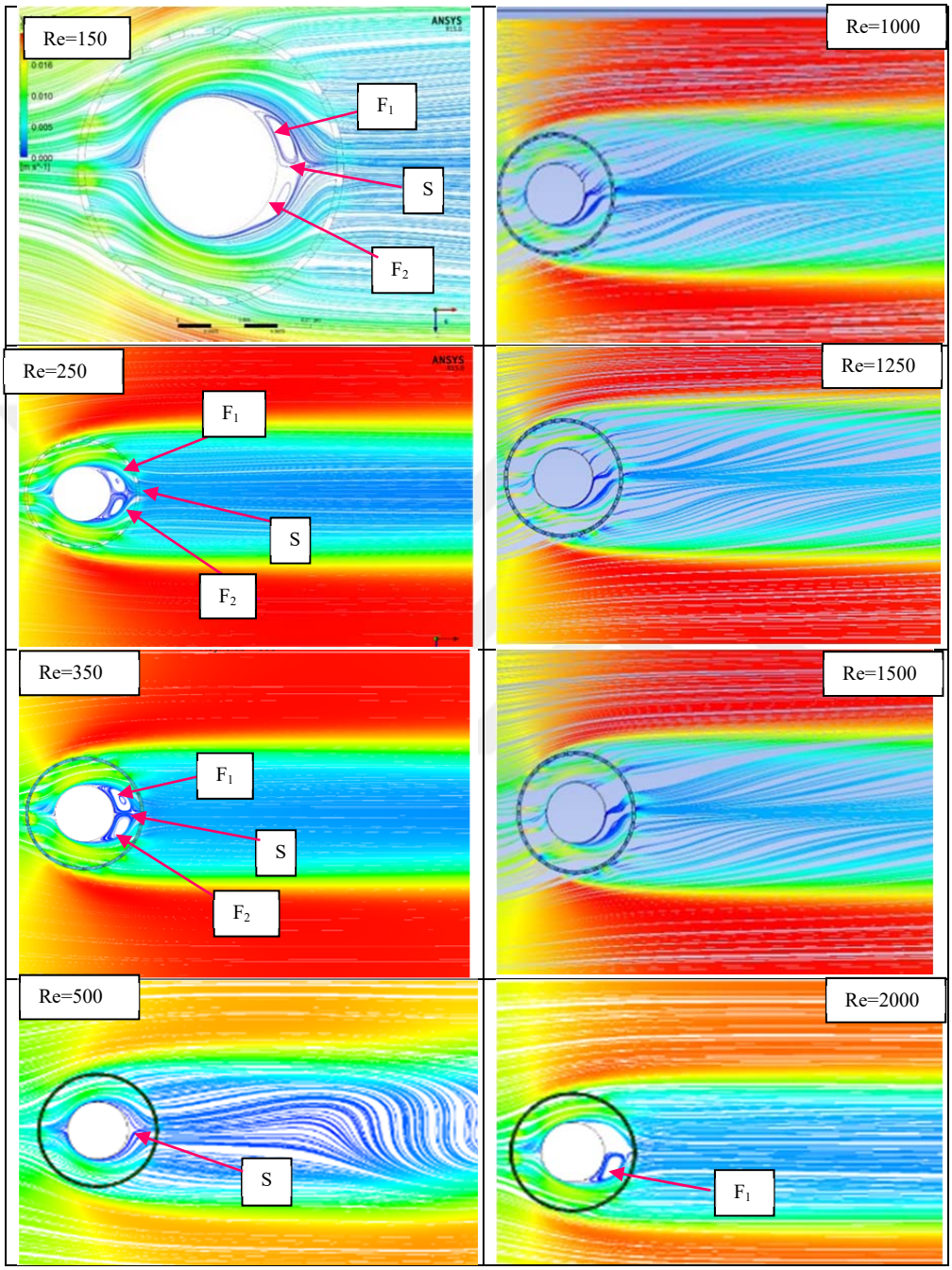

Figure 4.11. Time averaged streamlines <ψ> of inner and perforated circular Cylinder in the wake region from Re=150 to 2000 (Numerıcal Results)

In the Figure 4.12 , It indicates the changes of saddel point location with increacing of Reynolds number after located perforated cylinder. According to these data, 0.78% reduction is visible in saddel point distance value at Re=2000 as a maximum in the other hand the minimum value is 0.75% that belongs to Re= 150, these reduction percents confirm for controling of wake ragion as a good agreement results in this study.

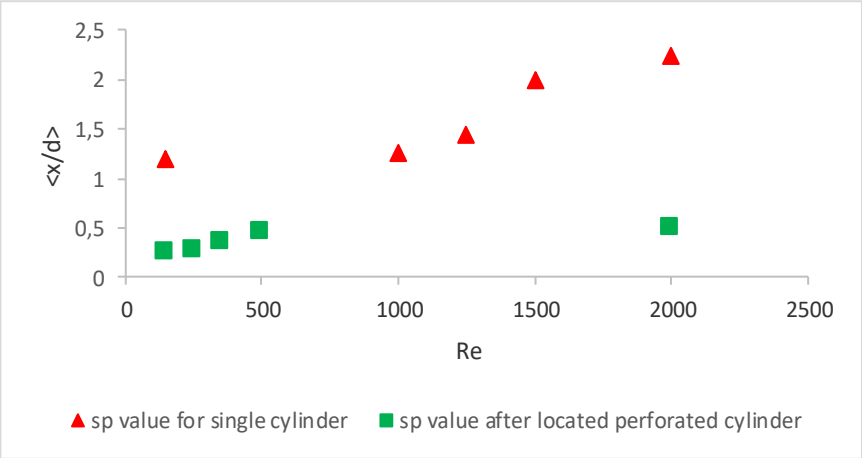

Figure 4.12. Changes Saddel point location with increacing of Reynolds number and compersion between single with efeccet of perforated cylinder at Re=150 to 2000 (Acoording Numerical results)

When we look at the time averaged Pressure contours <P> in figure 4.11 at first glance, it can be seen the pressure drops by increasing of the Reynolds numbers due to over come the Inertia forces to viscous forces,This trend can also be seen in the flow of the single solid cylinder and after the placed of the perforated cylinder, we also see the pressure reduction process with the increase of the flow momentum because of increasing of Reynolds numbers.at the figure 4.13 that the pressure difference between front and rear side of the cylinder decreased with increasing Reynlds number that it is main resion to decrease in drag coefficient , and this results have good agreement with results shown at the figure 4.20.

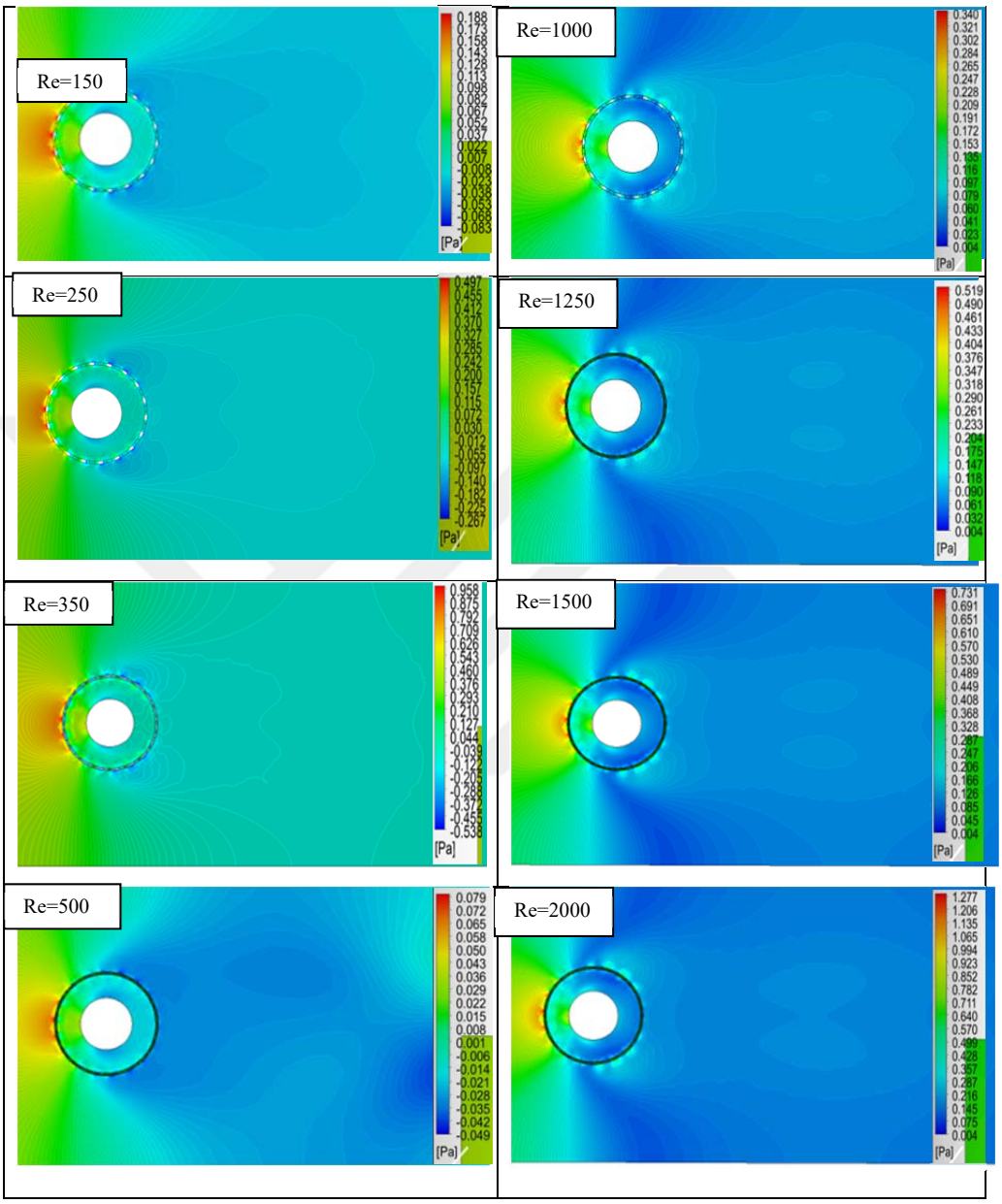

Figure 4.13. Time averaged pressure contour for diffrent Reynolds numbers. (Numerical)

Figure 4.14 <a> illustrates a representation of the distribution of planar turbulent kinetic energy (TKE) values with respect to the spanwise direction for various streamwise locations. And Figure 4.14 <b> shows The variation of planar TKE along spanwise direction for different cases at different location of x/d with expermental results.

As shown also in Figure 4.15 for single cylinder, like the previous results discussed so far, the TKE values do show a reduction after placement of the perforated cylinder, for all distances the total kinetic energy decreases notably after the perforated cylinder placement. It is seen that before deployment of the perforated cylinder, the minimum and maximum values for the TKE are around 0.01 and 0.05, respectively. However, according to the CFD simulations depicted in Figure 4.12<a>, after placement of the perforated cylinder, all regions show zero TKE values up to three decimal points that is the flow becomes mostly laminar rather than being turbulent.

Also be pointed out that concentration of TKE level along the shear layers increases as a result of Kelvin-Helmholtz vortices occurred due to the high amount of velocity difference between free stream and the wake region. Increasing the Reynolds number to a higher value, the maximum value of TKE is reduced dramatically and the location of peak value of TKE moves further downstream, it can be seen clearly at figure 4.14 Moreover, the rate of reduction in magnitude of peak values of TKE which gradually increases by increasing Reynolds Number.

Since the vortices are suppressed, entrainment of the fresh fluid with high momentum into the wake region from the shear layers is eliminated which results in large velocity in the wake region.

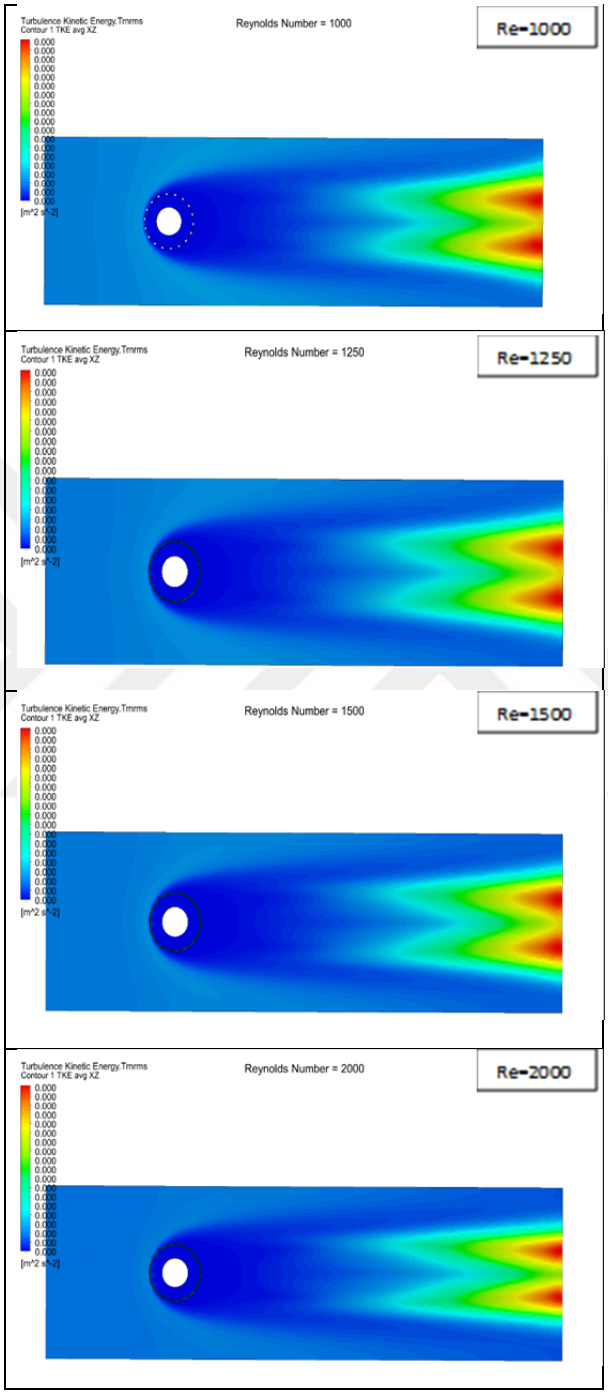

Figure 4.14. Time averaged Turbulence Kinetic Energy, <ψ>, for various Reynolds Numbers. (Numerical Results)

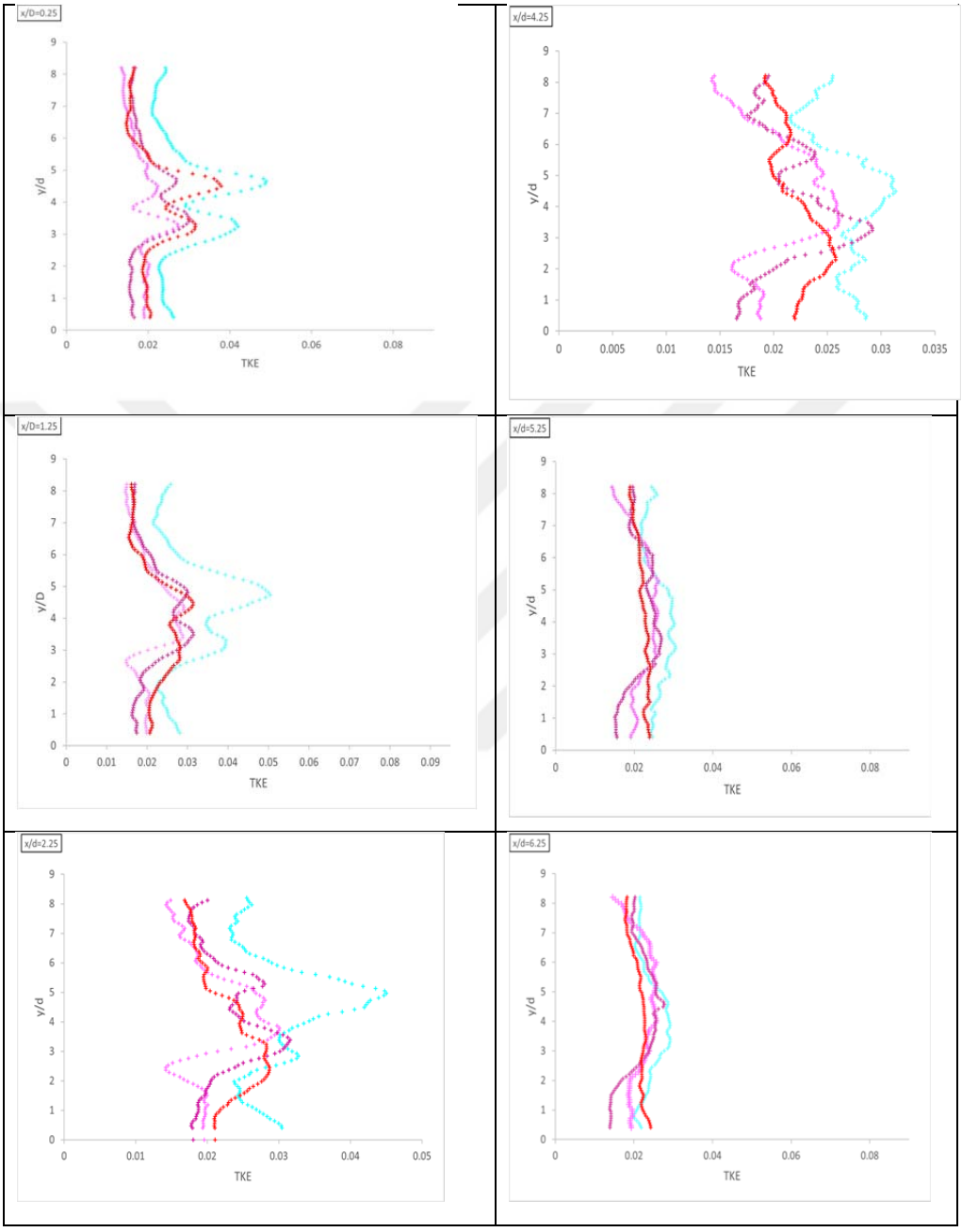
x/D=0.25
y/d
TKE
x/d=4.25
y/d
TKE
x/D=1.25
y/D
TKE
x/d=5.25
y/d
TKE
x/d=2.25
y/d
TKE
x/d=6.25
y/d
TKE

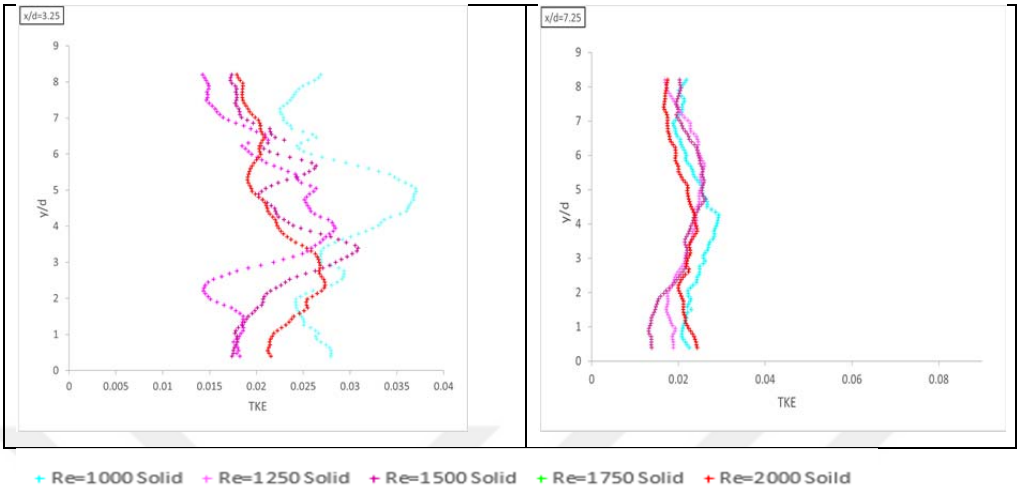

Figure 4.15. The variation of planar TKE along spanwise direction with the solid cylinder employment for different cases at different location of <x/d>.

Figure 4.16. shows the impact of perforated cylinder around single cylinder Instantaneous dye visualization pictures for various reynolds number with numerical results. When we look at the flow configuration at this figure 4.16, the narrow wake region and absence of Karman Vortex Street draws attention. So, these PIV results at the figure 4.6 match up with numerical visualization results and this configuration can be regarded as successful to control the flow. Creating of karman street and vortex formation was been seen very far from of cylinder for instance at the reynold 500, It is seen at least 4d more then of cylinder center. There fore this configuration also seems to be effective controling methode.

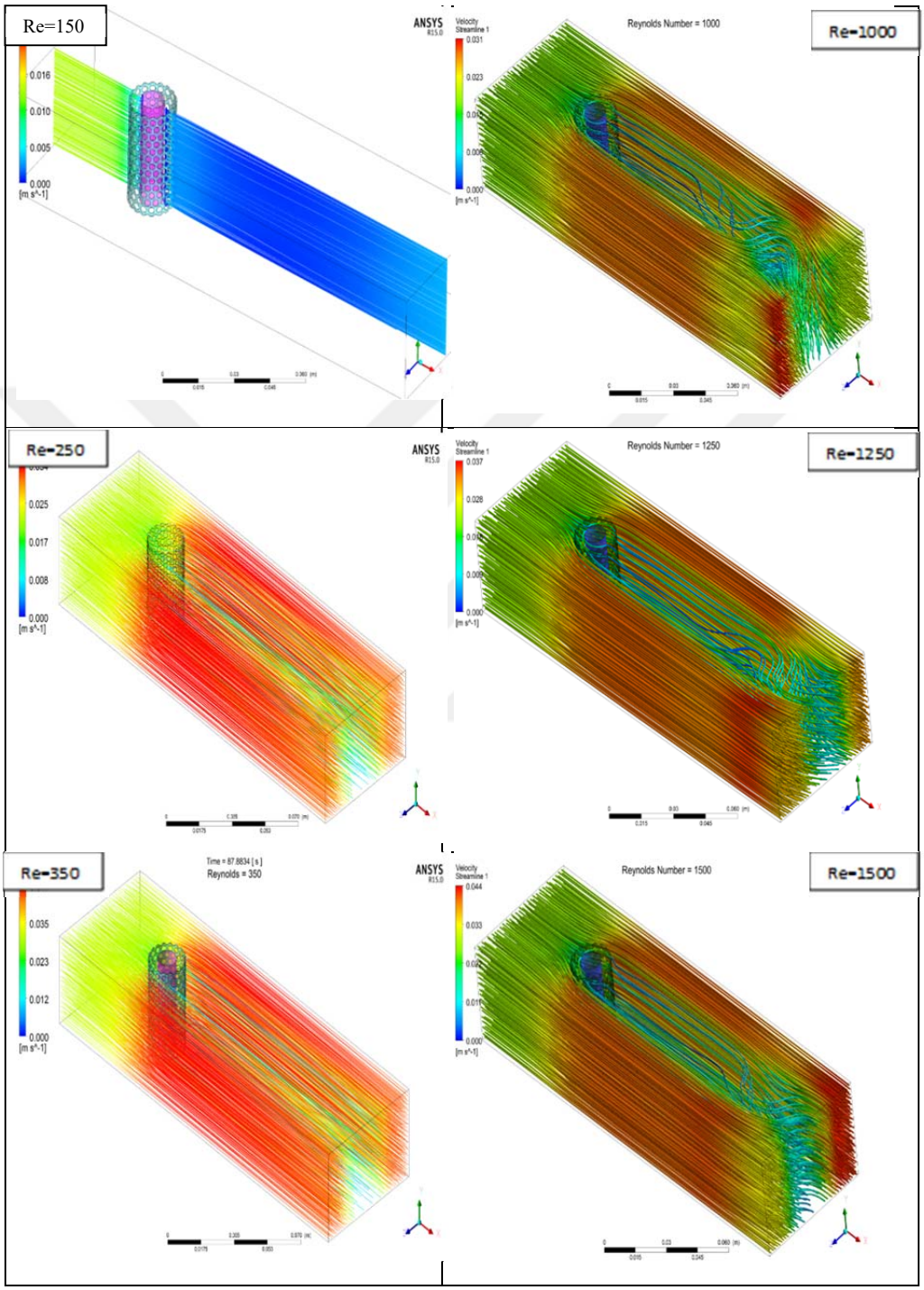
Re=150
0.016
0.010
0.005
0.000
[m s^-1]
ANSYS
Velocity
Streamline 1
Reynolds Number = 1000
Re=1000
Re=250
0.025
0.017
0.008
0.000
[m s^-1]
Reynolds Number = 1250
Re=1250
Re=350
Time = 87.8834 [s]
Reynolds = 350
0.035
0.023
0.012
0.000
[m s^-1]
Reynolds Number = 1500
Re=1500

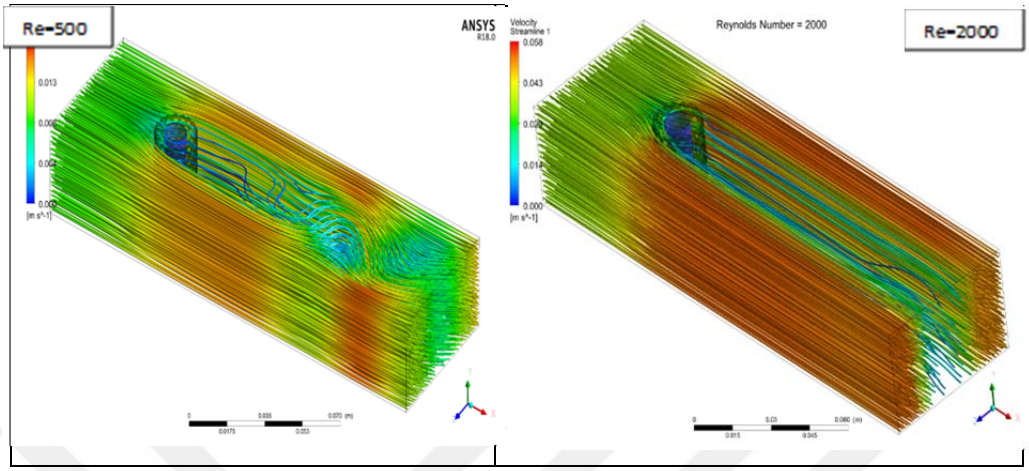

Figure 4.16. Instantaneous dye visualization pictures for various porosity of perforated cylinder, at different Reynolds Numbers. (Numerical results)

Figure 4.17 shows the effect of the perforated cylinder use on the contours of normalized velocity <u/U> in flow direction. It demonstrates the expermental results of velocity profiles for both solid cylinder and perforated cylinder along span wise direction at various positions of stream wise direction.In this figure, the streamwise distance, x is non dimensionalized with the diameter of the single solid cylinder, d. It is shown that the deployment of perforated cylinder will eliminates the region of negative <u/U> contours behind the cylinder in both longitudinally (streamwise) and in traverse (spanwise) directions for all tested Reynolds numbers the placement of the perforated cylinder accelerates the flow because of the holes provided by the surface of the perforated cylinder. This is in accordance with the results obtained from time-averaged streamline patterns which denotes that the utilization of perforated cylinder makes the focal and saddle points either disappear or which went quite close to the solid cylinder after placement of the perforated cylinder. It is shown on the wake region, like as x/d = 0.25 and 1.25, the magnitude of negative velocity is at the peak points for the solid circular cylinder, that negative peak point goes to positive side at the end of the field of x/d = 7.25. the

impact of jet-like flow for perforated cylinder can be perspicuously comprehensible along the span-wise direction. For x/d=0.25 to x/d=2.25 minimum velocity can be seen on the negative part in this study. This situation should also give rise to decrease in the drag force over the cylinder surface. The jet-alike phenomena described in the previous studies is clearly seen. This can be more understood by looking at the vorticity distribution assessed.

Figure 4.18 anf figure 4.19 is obvoused streamwise Reynolds normal stress, <u′u′>and <v′v′> transversal Reynolds normal stress, with attention to spanwise direction at the different downstream positions of x/d = 0.25, 1.25,2.25,3.25,4.25,5.25,6.25 and 7.25.

For the streamwise Reynolds normal stress, it is obvious from the figures presented that the minimum amountsof <u′u′> tot he solid and perforated cylinder, for both have had a desire to touch in the average amount of the spanwise direction (y/d = 3.5) . As expected, the values of <u′u′>for single cylinder has larger than the perforated cylinder at all reynolds number at variouse location, and alsoto the single cylinder, two clear peaks are observable at any stream wise location.

The peak amount of <u′u′>are alittle more than 0.075 for the solid cylinder at x/d =2.25 and 3.25; however, it has been limited from 0.01 to 0.02 at all stream-wise locations for state after located the perforated cylinder at the diffrent Reynolsd number. Acoording figure 4.16 the values of<u′u′> come close to zero value at the all x/d distance, and it can be conclude that there is approximately any bluff body to been barricade against the flow.

Figure of 4.19 ilistrude the transverse Reynolds normal stress, <v’v’> with respect to spanwise direction for various Reynolds numbers at different downstream locations of x/d. At first glance, the transversal Reynolds normal stress amounts can be understod that There are the specific differences between solid and perforated cylinders. According to these results, even for the low x/d ratits, there is a big gap between solid and perforated cylinder values and there are peak values for all of the cases.

Also At the figure 4.19, this gap amongst oscillate results distribution of the single and perforated cylinder was ambiguously get to near along the spanwise direction at the higher x/d raties.

Having the streamwise Reynolds normal stress and transverse Reynolds normal stress, we can show the planar turbulent kinetic energy distribution. Figure 4.19 illustrates a representation of the distribution of planar turbulent kinetic energy (TKE) values with respect to the spanwise direction for various streamwise locations. with using of stream wise Reynolds stress and transverse Reynolds stress, distributionof turbulent kinetic energy able to calculate like previous studies.

According to Figur4.20 aditinaly, supplays a profound idea of the distribution of turbulent kinetic energy (TKE) amounts with respect to the spanwise way for diffrent streamwise positions. The significant various of the distribution for single cylinder would be the seeing of the weekend of two distinct peak points all the location of saddle point, also it would be perfect to see back Figure 4.6 to recognize the saddle point as a result of the templates of streamlines models. The two distinct peaks happen after that for the rest of the stream-wise position as expected due to the dominance of separated shear layersafter placment of perforated cylinders around single cylinder.

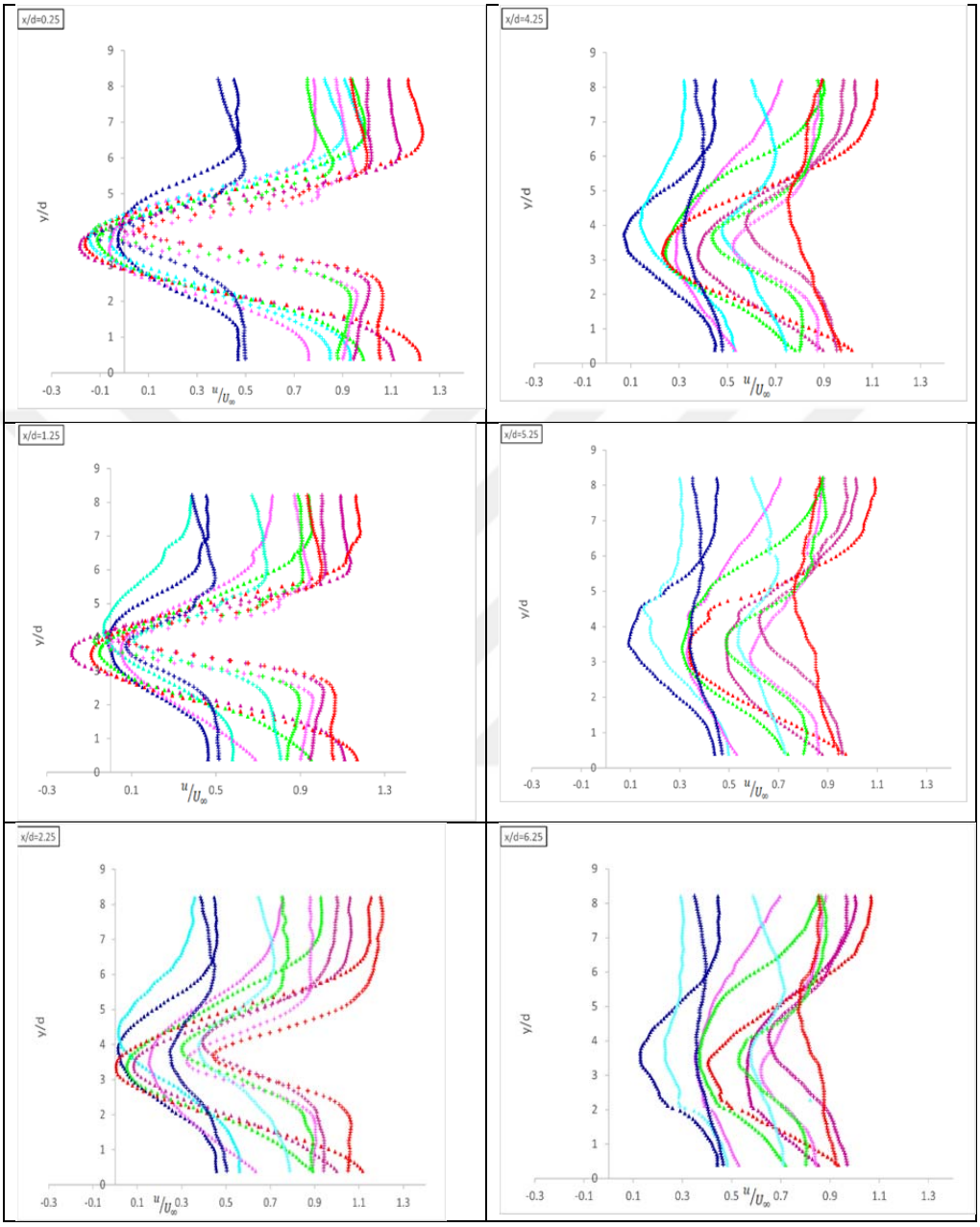
x/d=0.25
x/d=4.25
x/d=1.25
x/d=5.25
x/d=2.25
x/d=6.25
y/d
u/u∞

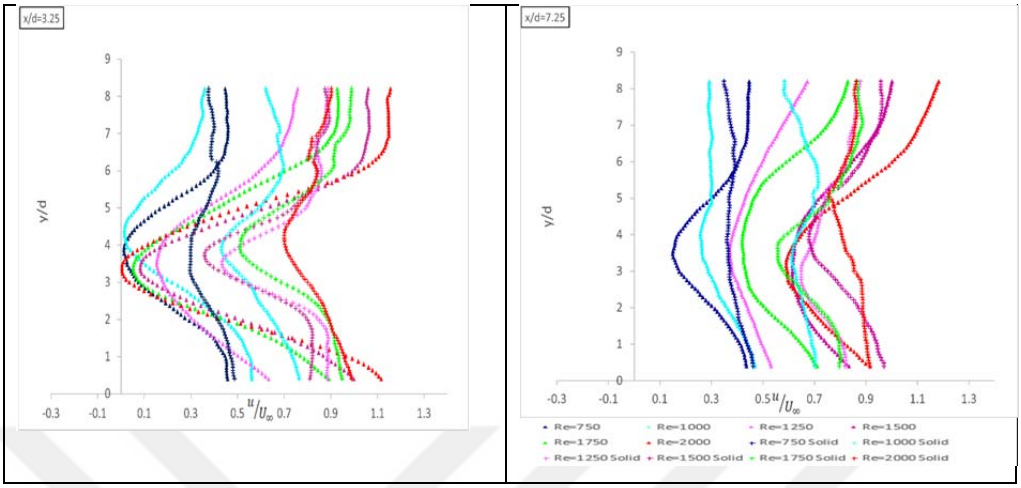

Figure 4.17. The variation of planar velocity along spanwise direction for different cases at different location of x/d.(Expermental results)

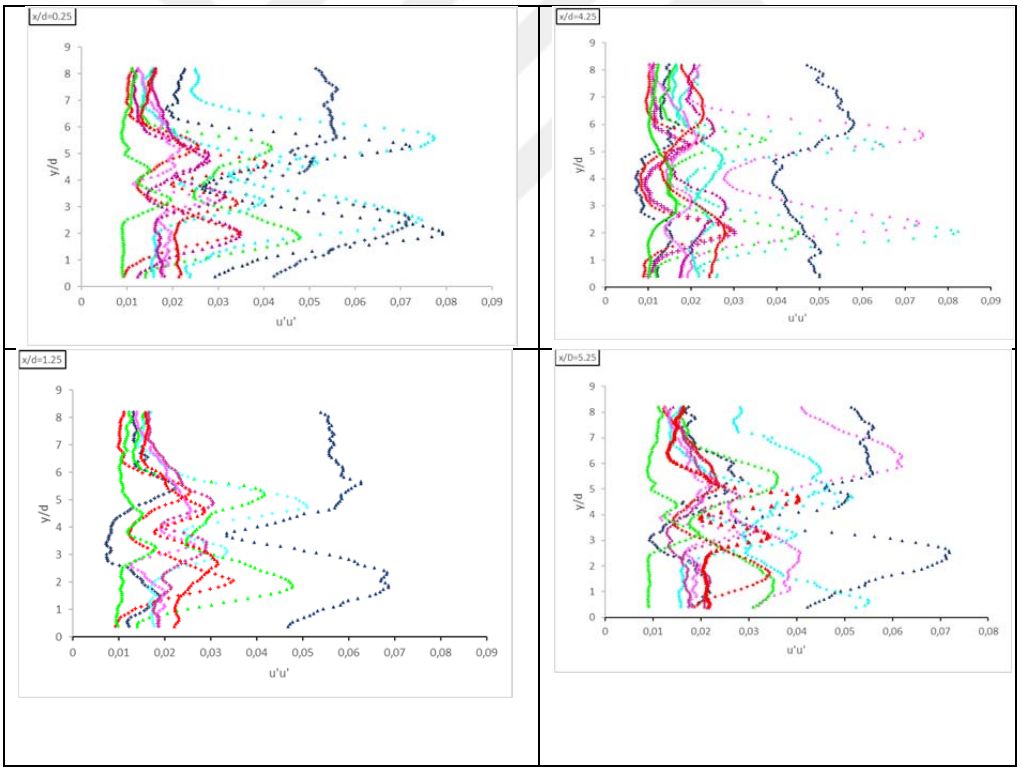

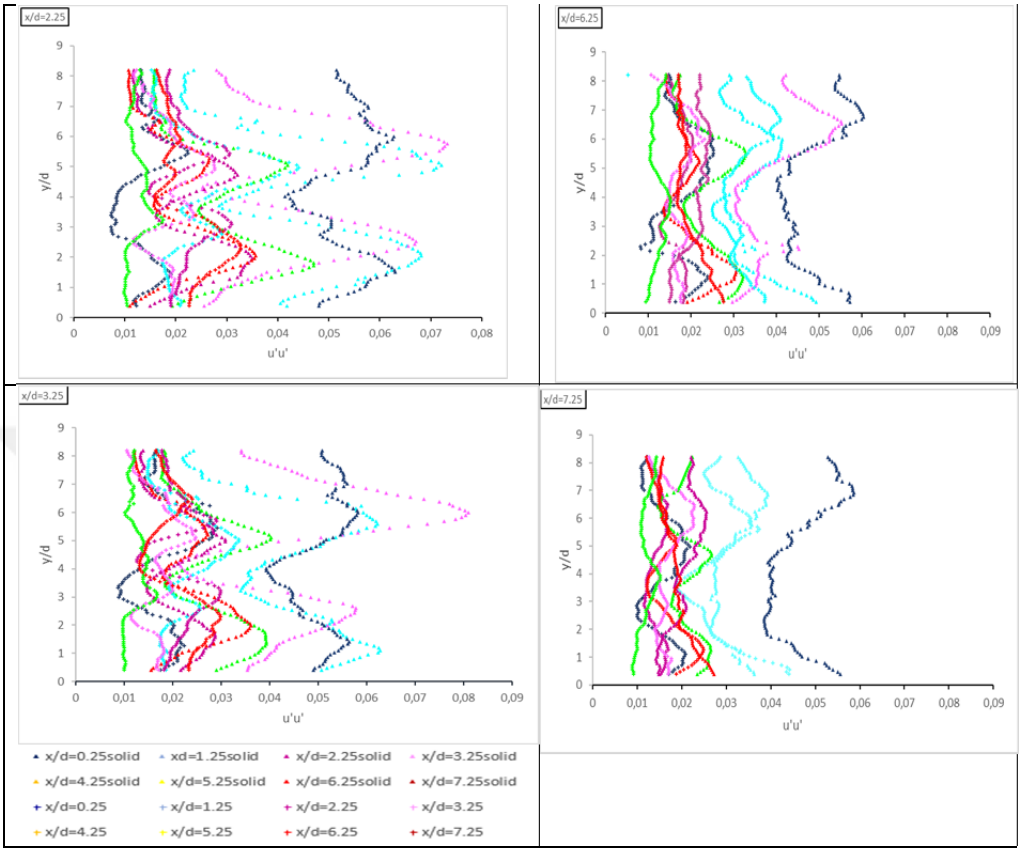

Figure 4.18. The variation of <u'u'> along span-wise direction for different cases at various locations of x/d (Experimental results)

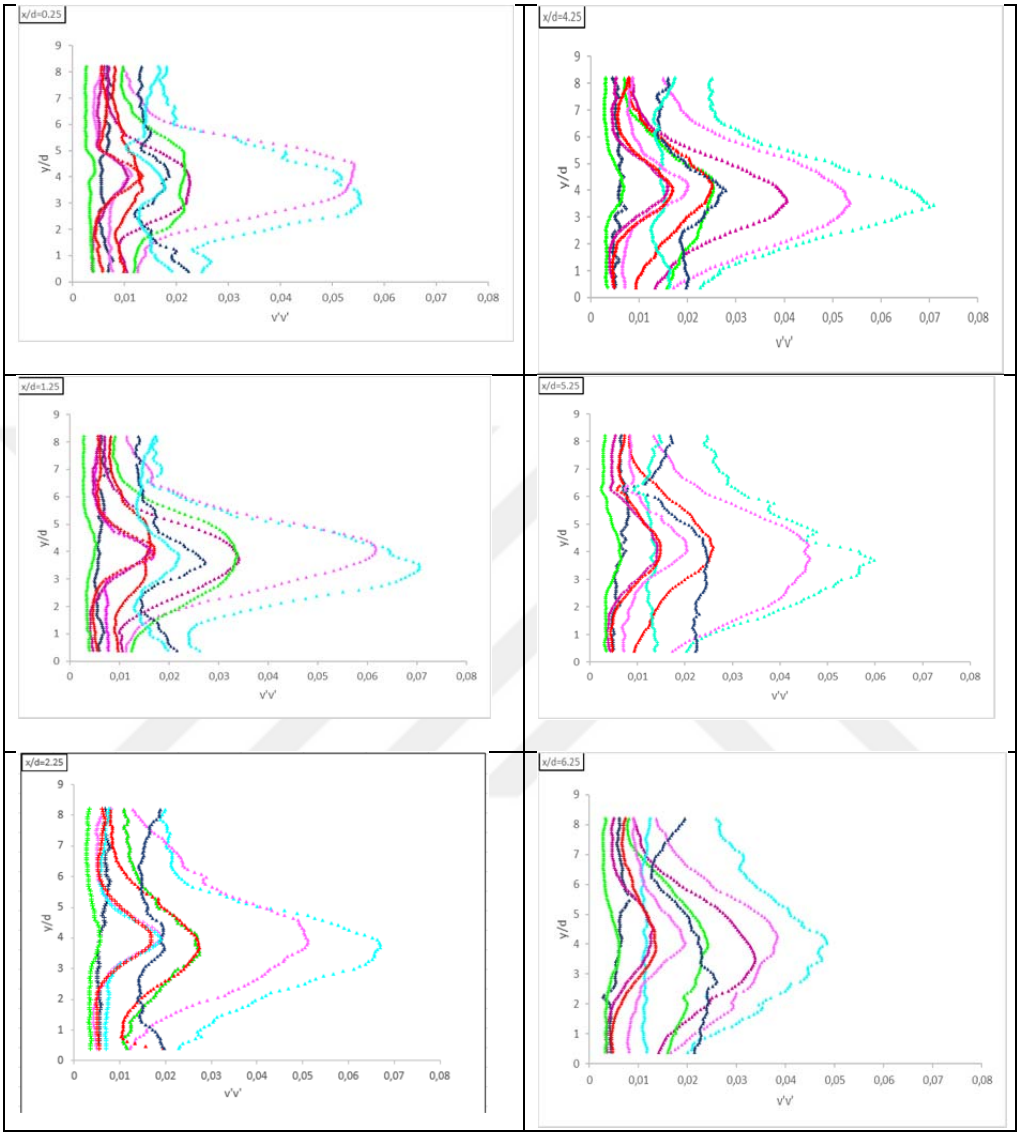
x/d=0.25
x/d=4.25
x/d=1.25
x/d=5.25
x/d=2.25
x/d=6.25
y/d
v'v'
0
1
2
3
4
5
6
7
8
9
0,01
0,02
0,03
0,04
0,05
0,06
0,07
0,08

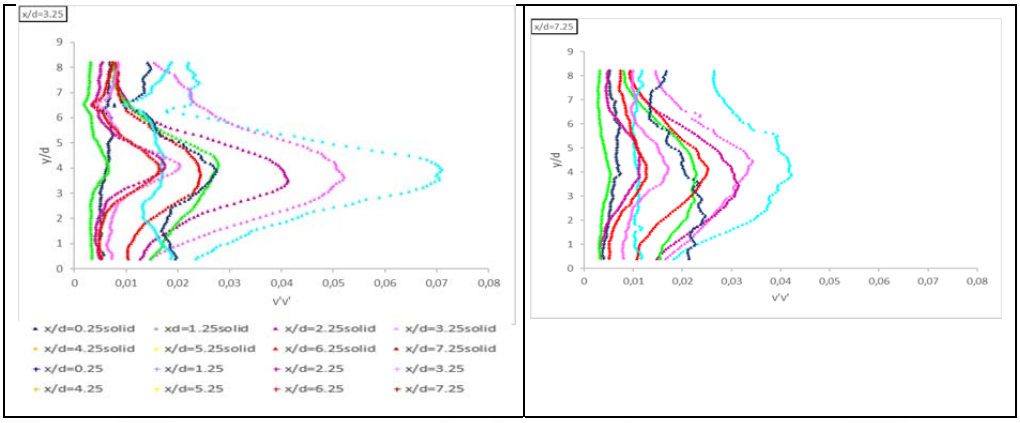

Figure 4.19. The variation of <v'v'> along span-wise direction for different cases at various locations of x/d. (Experimental results)

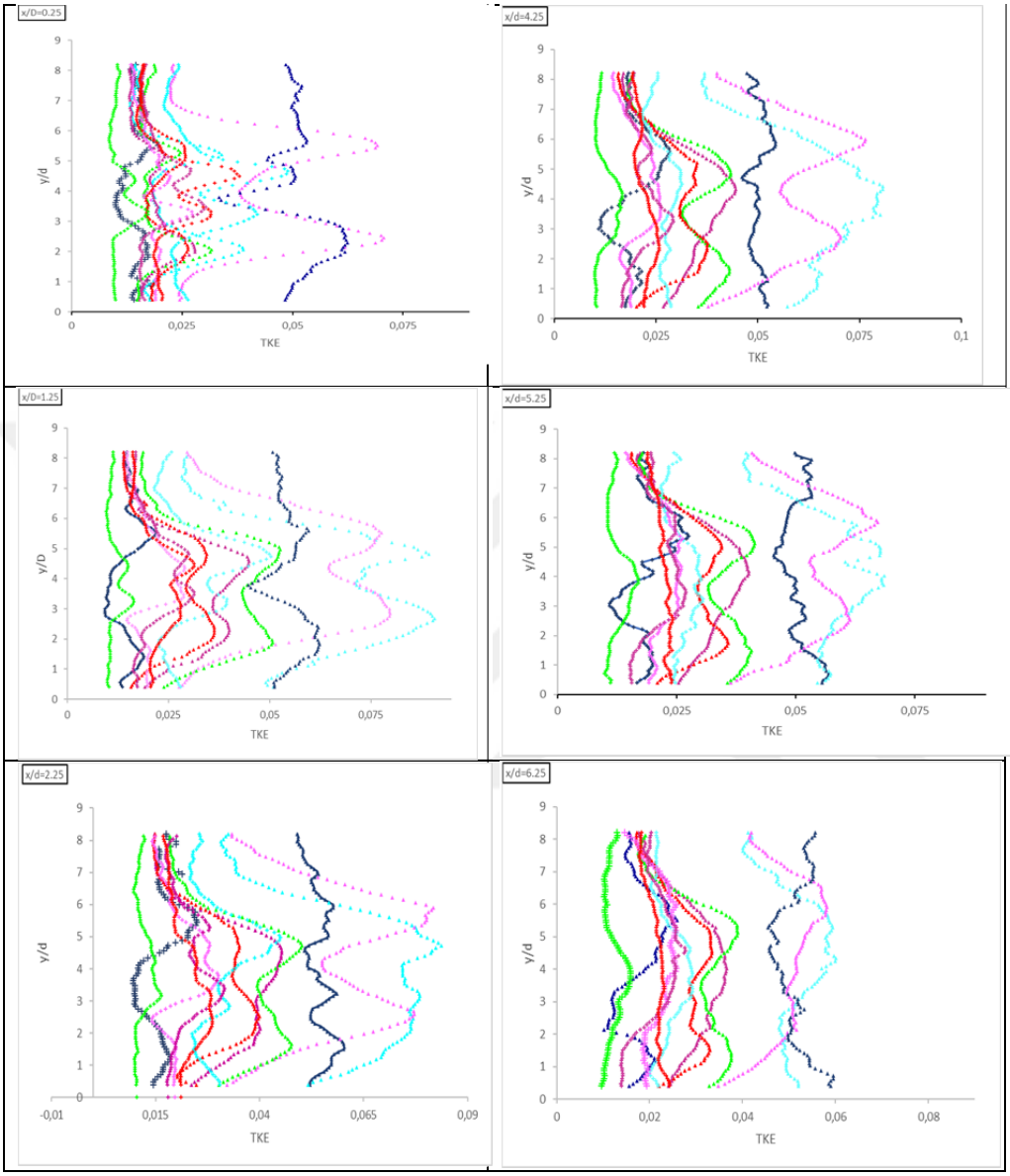
x/D=0.25
y/d
TKE
x/d=4.25
y/d
TKE
x/D=1.25
y/D
TKE
x/d=5.25
y/d
TKE
x/d=2.25
y/d
TKE
x/d=6.25
y/d
TKE

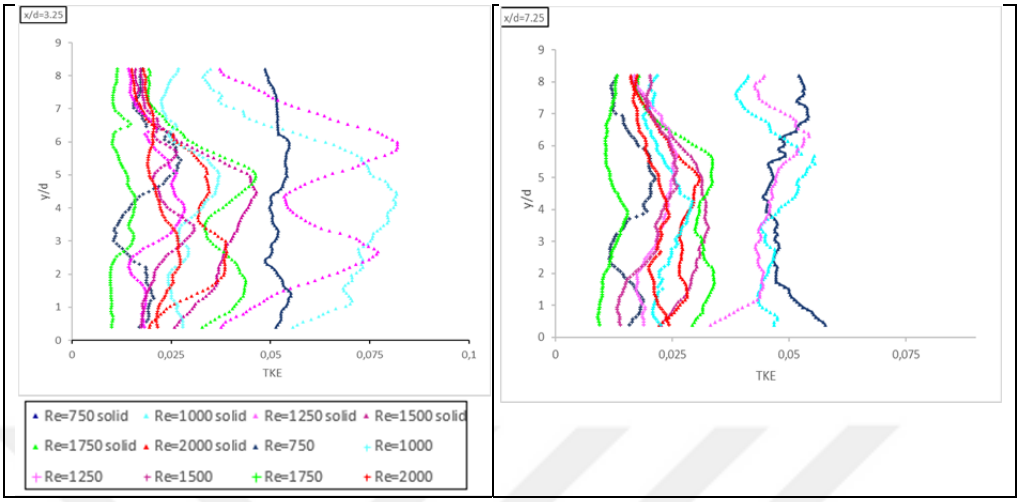

Figure 4.20. The variation of planar TKE along span-wise direction different Reynolds at different location of x/d.(Expermental results)

4.5. The Effect of Perforated Cylinder on Drag coefficient

Figure 4.20 shows variation of the time averaged drag coefficient of the cylinder, $<C_d>$ with respect Reynolds nomber, β=0.5 and d/D=0.5.Firstly, Force measurement is performed for the solid cylinder in order to compare the magnitude of drag coefficient, $<C_d>$ with results of current control method. The time averaged drag coefficient of the solid single cylinder is calculated as $<C_d>$ =1.54 for the Reynolds number Re=150. Using the perforated cylinder remarkably affects the drag coefficient, $<C_d>$ of the cylinder. It is obtained that the variation of the drag coefficient, $<C_d>$ of the cylinder with the porosities of perforated cylinder have similar trend for Re=150. The drag coefficient, $<C_d>$ of the cylinder is reduced by 45% for the porosity value of β=0.5 at the Re=150. At the perforated cylinder, the momentum transfer into the gap is reduced, so that the drag coefficient, $<C_d>$ of the cylinder is remarkably lower than the solid single cylinder. However, the vortex formation of the cylinder is observed in the gap region between the cylinder and the perforated cylinder for all cases. Moreover, it should also be pointed out that even for the porosity value of β=0.5, the drag coefficient,

<C_d> of the cylinder is obtained with 20% and 22% lower than the bare cylinder case at Re=1000 and 2000, respectively.

The force measurements were also performed for the cylinder along with perforated cylinders, and also the total drag coefficient was separately calculated based on both the frontal area of cylinder.

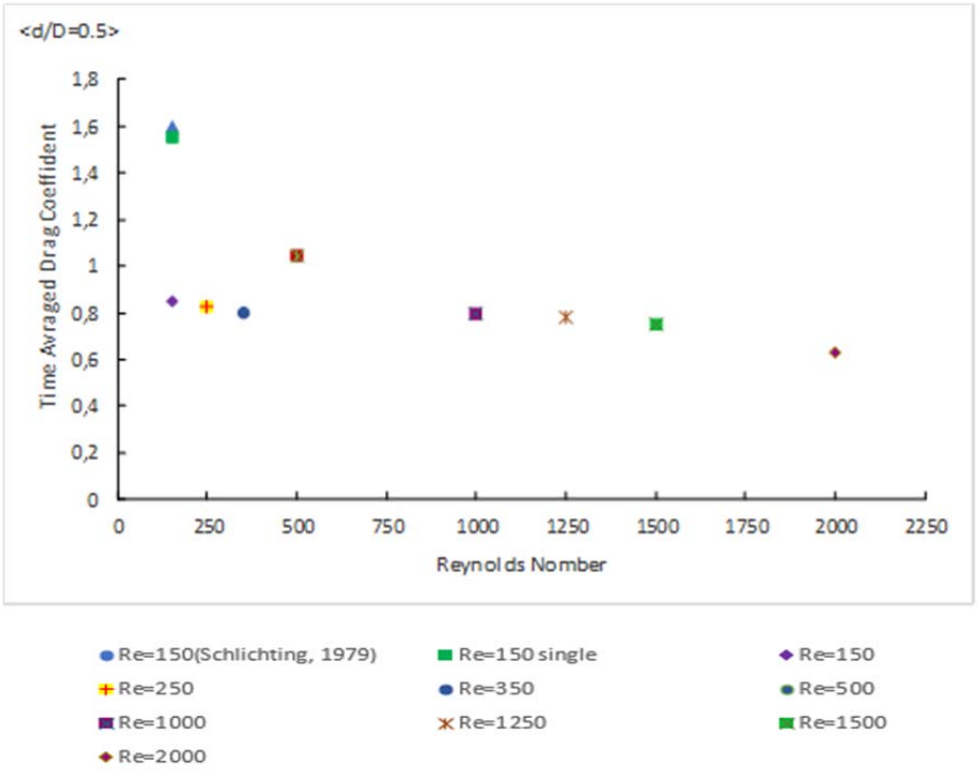

Figure 4.21. Variation of the time averaged drag coefficient of the cylinder, <C_d> with respect to the porosity, at the various Reynolds nomber (Numerical Results)

In conclusion, the flow structure downstream of cylinder is significantly affected by porosity of perforated cylinder, <β=0.5>. The drag results and the PIV measurements are in close agreement with each other in the scope of this investigation. This reveal that the Cd can be effectively reduced by applying perforated shrouds cylinder.

5. CONCLUSIONS AND RECOMMENDATIONS

One of the basic research topics to reduce and control or eliminate the adverse effects on downstream of bluff bodies is using the shrouds in this regard, but it has not been fully investigated at the low Reynolds numbers up to now. The perforated cylinder was utilized in this investigation as a shroud around a solid circular cylinder.

The objective of the present research is to investigate the effects of the placement of a perforated cylinder with a constant porosity and diameter on the flow structure such as vortex shedding, streamlines, wake ragion, vorticity and Drag cofficient over the cylinder in downstream direction by using CFD simulations along with the PIV technique in deep water at the low Reynolds numbers. The diameter of the cylinder was kept constant as d=10 mm where the free stream velocity was changed which corresponds to the Reynolds number of Re=750,1000,1250,1500,1750 and 2000 at PIV method and Re=150,250,350,500,750,1000,1250,1500,2000 with CFX. Fixed porosity value which are β=0.5. Firstly, it was focused on the flow structure in the gap region between the cylinder and the perforated cylinder as well as the near wake region of the perforated cylinder, and to investigate the effect of the perforated cylinder on the drag reduction that led to have reduction of vibration around cylinder.

It can be concluded in the light of obtained PIV results that the flow structure of the cylinder in the near-wake region is significantly affected by the perforated cylinder for all Reynolds. At diameter ratio of d/D=0.5, the negative velocity contours for porosity values of β=0.5 indicate that the narrow gap is inadequate to transfer the momentum from inside of perforated cylinder into the near-wake region. The reverse flow, therefore, occurs in the near-wake region because of the momentum transfer from the shear layers of the perforated cylinder into the near – wake region. Also, the drag coefficient of cylinder is reduced by 45% for porosity value of Re=150. However, the vortex formation of the cylinder

is observed in the gap between the cylinder and the perforated cylinder for Re=150,250,350 and 2000 , with the difference that their length and value have become much smaller than compare of single cylinder and in the rest of the Reynolds values, they have been completely eliminated.It was seen that like other studies with higher Reynolds numbers becouse of the holes on the surface of the perforated cylinder do provide the jet like flow in the wake region, and the Karman vortex street has been eliminated in comparison with the solid cylinder case . it approved by according the results of the flow regime in the case of adding the perforated cylinder compared to the single solid cylinder case.

Since this study has revealed benign results on the drag reduction by using perforated cylinders, it can be expected that the results would benevolently guide the engineers for further investigations. The future work about this topic will be studied numerically and this study with attached plate would be excellent example as a reference for the researchers as well. At the total according to previous studies, the perforated shroud cases show better drag reduction relative to other cases and addinthially, suppression of Karman vortex street is receivable by indeed utilize of perforated cylinder around single cylinder.

Due to the failure of our PIV apparatus, it is a good idea to develop the experimental measurements for the post-deployment of the perforated cylinder. It is interpreted that the bluff body effect will be eliminated or weakened noticeably after placement of the perforated cylinder. Considering this, we may conclude that the constant porosity value of 0.5 is the optimum one like as it was before for higher Re numbers in the previous studies. Based on this limitation and since the placement of the perforated cylinder in this investigation was concentric with respect to the solid cylinder; as a possibility, the eccentric placement of the perforated cylinder may be tested in the future.

REFERENCES

A. Ekmekci, “Circular cylinders fitted with small-scale straight and helical wires: A comparative study on the wire-induced critical effects,” Exp. Therm. Fluid Sci., vol. 53, pp. 179–189, Feb. 2014, doi: 10.1016/j.expthermflusci.2013.12.003.

A. Kahraman, B. Sahin, and D. Rockwell, “Control of vortex formation from a vertical cylinder in shallow water: Effect of localized roughness elements,” Exp. Fluids, vol. 33, no. 1, pp. 54–65, Jul. 2002, doi: 10.1007/s00348-002-0467-y.

A. Thom, “The flow past circular cylinders at low speeds,” 1933, doi: 10.1098/RSPA.1933.0146.

Ahmed, A., and Bays-Muchmore, B., 1992. Transverse Flow over a Wavy Cylinder. Phys. Fluids A, 4: 1959-1967.

Amitay, M., Honohan, A., Trautman, M., and Glezer, A., 1997. Modification of the Aerodynamic Characteristics of Bluff Bodies Using Fluidic Actuators. AIAA 97-2004.

Assi, G.R.S., Bearman, P.W., Kitney, N., and Tognarelli, M.A., 2010. Suppression of Wake-Induced Vibration of Tandem Cylinders with Free-to-Rotate Control Plates. Journal of Fluids and Structures, 26:1045–1057.

B. Gozmen, H. Akilli, and B. Sahin, “Passive control of circular cylinder wake in shallow flow,” Measurement, vol. 3, no. 46, pp. 1125–1136, 2013, doi: 10.1016/j.measurement.2012.11.008.

B. Molin, “A Potential Flow Model for the Drag of Shrouded Cylinders,” J. Fluids Struct., vol. 7, no. 1, pp. 29–38, Jan. 1993, doi: 10.1006/jfls.1993.1003.

B. Molin, “Hydrodynamic modeling of perforated structures,” Appl. Ocean Res., vol. 33, no. 1, pp. 1–11, Feb. 2011, doi: 10.1016/j.apor.2010.11.003.

Bandyopadhyay, PR., 1986. Review—Mean Flow in Turbulent Boundary Layers Disturbed to Alter Skin Friction, Trans. ASME Journal of Fluids Engineering 108, 127-140.

Bao, Y. and Tao, J., 2013. The Passive Control of Wake Flow behind a Circular Cylinder by Parallel Dual Plates. Journal of Fluids and Structures, 37:201-209.

Bearman, P., and Brankovic, M., 2003. Experimental Studies of Passive Control of Vortex-Induced Vibration. European Journal of Mechanics B/Fluids, 23: 9-15.

Bearman, P.W., 1965. Investigation of Flow behind a Two-dimensional Model with Blunt Trailing Edge and Fitted with Splitter Plates, Journal of Fluid Mechanics, 21, 241–255.

Bearman, P.W., 1965. Investigation of Flow behind a Two-dimensional Model with Blunt Trailing Edge and Fitted with Splitter Plates, Journal of Fluid Mechanics, 21, 241–255.

Bearman, 1967, The Effect of Base Bleed on the Flow behind a Two dimensional Model with a Blunt Trailing Edge, The Aeronautical Quaterly,18; 207-224.

Bearman,, 1984. Vortex Shedding From Oscillating Bluff Bodies. Annual Review of Fluid Mechanics, 16: 195-222.

Boorsma, K., Zang, X., and Molin, N., 2010. Landing Gear Noise Control Using Perforated Fairings. Acta Mechanica Sinica, 26:159-174.

Bovand, M., Rashidi, S., Dehghan, M., Esfahani, J.A., and Valipour, M.S., 2015. Control of Wake and Vortex Shedding Behind a Porous Circular Obstacle by Exerting an External Magnetic Field, J. Magn. Magn. Mater, 385:198-206.

C. J. Apelt, “The steady flow of a viscous fluid past a circular cylinder at Reynolds numbers 40 and 44,” 1958, Accessed: Dec. 17, 2021. [Online]. Available: https://reports.aerade.cranfield.ac.uk/handle/1826.2/3744

C.-K. Chyu and D. Rockwell, “NEAR-WAKE FLOW STRUCTURE OF A CYLINDER WITH A HELICAL SURFACE PERTURBATION,” J. Fluids Struct., vol. 16, no. 2, pp. 263–269, Feb. 2002, doi: 10.1006/jfls.2001.0419.

Chen, Z.H., and Aubry, N., 2005. Active Control of Cylinder Wake. Communications in Nonlinear Science and Numerical Simulation, 10:205-216.

Choı, H., Jeon, W-P., and Kim, J., 2008. Control of Flow over a Bluff Body. Annual Review of Fluid Mechanics, 40:113-139.

Cimbala, M., and Garg, S., 1991. Flow in the Wake of a Freely Rotatable Cylinder with Splitter Plate. AIAA Journal, 29:1001-1003.

D. Wei, H. Yoon, and J. H. Jung, “Characteristics of aerodynamic forces exerted on a twisted cylinder at a low Reynolds number of 100,” Comput. Fluids, vol. 136, Jul. 2016, doi: 10.1016/j.compfluid.2016.07.002.

Delaunay, Y. and Kaiktsis, L., 1999. Active Control of Cylinder Wakes: Use of Base Suction and Blowing. ESAIM: Proceedings, 7:104-119.

E. Firat, G. M. Ozkan, and H. Akilli, “PIV measurements in the near wakes of hollow cylinders with holes,” Exp. Fluids, vol. 58, no. 5, p. 39, Apr. 2017, doi: 10.1007/s00348-017-2334-x.

E. Pinar, G. M. Ozkan, T. Durhasan, M. M. Aksoy, H. Akilli, and B. Sahin, “Flow structure around perforated cylinders in shallow water,” J. Fluids Struct., vol. 55, pp. 52–63, May 2015, doi: 10.1016/j.jfluidstructs.2015.01.017.

E. Pinar, T. Durhasan, G. Ozkan, M. Aksoy, H. Akilli, and B. Sahin, “The effects of perforated cylinders on the vortex shedding on the suppression of a circular cylinder,” EPJ Web Conf., vol. 143, p. 02094, Jan. 2017, doi: 10.1051/epjconf/201714302094

Every, M.J., King, R., and Weaver, D.S., 1982. Vortex- Excited Vibrations of Cylinders and Cables and their Suppression. Ocean Engineering, 9: 135-

Hsiao, F.B., and Shyu, J.Y., 1991. Influence of Internal Acoustic Excitation upon Flow Passing a Circular Cylinder. Journal of Fluids and Structures, 5: 427-442.

Fujisawa, N., Takeda, G., and Ike, N., 2003. Flow Control around a Circular Cylinder by Internal Acoustic Excitation. Journal Fluid Structures, 17:903–913.

Gabbai, R.D., and Benaroya, H., 2004. An Overview of Modeling and Experiments of Vortex Induced Vibration of Circular Cylinder. Journal of sound and Vibration, 282:575-616

Galvao, R., Lee, E., Farrell, D., Hover, F., Triantafyllou, M., Kitney, N., and Beynet, P., 2008. Flow Control in Flow–Structure Interaction. Journal of Fluids and Structures, 24: 1216-1226.

Gao, Y., Fu, S., Wang, J., Song, L., and Chen, Y., 2015. Experimental Study of the Effects of Surface Roughness on the Vortex-Induced Vibration Response of a Flexible Cylinder. Ocean Engineering, 103: 40-54.

Kumar, R.A., Sohn, C-H., and Bangalore, H.L., 2008. Passive Control of Vortex-Induced Vibrations: An Overview. Recent Patents on Mechanical Engineering, 1:1-11.

Gerrard, J.H., 1966. The Mechanics of the Formation Region of Vortices behind Bluff Bodies. Journal of Fluid Mechanics, 25: 401-413.

Gozmen, B., Akilli, H., and Sahin, B., 2013. Passive Control of Circular Cylinder Wake in Shallow Flow. Measurement, 46:1125-1136.

Gozmen, B., and Akilli, H., 2014. Flow Control Downstream of a Circular Cylinder by a Permeable Cylinder in Deep Water. Wind structure Int. j., 19:389-404.

H. Akilli, B. Sahin, and N. Ozdil, “Suppression of vortex shedding of circular cylinder in shallow water by a splitter plate,” Flow Meas. Instrum. - FLOW MEAS INSTRUM, vol. 16, pp. 211–219, Aug. 2005, doi: 10.1016/j.flowmeasinst.2005.04.004.

H. Akilli, C. Karakus, A. Akar, B. Sahin, and N. F. Tumen, “Control of Vortex Shedding of Circular Cylinder in Shallow Water Flow Using an Attached Splitter Plate,” J. Fluids Eng., vol. 130, no. 4, Apr. 2008, doi: 10.1115/1.2903813.

H. Lim and S.-J. Lee, “Flow control of a circular cylinder with O-rings,” Fluid Dyn. Res., vol. 35, pp. 107–122, Aug. 2004, doi: 10.1016/j.fluiddyn.2004.05.001.

H. Nisi and A. W. Porter, “LXXXVI. On eddies in air,” Lond. Edinb. Dublin Philos. Mag. J. Sci., vol. 46, no. 275, pp. 754–768, Nov. 1923, doi: 10.1080/14786442308565237.

He, J.W., Chevalier, M., Glowinski, R., Metcalfe, R., Nordlander, A. and Periaux, J., 2000. Drag Reduction by Active Control for Flow Past Cylinders. In Computational mathematics driven by industrial problems, Berlin, 287–363.

Hsiao, F.B., and Shyu, J.Y., 1991. Influence of Internal Acoustic Excitation upon Flow Passing a Circular Cylinder. Journal of Fluids and Structures, 5: 427-442.

Igarashi, T., 1978. Flow Characteristics around a Circular Cylinder with a Slit. Bulletin of the Japan Society of Mechanical Engineers, 21;656–664.

Ingham, D.B., 1983. Steady Slow Past a Rotating Cylinder, Computers & Fluids, 11(4); 351-366

Ingham, D.B., and Tang, T., 1990. A Numerical Investigation into the Steady Flow Past a Rotating Circular Cylinder at Low and Intermediate Reynolds Numbers, Journal of Computational Physics, 87(1);91-107.

J. H. Gerrard, “Flow around Circular Cylinders; Volume 1. Fundamentals. By M. M. Zdravkovich. Oxford Science Publications, 1997. 672 pp. £120.,” J. Fluid Mech., vol. 350, pp. 375–378, Nov. 1997.

Jukes, T. N., and Choi, K.S., 2009. Flow Control around a Circular Cylinder Using Pulsed Dielectric Barrier Discharge Surface Plasma. Physics of Fluids, 21:127-139.

Kumar, R.A., Sohn, C-H., and Bangalore, H.L., 2008. Passive Control of Vortex-Induced Vibrations: An Overview. Recent Patents on Mechanical Engineering, 1:1-11.

Kuo, C.-H., and Chen, C.-C., 2009. Passive Control of Wake Flow by Two Small Control Cylinders at Reynolds Number 80. Journal of Fluids and Structures, 25:1021–1028.

Kuo, C.-H., Chiou, L.-C., and Chen, C.-C., 2007. Wake Flow Pattern Modified by Small Control Cylinders at Low Reynolds Number. Journal of Fluids and Structures, 23:938–956.

L. Najafi, E. Firat, and H. Akilli, "Time-averaged near-wake of a yawed cylinder," Ocean Eng., vol. C, no. 113, pp. 335–349, 2016, doi: 10.1016/j.oceaneng.2015.12.045.

Lim, H.C., and Lee, S.J., 2004. PIV Measurements of Near Wake behind a U-Grooved Cylinder. Journal of Fluids and Structures, 18:119–130.

Lee, S-J., and Kim, H-B., 1997. The Effect of Surface Protrusions on the Near Wake of a Circular Cylinder, Journal of Wind Engineering and Industrial Aerodynamics, 69–71:351-361.

Lee, S-Y., and Lee, J-Y., 2006. Flow Structure of Wake behind a Rotationally Oscillating Circular Cylinder, Journal of Fluids and Structures, 22(8);1097-1112.

M. C. Valencia-Cárdenas and C. A. Riveros-Jerez, "Numerical Based Approach for Predicting the Response of Flexible Risers Under Oscillatory Flows at Low Re and KC Numbers," Sci. Tech., vol. 24, no. 1, pp. 113–124, 2019.

M. Kawaguti, "Numerical Solution of the Navier-Stokes Equations for the Flow around a Circular Cylinder at Reynolds Number 40," J. Phys. Soc. Jpn., vol. 8, no. 6, pp. 747–757, Nov. 1953, doi: 10.1143/JPSJ.8.747.

M. Silva-Ortega and G. R. S. Assi, “Suppression of the vortex-induced vibration of a circular cylinder surrounded by eight rotating wake-control cylinders,” J. Fluids Struct., vol. 74, pp. 401–412, Oct. 2017.

Marris, A.W., 1964. A Review on Vortex Streets, Periodic Wakes, and Induced Vibration Phenomena. Journal of Basic Engineering, 86(2), 185-193.

Miau, J.J., Yang, J.H., and Lee, K.R., 1993. Suppression of Low Frequency Variations in Vortex Shedding by a Splitter Plate behind a Bluff Body, Journal of Fluids and Structure, 7:897-912.

Mimeau, C., Mortazavai, I., and Cottet, G-H., 2014. Passive Flow around a Semi-Circular Cylinder Using Porous Coatings. International Journal of Flow Control, 6(1);43-60.

Molin, B., 1993. A Potential Flow Model for the Drag of Shrouded Cylinders. Journal of Fluids and Structures, 7: 29-38.

Nakamura, Y., 1996. Vortex Shedding from Bluff Bodies with Splitter Plates, Journal of Fluids and Structures, 10(2):147-158.

Nakamura, H., Igarashi, T., 2008. Omnidirectional Reductions in Drag and Fluctuating Forces for a Circular Cylinder by Attaching Rings. Journal of Wind Engineering, 96:887–899.

Nebres, J., Batill, S., 1993. Flow about a Circular Cylinder with a Single Large-Scale Surface Perturbation. Experiments in Fluids, 15(6):369-379.

Nosenchuck, D.M., Brown, G.L., Culver, H.C., Eng. T.I., and Huang, I.S., 1995. Spatial and Temporal Characteristics of Boundary Layers Controlled with the Lorentz Force. Twelfth Australasian Fluid Mechanics

O.-S. Gim, S.-H. Kim, and G.-W. Lee, “Flow control behind a circular cylinder by control rods in uniform stream,” Ocean Eng. - OCEAN ENG, vol. 38, Dec. 2011, doi: 10.1016/j.oceaneng.2011.09.030. of the Mean and Fluctuating Forces of Wavy (varicose) Cylinders in a Cross-Flow. Journal of Fluids and Structures, 19: 321–334.

Ozkan, G.M., Oruc, V., Akili, H. and Sahin, B., 2012. Flow Around a Cylinder Surrounded by a Permeable Outer Cylinder in Shallow Water. Experiments in Fluids 53:1751-1793

Ozkan, G.M., Firat, E., and Akili, H., 2017. Passive Flow Control in the Near Wake of a Circular Cylinder Using Attached Permeable and Inclined Short Plates. Ocean Engineering, 134:35-49.

Oruc, V., 2017. Strategies for the Applications of Flow Control Downstream of a Bluff Body. Flow Measurement and Instrumentation, 53:204-214.

Price, P., 1956. Suppression of the Fluid-Induced Vibration of Circular Cylinders. J. Eng. Mech. Div., Am. Soc. Civ. Eng., 82: 1030.

R. Galvao et al., "Flow control in flow-structure interaction," J. Fluids Struct., vol. 24, pp. 1216–1226, Nov. 2008, doi: 10.1016/j.jfluidstructs.2008.07.006.

Roshko, A. 1954. On the Development of Turbulent Wakes from Vortex Streets. NACA Rep. 1191.

Ruck, B., Klausmann, K., and Wacker, T., 2012. The Flow Around Circular Cylinders Partially Coated with Porous Media. AIP Conference Proceedings 1453;49-54.

S. Behara and S. Mittal, "Flow past a circular cylinder at low Reynolds number: Oblique vortex shedding," Phys. Fluids - PHYS FLUIDS, vol. 22, May 2010, doi: 10.1063/1.3410925.

S. Sen, S. Mittal, and G. Biswas, "Steady separated flow past a circular cylinder at low Reynolds numbers," J. Fluid Mech., vol. 620, pp. 89–119, Feb. 2009, doi: 10.1017/S0022112008004904.

S. Taneda, "Experimental Investigation of the Wakes behind Cylinders and Plates at Low Reynolds Numbers," J. Phys. Soc. Jpn., vol. 11, pp. 302–307, Mar. 1956, doi: 10.1143/JPSJ.11.302.

S.-J. Lee, S.-I. Lee, and C.-W. Park, "Reducing the drag on a circular cylinder by upstream installation of a small control rod," Fluid Dyn. Res., vol. 34, no. 4, p. 233, Apr. 2004, doi: 10.1016/j.fluiddyn.2004.01.001.

Sarpkaya, T., 1979. Vortex-Induced Oscillations. Journal of Applied Mechanics, 46: 241–258.

Sarpkaya, T., 1979. Vortex-Induced Oscillations. Journal of Applied Mechanics, 46: 241–258.

Schubauer, G. B., and Skramstad, H. K., 1947. Laminar Boundary Layer Oscillations and Transitions on a Flat Plate. J Aero Sci., 14:69–79

T. Durhasan, E. Pinar, G. M. Ozkan, H. Akilli, and B. Sahin, “The effect of shroud on vortex shedding mechanism of cylinder,” Appl. Ocean Res., vol. 84, pp. 51–61, Mar. 2019, doi: 10.1016/j.apor.2019.01.007.

T. Durhasan, E. Pinar, G. Ozkan, M. Aksoy, H. Akilli, and B. Sahin, “PIV measurement downstream of perforated cylinder in deep water,” Eur. J. Mech. - BFluids, vol. 72, Jun. 2018, doi: 10.1016/j.euromechflu.2018.06.001.

T. Durhasan, M. M. Aksoy, E. Pinar, G. M. Ozkan, H. Akilli, and B. Sahin, “Vortex street suppression of a circular cylinder using perforated semi-circular fairing in shallow water,” Exp. Therm. Fluid Sci., vol. 79, pp. 101–110, Dec. 2016, doi: 10.1016/j.expthermflusci.2016.07.001.

T. Zhou, S. F. Mohd. Razali, Z. Hao, and L. Cheng, “On the study of vortex-induced vibration of a cylinder with helical strakes,” J. Fluids Struct., vol. 27, no. 7, pp. 903–917, Oct. 2011, doi: 10.1016/j.jfluidstructs.2011.04.014.

V. Strouhal, “Ueber eine besondere Art der Tonerregung,” Ann. Phys., vol. 241, pp. 216–251, Jan. 1878, doi: 10.1002/andp.18782411005.

W. Xu, L. Yingsen, Q. Han, C. Ji, and A. Cheng, “The effect of yaw angle on VIV suppression for an inclined flexible cylinder fitted with helical strakes,” Appl. Ocean Res., vol. 67, pp. 263–276, Sep. 2017, doi: 10.1016/j.apor.2017.07.014.

W.-L. Chen, D.-B. Xin, F. Xu, H. Li, J.-P. Ou, and H. Hu, “Suppression of vortex-induced vibration of a circular cylinder using suction-based flow control,” J. Fluids Struct., vol. 42, pp. 25–39, Oct. 2013, doi: 10.1016/j.jfluidstructs.2013.05.009.

Wang, J., Zheng, H., and Tian, Z., 2015. Numerical Simulation with a TVD-FVM Method for Circular Cylinder Wake Control by a Fairing, Journal of Fluids and Structures, 57;15-31.

Williamson, C.H.K., and Govardhan, R., 2004. .Vortex-Induced Vibrations. Annual Review of Fluid Mechanics, 36:413-455.

Williamson 1996b, Vortex dynamics in the cylinder wake. Annual Review of Fluid Mechanics, 539.

Williamson. 1988,The existence of two stages in the transition to three-dimensionality of a cylinder wake. Physics of Fluids.

Y. Jin, J.-T. Kim, S. Cheng, O. Barry, and L. P. Chamorro, “On the distinct drag, reconfiguration and wake of perforated structures,” J. Fluid Mech., vol. 890, May 2020, doi: 10.1017/jfm.2020.98.

Zdravkovich, M. M, and Soutworth, P.J., 1973. Effect of Shroud Eccentricity on Suppression of Flow Induced Vibrations. Journal of Sound and Vibration, 27(1); 77-84.

Zdravkovich, M. M, and Soutworth, P.J., 1973. Effect of Shroud Eccentricity on Suppression of Flow Induced Vibrations. Journal of Sound and Vibration, 27(1); 77-84.

Zdravkovich, M. M., 1981. Review and Classification of Various Aerodynamic and Hydrodynamic Means for Fuppressing Vortex-Shedding. Journal of Wind Engineers and Industrial Aerodynamics, 7:145–189.

Zdravkovich, M. M., 1981. Review and Classification of Various Aerodynamic and Hydrodynamic Means for Fuppressing Vortex-Shedding. Journal of Wind Engineers and Industrial Aerodynamics, 7:145–189.

Zhang, H., Fan, B.-C.., and Chen, Z.-H., 2010. Computations of Optimal Cylinder Flow Control in Weakly Conductive Fluids. Computers and Fluids, 39:1261–1266.

Zhao, M., and Cheng, L., 2010. Finite Element Analysis of Flow Control Using Porous Media. Ocean Engineering, 37:1357-1366.

Zou, L., and Lin, Y., 2009. Force Reduction of Flow around a Sinusoidal Wavy Cylinder. Journal of Hydrodynamics, 21(3):308-315.

Zhao, M., and Cheng, L., ZHOU, T., 2009. Direct numerical simulation of three dimensional flow past a yawed circular cylinder of infinite length. Journal of Fluids and Structures 25, 831-847

Zhou, B., Wang, X., Guo, W., Gho, W.M., and Tan, S.K., 2015. Experimental Study on Flow Past a Circular Cylinder with Rough Surface. Ocean Engineering, 109:7-13

BIOGRAPHY

Leila NAJAFI, she graduated as a Mechanical Engineer from Tabriz university in Iran. He finished her master education in Mechanical Enginnering Department of Cukurova University in February 2014 and began her Doctor of Philosophy at the same department in 2014.

She is married and has tow twin daughter. She is working as a General Manager in Recycle paper factoray (MRS KAGIT KARTON) from 2017 up to now.